University of Massachusetts Medical School

eScholarship@UMMS

GSBS Dissertations and Theses   Graduate School of Biomedical Sciences

2016-12-01

Identification of Essential Metabolic and Genetic Adaptations to the Quiescent State in Mycobacterium Tuberculosis: A Dissertation

Emily S. C. Rittershaus
University of Massachusetts Medical School

Let us know how access to this document benefits you.

Follow this and additional works at: https://escholarship.umassmed.edu/gsbs_diss

Part of the Bacteriology Commons, Cellular and Molecular Physiology Commons, Immunology of Infectious Disease Commons, and the Microbial Physiology Commons

Repository Citation

IDENTIFICATION OF ESSENTIAL METABOLIC AND GENETIC ADAPTATIONS
TO THE QUIESCENT STATE IN *MYCOBACTERIUM TUBERCULOSIS*

A Dissertation Presented

By

EMILY S. C. RITTERSHAUS

Submitted to the Faculty of the

University of Massachusetts Graduate School of Biomedical Sciences, Worcester

in partial fulfillment of the requirements for the degree of

DOCTOR OF PHILOSOPHY

Program in Molecular Genetics and Microbiology

IDENTIFICATION OF ESSENTIAL METABOLIC AND GENETIC ADAPTATIONS
TO THE QUIESCENT STATE IN *MYCOBACTERIUM TUBERCULOSIS*

A Dissertation Presented By

EMILY S. C. RITTERSHAUS

This work was undertaken in the Graduate School of Biomedical Sciences
Program in Molecular Genetics and Microbiology

The signature of the Thesis Advisor signifies validation of Dissertation content

Christopher Sassetti, Thesis Advisor

The signatures of the Dissertation Defense Committee signify completion and
approval as to style and content of the Dissertation

Craig Peterson, Member of Committee

Daniel Bolon, Member of Committee

Beth McCormick, Member of Committee

Sabine Ehrt, External Member of Committee

The signature of the Chair of the Committee signifies that the written dissertation
meets the requirements of the Dissertation Committee

Jon Goguen, Chair of Committee

The signature of the Dean of the Graduate School of Biomedical Sciences
signifies that the student has met all graduation requirements of the School.

Anthony Carruthers, Ph.D.,

Dean of the Graduate School of Biomedical Sciences

December 1, 2016

Acknowledgements

You are the best. If I were to express everything I want to thank you for this document would be twice as long.

I want to acknowledge University of Massachusetts Medical School for the incredible research institution that it is. I am so grateful to have been accepted into its Graduate School of Biomedical Science. Thank you to the Department of Microbiology and Physiological Systems and everyone that entails. I have made many good friends and have learned so much. Finally, thank you to my thesis committee for taking the time to guide me in the right direction. It takes a village.

Abstract

Mycobacterium tuberculosis stably adapts to respiratory limited environments by entering into a nongrowing but metabolically active state termed quiescence. This state is inherently tolerant to antibiotics due to a reduction in growth and activity of associated biosynthetic pathways. Understanding the physiology of the quiescent state, therefore, may be useful in developing new strategies to improve drug efficiency. Here, we used an established *in vitro* model of respiratory stress, hypoxia, to induce quiescence. We utilized metabolomic and genetic approaches to identify essential and active pathways associated with nongrowth. Our metabolomic profile of hypoxic *M. tuberculosis* revealed an increase in several free fatty acids, metabolite intermediates in the oxidative pathway of the tricarboxylic acid (TCA) cycle, as well as, the important chemical messenger, cAMP. In tandem, a high-throughput transposon mutant library screen (TnSeq) revealed that a cAMP-regulated protein acetyltransferase, MtPat, was conditionally essential for survival in the hypoxic state. Via ^{13}C-carbon flux tracing we show an MtPat mutant is deficient in re-routing hypoxic metabolism away from the oxidative TCA cycle and that MtPat is involved in inhibiting fatty-acid catabolism in hypoxia. Additionally, we show that reductive TCA metabolism is required for survival of hypoxia by depletion of an essential TCA enzyme, malate dehydrogenase (Mdh) both in *in vitro* hypoxia and *in vivo* mouse infection.

Inhibition of Mdh with a novel compound resulted in a significantly greater killing efficiency than the first-line anti-*M. tuberculosis* drug isoniazid (INH). In conclusion, we show that understanding the physiology of the quiescent state can lead to new drug targets for *M. tuberculosis*.

Table of Contents

List of Tables

List of Figures

List of Copyrighted Materials Produced by the Author

Rittershaus ES, Baek SH, Sassetti CM. *The normalcy of dormancy: common themes in microbial quiescence.* Cell Host Microbe. 2013 Jun 12;13(6):643-51. PubMed PMID: 23768489; NIHMSID: NIHMS490114; PubMed Central PMCID: PMC3743100.

Preface

Portions of this thesis have appeared in the following publications:

Rittershaus ES, Baek SH, Sassetti CM. *The normalcy of dormancy: common themes in microbial quiescence.* Cell Host Microbe. 2013 Jun 12;13(6):643-51. PubMed PMID: 23768489; NIHMSID: NIHMS490114; PubMed Central PMCID: PMC3743100.

Rittershaus ES, Baek SH, Nambi S, Murphy K, Papavinasasundaram K, Lescyk J, Shaffer S, Chen YS, Sacchettini J, Baker R, Sassetti CM. *Hypoxic survival in Mycobacterium tuberculosis requires a cAMP-mediated metabolic switch.* Manuscript in preparation.

Chapter I. Introduction

Abstract

All microorganisms are exposed to periodic stresses that inhibit growth. Many bacteria and fungi weather these periods by entering a hardy, nonreplicating state, often termed quiescence or dormancy. When this occurs during an infection, the resulting slowly growing pathogen is able to tolerate both immune insults and prolonged antibiotic exposure. While the stresses encountered in a free-living environment may differ from those imposed by host immunity, these growth-limiting conditions impose common pressures, and many of the corresponding microbial responses appear to be universal. In this review, we discuss the common features of these growth-limited states, which suggest new approaches for treating chronic infections such as tuberculosis.

Overview

A defining feature of *Mycobacterium tuberculosis*, the causative agent of tuberculosis, is its slow growth. The maximal doubling time of this bacterium is approximately 20 hours and is significantly slower when exposed to stresses such as those encountered in the host. Indeed, the bacterial population found in chronically infected animals replicates only once every 100 hours or more (Gill et al., 2009; Muñoz-Elías et al., 2005), and subpopulations of bacteria are thought to cease growth entirely for significant periods. The importance of this relatively quiescent behavior is difficult to overstate, as it likely underlies the chronicity of the infection as well as the requirement for extended antibiotic therapy.

Dormancy, latency, and persistence are conceptually related terms used to describe the propensity of *M. tuberculosis* to arrest its growth in response to host-imposed stress. Because this behavior is very different from well-studied model organisms or agents of acute infection, it is sometimes considered an unusual selective adaptation specific to the pathogenic mycobacteria. While this trait is likely adaptive, it is by no means unusual. In fact, slow to negligible replication is the norm in the microbial world, where organisms often inhabit environments that are incompatible with rapid growth. In this review, we will consider mycobacterial dormancy in this broader ecological context.

Three Strategies to Weather the Storm

All microbes are subjected to changing environments, and the basic requirements for growth (carbon, nitrogen, phosphorus, water, etc.) are not always available. The evolutionary success of virtually all microbial species requires the ability to weather these periods, and the spectrum of survival strategies used by different microbial species has been studied for decades (Steinhaus and Birkeland, 1939). In general, these strategies can be described as variations of three general themes (Figure 1.1).

Bust and Boom

The physiology of organisms that evolved in consistently nutrient-rich environments, such as the bacteria *Escherichia coli*, are tuned to maximize growth rate (Neidhardt, 1999). Under nutrient-replete conditions in which bacterial metabolism is often studied, these organisms maximize their growth at the expense of economy by using relatively inefficient fermentative pathways to generate energy (Wolfe, 2005). Upon nutrient exhaustion the majority of these bacterial populations die, leaving a few viable organisms that subsist on the corpses of their siblings. Slow growth and cell death are balanced during this period (Finkel, 2006). When environmental conditions become more favorable, the few survivors resume growth. The ability to replicate rapidly is likely to be an essential component of this strategy, as these organisms must outcompete neighboring microbes to consume the newly introduced nutrients.

Figure 1.1. Strategies to Overcome Growth-Limiting Stress

All microorganisms encounter periods during which growth is impossible.

Three fundamental themes describe the strategies used to weather these

periods. ''Bust and boom'' describes a strategy that relies on the dynamic

persistence of a small subpopulation, ''sporulation'' is defined by the

production of metabolically inactive spores, and ''quiescence'' describes a

metabolically active nonreplicating cell that is resistant to many environmental

insults. These strategies differ in several important respects including the

population density of persistent organisms, the sensitivity of these cells to

toxins and antibiotics, and the differential dependence on rapid growth to

repopulate the niche.
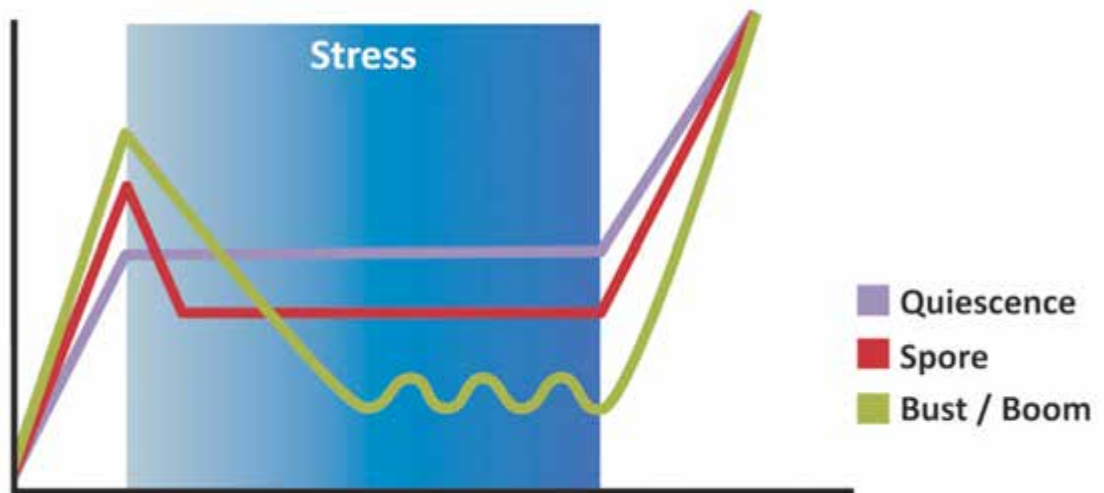
Cellular Quiescence

A distinct strategy for surviving periods of growth-limiting stress appears to be favored by both *M. tuberculosis* (Betts et al., 2002; Mitchison and Coates, 2004; Wayne, 1976) and many environmental bacteria (Lewis and Gattie, 1991). When these organisms are exposed to growth-limiting stress, the bulk of the bacterial population slows or arrests its growth and can persist in a viable nonreplicating state for months or even years (Corper and Cohn, 1933). These "quiescent" cells can be differentiated from truly dormant spore-like forms because they display nominal metabolic capacity, maintain their membrane potential, and do not undergo obvious morphological differentiation (Gengenbacher et al., 2010; Rao et al., 2008). This strategy allows the viable bacterial population size to be maintained throughout the period of stress (Jones and Lennon, 2010), relieving the emphasis for rapid growth seen in the bust-and-boom model.

True Dormancy

Sporulation is the purest form of microbial dormancy. When exposed to growth-restricting stress, some bacteria undergo an asymmetric cell division to produce a hardy metabolically inactive daughter cell called a spore (Stragier and Losick, 1996). Upon exposure to favorable environmental conditions, a fraction of spores germinate and initiate rapid growth to reestablish the population. This strategy could be viewed as a combination of the first two. The spore, while fundamentally

distinct, shares many structural and biochemical features with quiescent cells, which promote long-term survival. Upon germination, however, rapid growth may be advantageous to repopulate the niche. Indeed, the 10 min replication time of some spore-forming species of the clostridia bacteria are among the fastest known (Kreidl et al., 2002).

Historically, the strategies at either end of this spectrum have been most heavily studied. This is due to the experimental tractability of rapidly growing organisms, not because these strategies are more common or important. Indeed, it has been estimated that 60% of the microbial biomass on earth exists in a quiescent state (Cole, 1999; Lewis and Gattie, 1991). Despite its ubiquity, we still know relatively little about the regulatory mechanisms and physiological changes that define microbial quiescence. While these cellular adaptations are not exactly the same for all organisms or under all conditions, common themes can be defined (Figure 1-2). In this review, we will consider the general adaptations that are required for quiescence in diverse microorganisms and discuss how these insights might be used to develop more effective therapies for chronic infections such as tuberculosis.

Common Features of Quiescent Cells

Figure 1.2. Common Themes in Microbial Quiescence

Growth arrest can be induced by many stimuli and can have a variety of consequences on the cell. Shown are common growth-limiting stresses encountered by environmental microbes and pathogens. With a few notable exceptions, most of the growth-limiting stresses encountered in these environments are similar. Some responses to these insults are linked to a particular stress. For example, specific DNA repair pathways are necessary to resist oxidative and nitrosative stress, and the remodeling of carbon metabolism will be different in hypoxic versus normoxic conditions. In contrast, other re- sponses appear to be secondary to growth arrest per se. For example, a wide variety of growth-inhibiting stresses trigger carbon storage and cell wall re- modeling, and the maintenance of energy homeostasis is universally required for viability. PMF, proton motive force; ROS, reactive oxygen species; RNI, reactive nitrogen intermediate.
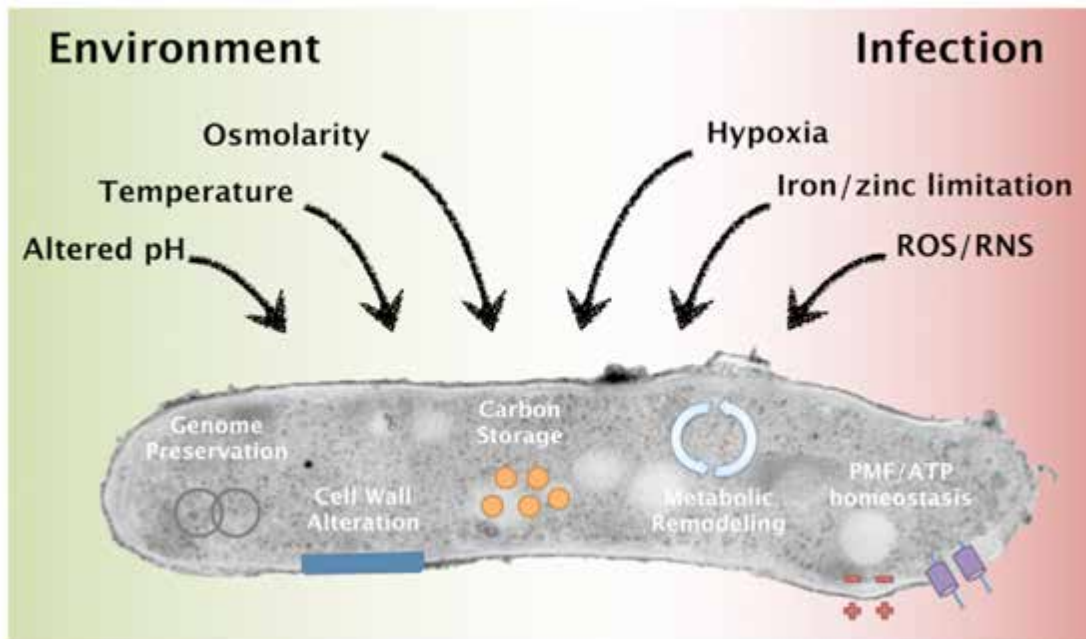
Carbon Storage

An almost universal property of quiescent cells is the accumulation of carbon stores, although the chemical structure of the storage form can differ. During low growth states, the yeast *Saccharomyces cerevisiae* accumulates glycogen, trehalose, and triglycerides as the main forms of metabolizable carbon (Gray et al., 2004). The bacterial pathogen *Vibrio cholerae* accumulates glycogen in preparation for survival in nutrient-poor environments (Bourassa and Camilli, 2009). Additionally, many bacteria store fatty acids in the form of triglycerides (Daniel et al., 2004; Kalscheuer et al., 2007) and wax esters (Sirakova et al., 2012). Both triglycerides and wax esters also accumulate in plant seeds (Radunz and Schmid, 2000), indicating that this mode of storage is advantageous for organisms that represent vastly separated domains of life. In addition, linear plastic polymers like polyhydroxyalkanoates and poly-b-hydroxybutyric acid can serve as a carbon repository in a variety of bacteria living in the soil and the rhizosphere (Kadouri et al., 2005).

What is the purpose of carbon storage? The most intuitive answer is that these cells are simply "storing nuts for winter," and these nutritional stores can be rapidly mobilized to fuel growth when environmental conditions improve. This role has been most clearly demonstrated in the *S. cerevisiae* cell, where the trehalose stores that accumulate in stationary cultures are immediately consumed upon addition of fresh media to fuel rapid regrowth (Shi et al., 2010). Glycogen may serve a similar role in *V. cholerae*, a bacterium whose life cycle relies on periodic

switches from the nutrient-replete mammalian gut to nutrient- poor aquatic environments (Bourassa and Camilli, 2009).

Carbon storage has also been found to play an important role in remodeling cellular carbon fluxes and facilitating entry into the quiescent state. Diverse stresses, such as low oxygen, low pH, or low iron, all induce a storage response in *M. tuberculosis* through the activation of a common sensor-kinase system, DosRST (Bacon et al., 2007; Baek et al., 2011; Daniel et al., 2011). The DosS sensor likely responds to alterations in cellular redox state in these contexts (Honaker et al., 2010), and triggers the synthesis of triglycerides that are stored in large cytosolic inclusions (Garton et al., 2002). The impact of this response appears to extend beyond the generation of nutrient stores. That is, disruption of the triglyceride biosynthesis pathway in *M. tuberculosis* reverses the growth arrest that is normally caused by these stresses, but has little effect on the subsequent recovery of growth when the stress is relieved (Baek et al., 2011). This inverse relationship between growth and triglyceride production appears to result from the redirection of acetyl-CoA from the TCA cycle, where it is used to generate energy during aerobic respiration, into lipid synthesis, where acetyl CoA serves as a building block for fatty acids. The growth-limiting effect of carbon storage is unlikely to be restricted to mycobacteria. For example, *S. cerevisiae* mutants that are unable to produce glycogen or trehalose consume more CO_2 than the wild-type strain during slow growth (Silljé et al., 1999), indicating higher TCA flux in the absence of carbon storage. The almost universal propensity of

microorganisms to accumulate acetyl CoA-derived carbon stores under growth-limiting stresses suggests that this may represent a common strategy for reducing growth and metabolic rate.

Cell Wall Modification

Virtually all bacteria are surrounded by an elastic meshwork of peptidoglycan that maintains cellular integrity under changing environmental conditions. This structure is composed of glycan chains, consisting of N-acetylglucosamine (NAG) and N-acetyl-muramic acid (NAM), crosslinked through short peptide moieties. Not surprisingly, the long-term survival of both spores and quiescent cells depends on specific alterations in the composition of this structure. For example, in stationary phase cultures, the Gram-positive bacteria *Staphylococcus aureus* generates a cell wall that is structurally different from the peptidoglycan found during exponential phase growth, in that it contains fewer pentaglycine bridges, which crosslink the glycan chains, and is significantly thicker (Zhou and Cegelski, 2012). Similarly, the level and gradient of crosslinking are important for the formation of bacterial spores. In the spore peptidoglycan layer of the soil-dwelling bacteria *Bacillus subtilis*, the peptide side chains serving as crosslinkers are completely or partially removed from the NAM residues and replaced by muramic-d-lactam, a specificity determinant for germination autolytic enzymes, at every second NAM position in the cortex glycan strands. As a consequence, overall levels of crosslinking are markedly

decreased in the spore cortex as compared to the vegetative cell wall (Atrih et al., 1996). Thus, common features of the peptidoglycan in both quiescent cells and spores are reduced crosslinks and increased peptidoglycan mass.

The regulation of these modifications is likely complex, but recent observations suggest that extracellular D-amino acids, such as D-methionine and D-leucine, could play an important role. D-amino acids accumulate to millimolar levels in the supernatants of stationary phase bacterial culture, where they regulate cell wall synthetic enzymes and are incorporated into the peptidoglycan polymer. The increased abundance of D-amino acids in cultures of nongrowing cells and their ability to alter the osmotic sensitivity of *V. cholerae* (Lam et al., 2009) suggests a likely role in remodeling the cell wall for quiescence.

Like many other bacteria, *M. tuberculosis* may vary the cross- linking of its peptidoglycan in slow growth states (Lavollay et al., 2008). During exponential growth, *M. tuberculosis* peptidoglycan is cross-linked largely via linkages between the third and fourth amino acids in the stem peptide, the chain of amino acids in peptidoglycan that crosslinks adjacent strands (i.e., 4/3 linkages). However, in stationary phase the cell wall primarily consists of 3/3 crosslinks. While not all investigators have observed these changes (Kumar et al., 2012), altered crosslinking could significantly change the physical characteristics of the cell wall. In addition, 3/3 crosslinks are made by transpeptidases that are insensitive to b-lactam antibiotics that inhibit cell wall synthesis, suggesting the

reduction in 4/3 linkages may reduce antibiotic susceptibility. Indeed, when the L,D-transpeptidase (MT2594/Rv2518c) responsible for making the 3/3 link- ages in *M. tuberculosis* was inactivated, the bacteria became more susceptible to the b-lactam antibiotic amoxicillin, and persistence in animals was attenuated (Gupta et al., 2010).

The mycobacterial cell wall is much more complex than those surrounding the organisms discussed above, and the full complement of alterations that accompany quiescence have yet to be defined. Mycobacterial peptidoglycan is conjugated to an additional glycan layer and finally to a functional outer membrane composed of very long chain fatty acids called mycolic acids. Surrounding this hydrophobic layer is a capsule that is largely comprised of the polysaccharide α-glucan. Thickening of the mycobacterial cell wall upon hypoxia-induced stasis was first demonstrated more than 30 years ago (Wayne, 1976). More recently, a computational model of the *M. tuberculosis* response to hypoxia was used to predict a large increase in production of cell wall components like mycolic acids and peptidoglycan (Fang et al., 2012). This prediction is consistent with electron microscopy studies that demonstrate thickening of the outer mycolic acid and/or capsule layers of the cell wall (Cunningham and Spreadbury, 1998). A major physiological outcome of these changes is decreased permeability of the cell wall, and the uptake of several classes of antibiotics into quiescent *M. tuberculosis* is significantly decreased relative to replicating cells (Sarathy et al., 2013).

In addition to its structural roles, cell wall metabolism also appears to play an important role in generating signals that regulate the germination of spores and the exit from quiescence. In *B. subtilis*, the PrkC Ser/Thr kinase responds to the presence of extracellular peptidoglycan fragments and induces spore germination (Shah et al., 2008). These fragments are released by growing cells, providing a mechanism by which the spore can sense the presence of a favorable growth environment using cues from neighboring bacteria. *M. tuberculosis* expresses a similar Ser/Thr kinase, PknB, which is also capable of binding extracellular peptidoglycan fragments (Mir et al., 2011) and regulates cell wall synthesis and growth (Gee et al., 2012). Activation of this kinase could explain the ability of spent culture medium to promote the regrowth of quiescent mycobacteria, as this activity depends on secreted lysozyme-like proteins (Mukamolova et al., 1998) that could act by liberating peptidoglycan-derived PknB ligands.

Macromolecular Synthesis and Stability

It may seem intuitive that RNA and protein synthesis will proceed at negligible rates in the quiescent cell. However, the dynamics of macromolecular synthesis are more complicated than they appear and vary during the entry, maintenance, and exit from quiescence. During entry and exit, protein synthesis accelerates. Protein turnover increases 5-fold in famished *E. coli* cells due to proteases that are produced in early stationary phase. This enhanced protein turnover during

the transition to the growth- limited state facilitates de novo protein synthesis in the absence of an exogenous carbon source (Shaikh et al., 2010), and the required amino acids are provided by peptidase-dependent autophagy, in which amino acids are produced via protein hydrolysis and degradation (Reeve et al., 1984). Similarly, increased protein turnover may also be required for exiting the quiescent state. Regrowth of *M. tuberculosis* from hypoxia- induced stasis is accompanied by an increase of the ClgR regulatory protein, which induces expression of the ClpXP protease that uses ATP hydrolysis to unfold proteins for subsequent degradation (Sherrid et al., 2010). Here, increased protein turn- over is a likely indicator of the wholesale metabolic remodeling necessary to shift between growth states.

Once quiescence is established, however, it is reasonable to assume that the synthesis of RNA and protein will slow considerably. Indeed, quiescence in *S. cerevisiae* is accompanied by a 3- to 5-fold decrease in overall transcription rate (Choder, 1991), and a 20-fold decrease in protein synthesis (Fuge et al., 1994). The mechanisms underlying the reduction of macromolecular synthesis in slowly growing *E. coli* have been explored in great detail. While the rate of nascent RNA and polypeptide chain elongation remains relatively constant, the number of synthetic sites decreases (Pedersen, 1986). As approximately half of the mass of the rapidly growing *E. coli* cell is comprised of protein synthesis machinery, the economy realized by this strategy is evident (Neidhardt, 1999). The same analysis has not been performed on nonreplicating cells, and it remains likely that

both initiation and elongation rate slow. This could be the result of specific

regulatory systems, such as the stringent response, which controls ribosomal

RNA transcription during stress (Stallings et al., 2009), and is critical for *M.*

tuberculosis survival in both hypoxia- and starvation-induced stasis (Primm et al.,

2000). In addition, low levels of nucleotide triphosphates and amino acids could

nonspecifically limit elongation rate. This would be consistent with the proposed

mechanism by which the drug pyrazinamide kills nonreplicating *M. tuberculosis*

by inhibiting trans-translation, a mechanism for recycling stalled ribosomes (Shi

et al., 2011).

The apparent reduction in RNA synthesis upon mycobacterial entry into

quiescence is coupled to a 15-fold increase in mRNA stability (Rustad et al.,

2013), and these stable mRNAs are required to sustain pools of essential

proteins (Rao and Li, 2009). This phenomenon is not unique to mycobacteria. In

both *S. aureus* and *S. cerevisiae*, mRNA transcripts are globally stabilized in

response to stationary phase and stress (Anderson et al., 2006; Jona et al.,

2000). In addition, slow growth induces the preferential stabilization of a set of

transcripts in *E. coli* (Georgellis et al., 1993), indicating that survival requires the

continual synthesis of select proteins. In support of this model, studies have

shown that stationary phase *E. coli* requires the continual expression of a subset

of genes that are controlled by the σ^S subunit of the RNA polymerase, including

many genes involved in cellular stress responses (Talukder et al., 1996).

Additionally, a subset of mRNAs is strongly induced in quiescent *S. cerevisiae*

(Werner-Washburne et al., 1996). In sum, while the rate of macromolecular synthesis clearly decreases in quiescent cells, continual transcription and translation occurs. The ability of RNA polymerase and DNA gyrase inhibitors to kill non- replicating mycobacteria indicates that these activities may also be required for survival (Betts et al., 2002; Sala et al., 2010). Energetics and Metabolism during Quiescence Maintenance of membrane potential and ATP synthesis is not required for sustaining the viability of spores, even though a repertoire of ATPases and ATP-dependent regulatory proteins is utilized during the initiation of germination (Errington, 2003). In contrast, quiescent bacteria maintain their membrane potential (Pernthaler and Amann, 2004; Rao et al., 2008), and energy homeostasis appears to be critical for survival. In nonreplicating *M. tuberculosis* cells starved for oxygen or nutrients, ATP levels are maintained at a steady level, which is only 5-fold lower than replicating cells (Gengenbacher et al., 2010; Rao et al., 2008). This maintenance of ATP homeostasis is clearly important, as disruption of the proton motive force or chemical inhibition of the F_0F_1 ATP synthase involved in ATP synthesis induces cell death in nutrient-starved or hypoxic cultures (Rao et al., 2008; Sala et al., 2010). Diverse strategies can be used to maintain energy homeostasis. Both respiratory and fermentative path- ways can support the long-term survival of bacteria in stationary phase (Duwat et al., 2001). Similarly, *M. tuberculosis* harbors a number of respiratory systems utilizing both oxygen and nitrate as terminal electron acceptors (Boshoff and Barry, 2005). When respiration is not

possible, recent data suggest that fermentation can lead to succinate secretion, which plays an important role in maintaining membrane potential (Watanabe et al., 2011; Eoh and Rhee, 2013). This general strategy is used by a number of Gram-positive and Gram-negative organisms under respiration-limited conditions (Engel et al., 1994; Schnorpfeil et al., 2001).

While the overall rate of carbon utilization decreases in quiescence, a few metabolic pathways display enhanced flux (Sauer et al., 1999; Zhang et al., 2009). The specific pathways used to maintain the quiescent cell are diverse, and their relative importance depends on the peculiarities of both the organism and the environment. However, common themes have emerged, such as a central role for the glyoxylate shunt in adapting to the growth- limited state. This pathway consists of isocitrate lyase and malate synthase and is responsible for the conversion of isocitrate and acetyl-CoA into malate and succinate. This bypasses a segment of the TCA cycle that is normally siphoned to produce biosynthetic precursors. While initially considered simply as an anapleurotic system that is used to replenish TCA intermediates during growth on nonglycolytic carbon sources such as lipids (Muñoz-Elías and McKinney, 2005), recent studies indicate that these reactions are an essential component of metabolic cycles that sustain diverse bacterial species in slowly growing states. The glyoxylate shunt is an essential component of the phosphoenolpyruvate-glyoxylate cycle in *E. coli* (Fischer and Sauer, 2003) and the ''GAS'' pathway in mycobacteria (Beste et al., 2011). These pathways are important for the

utilization of glucose, in contrast to the canonical role for the glyoxylate shunt in lipid catabolism. In both cases, these cycles are used to uncouple glucose oxidation from the production of reducing equivalents, and may function to maintain the redox state of the cytosol. In the mycobacterial case, inhibition of isocitrate lyase causes cell death in both hypoxia- and starvation-induced quiescence, supporting the importance of these pathways in nongrowing states (Gengenbacher et al., 2010; Eoh and Rhee, 2013).

Preservation of Genome Integrity

Maintaining genome fidelity when little or no metabolic capacity is available for canonical DNA repair mechanisms is a challenge faced by both quiescent cells and dormant spores. One strategy common to both types of cells is altering chromosomal structure to a more chemically stable form. The chromosome of stationary phase *E. coli* assumes an extremely compact structure. A nucleoid-associated protein called Dps, which is expressed only in stationary phase, mediates biocrystallization of the nucleoid and protects DNA from damage (Martinez and Kolter, 1997). This compaction of DNA can be very dynamic as bacteria enter and exit different growth states. In the photosynthetic cyanobacterium, *Synechococcus elongates*, a circadian clock- controlled mechanism induces periodic chromosome compaction during the night (Smith and Williams, 2006), and the resulting alterations in DNA supercoiling control global gene expression patterns (Vijayan et al., 2009). *M. tuberculosis* might use

a similar mechanism to protect its chromosome. A mycobacterial histone-like protein, Lsr2, mediates chromosome compaction and protection from reactive oxygen and nitrogen species (Summers et al., 2012). The mechanisms underlying this protective ability are unclear but could be related to the reported association between Lsr2 and a FAD-binding flavoprotein that mediates general oxidative stress resistance (Du et al., 2012). The compact packaging of bacterial DNA can be also facilitated by cationic metabolites, such as polyamines, which have been implicated in the protection of DNA from chemical damage (Baeza et al., 1991). *M. tuberculosis* synthesizes a repertoire of polyamines that facilitate transcription and DNA replication (Marton and Pegg, 1995), although the roles of these compounds during cellular quiescence remain unknown.

Truly dormant spores are not able to actively maintain their chromosome but depend on the induction of DNA repair systems upon exit from the dormant state. While the nominal metabolic capacity of the quiescent cell likely allows a subset of DNA repair mechanisms to operate continuously, the relative activity of different systems in growing and nongrowing states remains uncertain, and distinct organisms favor different strategies. Some microorganisms arrest growth with a single chromosome (Valcourt et al., 2012), while others, such as *M. tuberculosis*, exits the cell cycle with two chromosomal copies (Wayne, 1977). Thus, high-fidelity recombinational repair mechanisms, which often dominate in growing cells, are only available to a subset of quiescent organisms. Despite the apparent presence of a recombinational template in nonreplicating *M.*

tuberculosis, this organism still appears to utilize more error-prone repair systems. For example, error-prone translesion polymerases, which replicate past DNA damage lesions, are important for the survival of slowly growing *M. tuberculosis* in chronically infected animals (Boshoff et al., 2003). Similarly, mycobacteria rely on nonhomologous end-joining (NHEJ), in which double strand breaks are imprecisely rejoined, to repair double-stranded breaks in quiescent states (Shuman and Glickman, 2007). The use of the low- fidelity NHEJ system under these conditions could be due to its dependence on ribonucleotides as opposed to deoxyribonucleotide triphosphates, which may be limiting in nonreplicating cells (Gong et al., 2005).

The particular DNA repair pathways used by quiescent organ- isms have significant implications for genome evolution. While the mutation rate of rapidly growing organisms is largely deter- mined by the error rate of the replisome (Kunkel, 2004), the fidelity of DNA repair systems might dominate in organisms that spend a significant portion of their existence in slowly growing states. Consistent with this model, it was recently estimated that the *M. tuberculosis* genome accumulates mutations at a similar rate in active and latent infection states (Ford et al., 2011), and mutations accumulate in a time-dependent and not replication-dependent manner (Ford et al., 2013). As drug resistance in *M. tuberculosis* is the product of spontaneous mutation, the specific DNA repair pathways that are operational in the quiescent state could determine the rate at which resistance emerges.

Strategies to Eradicate Quiescent Bacteria

Arguably, the most important factor limiting tuberculosis control efforts is the exceptionally long treatment course that is required to prevent relapse. While the standard regimen of antitubercular drugs rapidly kills replicating bacteria in vitro, the same drugs must be administered for at least 6 months to effectively treat an active TB infection. The reduced activity of antibiotics in the in vivo environment is not specific to mycobacteria and is often attributed to slowly replicating or quiescent populations of the pathogen (Eagle, 1952; McDermott, 1958). The antibiotic sensitivity of quiescent bacterial populations has been investigated extensively in the context of environmentally induced stasis in *M. tuberculosis* (Mitchison and Coates, 2004; Rao et al., 2008; Xie et al., 2005), drug-tolerant populations found in biofilms (Brown et al.,1988), and nonreplicating "persister" subpopulations that exist even in rapidly growing cultures (Balaban et al., 2004). In all situations, quiescent bacterial populations are less sensitive to existing antibiotics that target functions necessary for cell growth. In principle, the identification of cellular functions that are important for the regulation or maintenance of quiescence should suggest new strategies for eliminating nonreplicating bacterial populations and could be used to accelerate the treatment of chronic infections. The following three general approaches have been pursued to this end.

Inhibit Pathways that Are Essential in the Quiescent State

In the case of *M. tuberculosis* there is an anecdotal correlation between drugs that retain activity against nonreplicating cells in vitro and those that have the strongest sterilizing activity in vivo (Mitchison and Coates, 2004), although this correlation is not absolute. As a result, new drug candidates are generally tested for their ability to kill quiescent bacteria. Among the several new regimens under development, a combination that includes drugs retaining activity against nonreplicating cells, bedaquiline, PA-824, and moxifloxacin, showed the highest early bactericidal activity in a recent human trial (Diacon et al., 2012). While none of these drugs were developed specifically to kill in a growth rate- independent manner, all three might have been predicted to have this ability based on their mechanism of action. Bedaquiline inhibits the F_0F_1 ATP synthase, a function required for energy maintenance (Andries et al., 2005), PA-824 is a nitroimidazole that kills via nonspecific nitrosative (nitrogen radical-mediated) damage (Singh et al., 2008), and moxifloxacin produces DNA breaks at sites of ongoing transcription (Drlica et al., 2008). These observations suggest that specifically targeting other functions necessary for survival, such as those maintaining carbon flux, energy generation, or redox maintenance, might represent a productive strategy to produce more effective therapies (Table 1).

Table 1.1. Strategies to Eradicate Quiescent Bacterial Populations

Table 1. Strategies to Eradicate Quiescent Bacterial Populations

Pathways that May Be Essential during Quiescence	Known Drugs/Inhibitors	References
RNA synthesis	Rifampin	Betts et al., 2002; Mitchison and Coates, 2004
Proton motive force/ATP generation	Bedaquiline, possibly pyrazinamide	Gengenbacher et al., 2010; Rao et al., 2008; Zhang et al., 2003
DNA gyrase/DNA integrity	Fluorquinolones	Hussain et al., 2009; Sala et al., 2010
Trans-translation	Pyrazinamide	Mitchison and Coates, 2004; Shi et al., 2011
Cell wall remodeling	Carbapenem	Hugonnet et al., 2009
Glyoxylate shunt	None	Beste et al., 2011; Muñoz-Elias and McKinney, 2005
Reductive TCA branch	None	Eoh and Rhee, 2013; Watanabe et al., 2011
Strategies to Resensitize Quiescent Cells	**Examples**	**References**
Inhibit stringent response	Increases antibiotic sensitivity in P. aeruginosa biofilm	Nguyen et al., 2011
Modulate toxin/antitoxin systems	Determines the proportion of quiescent cells in a population	Lewis, 2007
Enhance antibiotic uptake	Metabolite supplementation increases aminoglycoside uptake	Allison et al., 2011
Impose nonspecific nitrosative damage	Nitromidazoles (e.g., Metronatazole, PA-824, Delamanid)	Singh et al., 2008
Enhance TCA activity	Sensitizes to multiple antibiotics	Baek et al., 2011; Kohanski et al., 2007
Strategies to Remove Quiescence-Inducing Cues		**References**
Biofilm dispersion	Disrupts starvation-induced quiescence	Potera, 2010
TNF modulation	Enhances anti-TB therapy	Bourigault et al., 2013
Immunosuppression	Accelerates antibacterial therapy in animal models	Assfalg et al., 2010; Lenaerts et al., 2003

Sensitize the Quiescent Cell to Existing Antibiotics

As an alternative to targeting what is likely a restricted set of pathways that are necessary for maintaining viability in the absence of replication, it may also be possible to alter the physiology of the quiescent cell to render it more antibiotic susceptible. Two recent studies have focused on increasing antibiotic activity by altering flux through central carbon metabolism. In *M. tuberculosis*, antibiotic efficacy is reduced as a result of carbon storage responses that lower TCA flux. Genetic mutations or nutritional supplements that inhibit triglyceride production, and thus drive activity of the TCA cycle, or directly enhance TCA flux were found to enhance antibiotic activity in quiescent cells in vitro and in animal models (Baek et al., 2011). A similar approach for enhancing TCA-dependent antibiotic activity by metabolite supplementation was subsequently found to enhance aminoglycoside activity in *E. coli* and *S. aureus* (Allison et al., 2011). Another promising approach is inhibiting the stringent response. This system coordinates cellular physiology during slow growth states in many bacteria, and genetic inhibition of the stringent response sensitizes *Pseudomonas aeruginosa* biofilms to antibiotics (Nguyen et al., 2011). While metabolite supplementation might not be practical for many infections of the deep tissues, and small molecule modulators of these pathways are not currently avail- able, these studies provide proof for the concept that quiescent cells can be rendered antibiotic susceptible.

Alter the Growth-Limiting Stress

Instead of directly modulating bacterial metabolism, it may be possible to enhance drug efficacy by removing the specific environmental pressures that induce quiescence. For example, nonreplicating, antibiotic-tolerant cells are found in relatively high numbers in bacterial biofilms (Lewis, 2007), and the disruption of the biofilm architecture increases antibiotic activity at least in part by reversing this differentiation (Musk and Hergenrother, 2006). Similarly, it may be possible to modulate the host immune pressures that induce the antibiotic tolerant state. Overt immunosuppression can enhance antibiotic activity in a number of models (Assfalg et al., 2010; Lenaerts et al., 2003). Even more subtle chemical modulation of tumor necrosis factor (TNF) signaling, which plays central roles in the inflammatory response, has been shown to accelerate antituberculosis therapy in animals (Bourigault et al., 2013).

Thus, both the host and the pathogen can be manipulated to increase antibiotic efficacy. A more detailed understanding of the specific pressures that limit growth during infection and the pathogen's adaptations to these stresses could lead to the rational development of new synergistic therapies that accelerate antibacterial treatment.

Conclusion and Specific Aims

The aim of this work was to better understand the physiology of the quiescent

state in *M. tuberculosis* in order to identify new strategies for drug treatment. As

detailed above, while there are many pathways that are down-regulated or

inactive in the nongrowing quiescent state, there are also active processes

involved in maintaining viability that require further study. Our approach to

identifying these active pathways was to harness the power of global and high-

throughput screens, metabolomics and TnSeq, to identify active pathways and

enzymes involved in the stable adaptation and survival of hypoxia. Specifically,

we wished to accomplish the following goals:

I.   Identify metabolic alterations in hypoxic *M. tuberculosis*

II. Identify conditionally essential genes in hypoxic *M. tuberculosis*

III. Understand the role of MtPat in hypoxic metabolic regulation

IV. Identify new targets for drug treatment in hypoxic *M. tuberculosis*

Chapter II. Results

Abstract

Upon inhibition of respiration, which occurs in hypoxic or nitric oxide-containing

host microenvironments, *M. tuberculosis* adapts a non-replicating 'quiescent'

state and becomes relatively unresponsive to antibiotic treatment. In this study,

we utilized a combination of metabolite profiling in tandem with comprehensive

mutant fitness analysis to identify regulatory or metabolic pathways that could be

targeted to kill quiescent cells under hypoxic conditions. Quantification of total

metabolite pools revealed alterations in the abundance of tricarboxylic acid (TCA)

cycle intermediates that correlated with increased cyclic AMP (cAMP). A parallel

genetic study identified a cAMP-controlled protein acetyl-transferase

(MtPat/Rv0998) that was essential for survival in hypoxia. MtPat promoted

survival by coordinately inhibiting both fatty acid catabolism and oxidative TCA

reactions, and favoring flux through reductive TCA reactions that maintain the

redox state of the cell. In the absence of this regulatory system, beta-oxidation

and continued flux through oxidative TCA reactions lead to reduction of the

NAD^+/NADH pool and reduced viability. Genetic inhibition of TCA enzymes

verified the relative importance of reductive reactions in hypoxic cultures and

murine lung, and established a specific role for malate dehydrogenase (Mdh) in survival. Chemical inhibition of Mdh caused more rapid cell death in hypoxia than did isoniazid, suggesting a new strategy for eradication of quiescent bacteria.

Introduction

Tuberculosis (TB) has proven difficult or impossible to control throughout much of the world. The resilience of this disease can be attributed to the huge reservoir of asymptomatic *Mycobacterium tuberculosis* (Mtb) infection, which is estimated to include as many as one billion individuals, and the remarkably long and complex treatment regimen that is necessary to prevent or cure infection. Despite the availability of drugs that rapidly kill (Mtb) *in vitro*, treatment of active TB disease still requires the administration of these agents for at least six months. This long and complex regimen is difficult to deliver and incomplete treatment is both ineffective and contributes to the selection of drug-resistant strains.

A defining feature of Mtb that limits antibiotic efficacy is its relatively slow growth rate and propensity to exit the cell cycle and adopt a hardy nonreplicating state during times of stress (Gengenbacher et al., 2010; Hett and Rubin, 2008; Voskuil et al., 2003; Wayne and Sohaskey, 2001). While Mtb does not replicate in this "quiescent" state it remains metabolically active (Baek et al., 2011; Eoh and Rhee, 2013; Watanabe et al., 2011), distinguishing quiescence from true microbial "dormancy" responses, such as sporulation. Despite this continual metabolic activity, quiescent Mtb becomes relatively tolerant to existing

antibiotics that target bacterial functions, such as transcription, translation, and cell wall synthesis, which are required primarily during active replication. Understanding which metabolic pathways remain necessary for the survival of quiescent Mtb could lead to the rational design of new drugs that are more effective in eradicating these cells.

A wide variety of stresses encountered during infection, such as low oxygen, low pH, iron starvation, and exposure to nitric oxide (NO), are capable of reducing mycobacterial growth and antibiotic efficacy. While the specific adaptation to each of these stresses is likely to differ, they all initially trigger the DosRST regulatory system that senses respiratory capacity by responding to the reduction state of the quinone pool (Voskuil et al., 2003). This response to respiratory limitation has been most thoroughly studied using a well-defined in vitro model in which hypoxia is used to arrest the growth of this obligate aerobe (Wayne and Hayes 1996; Rustad et al., 2008; Boshoff et al., 2004; Eoh and Rhee, 2013). Upon oxygen depletion, DosRST rapidly induces a 48-gene regulon that includes the Tgs1-encoded triglyceride synthase (Voskuil et al., 2003). The resulting carbon storage response redirects acetyl-CoA from growth promoting pathways into the formation of cytosolic lipid bodies, which correlates with the arrest of bacterial replication (Baek et al., 2011). This initial response is followed by more stable transcriptional and metabolic changes that promote long-term survival (Rustad et al., 2008; Watanabe et al., 2011; Eoh and Rhee, 2013; Galagan et al.,

2013; Baek et al., 2011). The outcome of this adaptation is a remodeling of the TCA cycle from the oxidative reactions that occur during respiration to a reductive pathway that regenerates NAD+ and produces succinate to sustain membrane potential, ATP synthesis, and anaplerosis. Indeed, these dual responses to respiration limitation serve to maintain cellular redox balance, since both lipid anabolism and reductive TCA consume NADH and regenerate NAD+.

These studies describe important responses to respiratory limitation and suggest pathways that might be important for the survival of quiescent Mtb. However, it remains unclear how metabolic alterations are regulated and which of these remodeled pathways are most important for survival of the quiescent cell. To understand the consequences of perturbing individual metabolic pathways in quiescent cells, we combined a comprehensive metabolite analysis of hypoxic Mtb with a parallel genome-wide genetic screen for mutants that were unable to survive under this condition. This combination of approaches identified a cAMP-dependent regulatory pathway that coordinates the switch from oxidative to reductive metabolism, and defined bacterial functions that can be targeted to kill quiescent Mtb. Inhibiting one such function, a non-redundant component of the reductive TCA pathway, resulted in rapid Mtb death in hypoxia and during infection. We conclude that this insight into the physiology of quiescent cells can inform the development of more effective TB therapies.

Materials and Methods

Mycobacterium tuberculosis H37Rv (ATCC 27294) was used. Cultures were grown using Middlebrook 7H9 media supplemented with 0.05% Tween-80 and OADC (Becton Dickinson) enrichment, or on 7H10 agar with OADC enrichment at 37˚C. For fatty acid-free media, 7H9 was supplemented with ADC, using fatty-acid free BSA (Sigma) and 0.05% tyloxapol (Sigma). For ^{13}C flux experiments, 7H10 media was supplemented with ADC using 0.05% D-Glucose-2-^{13}C (Sigma) and 0.05% acetate.

Hypoxic cultures were grown in 17 mL cultures in sealed glass vials (as described in Baek *et al*., 2011), or in 31 mL cultures in 45 ml glass serum vials (Wheaton) sealed with 20 mm rubber stoppers (Wheaton) and 20 mm aluminum crimp caps (Supelco). At indicated time points, 3 vials were opened and viable bacterial numbers were enumerated on 7H10 agar plates. Redox ratios were determined using the NAD/NADH Quantitation Kit (Sigma).

For metabolite abundance, metabolites were extracted from hypoxic (day 10) and aerobic cultures in quadruplicate. Cells were lysed in chloroform:methanol (2:1), dried and subjected to analysis via GC/MS and LC/MS as described in Griffin et al., 2012.

Transposon mutagenesis of H37Rv was carried out as described in Long *et al*.

(2015). Three independent libraries were generated and mixed together at equal

ratios based on optical density (A600). Hypoxic vials (31 mL) were inoculated in

replicates of eight with approximately 10^7 mutants at day zero. At day 21 and day

42, eight vials were opened per time point and approximately 50,000 mutant CFU

were spread onto each of three 7H10 petri plates (245mm x 245mm) including 25

µg/mL Kanamycin and 0.05% Tween-80 for an approximate total of 150,000

mutant CFU per replicate. Input library (control) was plated in replicates of eight

as described above for hypoxic samples. 7H10 agar plates were incubated for 28

days at 37ºC, after which genomic DNA was extracted independently from all

replicates. Sample preparation, sequencing and analysis were performed as

described in Nambi et al., 2015.

Genetic knockout of MtPat was achieved by hygromycin-marker replacement via

suicide vector pJM1 as previously described (Baek et al., 2011). For ^{13}C flux

experiments, bacteria were inoculated onto 0.45 µm HVLP membrane filters

(Millipore) and placed on top of 7H10 agar, and grown at 37˚C for 7-10 days, at

which point the filters were acclimated to room temperature and transferred to

7H10 agar plates including 0.05% D-Glucose-2-^{13}C and placed inside an

anaerobic chamber (BBL) with a GasPak (Beckton Dickinson) to deplete oxygen.

After two hours at RT, anaerobic chamber was placed at 37˚C for 7-10 days.

Filters containing bacteria were removed an added to 2 mL screw-capped tubes

with silica beads (pre-washed with HPLC-grade methanol) and 1 mL HPLC-grade acetonitrile:methanol:water (2:2:1). Lysis and quenching of metabolites was performed by bead-beating three times at 6.5 m/s for 30 seconds each. The supernatant was filtered using a 0.22 μm HVLP filter and kept at -80°C until further use. HPLC analysis was performed using an Agilent 6520 Accurate-Mass QTOF LC/MS system (Agilent Technologies Inc, Marshfield, MA, USA) with a Cogent Diamond Hydride TYPE-C Silica HPLC Column (100Å Pore Size) (MicroSolv, 70000-15P-2) and isocratic gradient as described in Eoh and Rhee, 2013. Peak area was measured for each metabolite of interest and flux ratio was determined by comparison of peak area for standard metabolite mass and peak area of metabolite mass +1 (i.e. 13C labeled-form).

For mouse infections, C57BL/6 mice were infected with approximately 200-300 CFU/lung of WT (H37Rv) or ΔMtPat via the aerosol route using a Glas-col aerosol exposure system. After approximately four weeks, isoniazid (INH) treatment was initiated and delivered via drinking water (100 μg/ml INH). Mice were sacrificed at weeks four and twelve and organs were extracted and CFU was enumerated as described in Baek et al., 2011.

Genetic knockdown constructs (Mdh-DAS, SucD-DAS) were made as described previously (Kim et al., 2013, Schnappinger et al., 2015). Knockdowns were induced with ATc (1 μg/mL) added to cultures in vitro or with doxycycline chow

for mouse infections. Knockdowns were confirmed in hypoxia using multiple-reaction-mode (MRM) Mass Spectrometry to detect the presence of specific target peptides. For hypoxic and aerobic cultures, ATc was added every seven days using a non-coring gas-tight syringe (Hamilton) with 1 µg/mL as the initial dose and 0.5 µg/mL as the subsequent doses. Pooled mouse infection (C57BL/6), qTag strain construction, and qPCR analysis were performed as described in Blumenthal et al., 2010.

The Sacchettini Lab at TAMU carried out the Mdh inhibitory compound screen. Inhibition of Mdh was measured by the conversion of s-malate to oxaloacetate and the decrease of reaction cofactor NADH (ex:340nm, em:460nm). Assay conditions were as follows: 100mM HEPES, 50mM KCl, pH7.5, 100 µM OAA, 250 µM NADH and 0.25nM Mdh. 3653 compounds were screened, of which 3321 have been shown to have whole-cell activity in Mycobacteria. Three active compounds were identified, and the most effective compound (Compound A) was selected for further testing. For hypoxic drug testing, Compound A (CHEM ID # 5104073) was solubilized in DMSO and filtered using PMSF sterile filters. 40 µM of Compound A, or 2 µg/ml of isoniazid (INH), or both, was added to hypoxic cultures every seven days after the initial 10 day stable adaptation to hypoxia. Compound A sensitivity assay was carried out in the presence of 1µg/mL ATc and differing concentrations of the compound as described in Franzblau et al., 1998. Viability was measured by the addition of alamarBlue Dye (Thermo Fisher)

and monitoring fluorescence excitation (ex: 570nm, em: 585nm).

Results

Quantifying total metabolite pools in quiescent *M. tuberculosis* reveals coordinated alterations in carbon metabolism and increased cAMP

The ultimate rationale for this study was to apply parallel metabolomic and genetic profiling to associate metabolic changes with the genes that regulate them. To accomplish this, we first utilized high-throughput metabolomics to identify metabolic pathways that are regulated during the adaptation to hypoxia. Mtb was cultured in sealed vials in which the bacterium gradually depletes the available oxygen over an initial growth period of five to seven days. Once the oxygen is consumed, Mtb ceases replication but maintains viability for several weeks. To capture the initial adaptation to the hypoxic condition, we extracted total metabolites from 10-day-old non-replicating cultures, and compared these to metabolites extracted from log-phase aerobic cultures. Approximately 200 distinct metabolites were quantified via a combination of gas and liquid phase chromatography coupled with mass spectrometry.

A clear change in metabolic state was apparent between the two conditions (Figure 2.1). In general, the abundance of biosynthetic precursors was decreased, reflecting the lack of necessity to increase biomass. This change was apparent in amino acid pools and also in the pentose phosphate pathway, which generates nucleotides. In contrast, we noted a general increase in abundance of

free fatty acids (linoleate, oleate, methylstearate, margarate, arachidate), sugar

alcohols (malitol, sorbitol) and glycogen precursors (maltose oligomers) (Figure

2.2). The accumulation of these compounds is consistent with a general shift

from carbon catabolism to storage. This observation is consistent with the known

accumulation of triglycerides under these conditions and suggests the presence

of diverse carbon storage programs in hypoxic *M. tuberculosis*.

A second notable effect was the differential abundance of some TCA

intermediates. Citrate, cis-aconitate, alpha-ketoglutarate, and acetyl-CoA were all

more abundant in the hypoxic extracts when compared with the aerobic extracts.

In contrast, the abundance of malate, fumarate, and succinate were unchanged

or less abundant in hypoxic extracts (Figure 2.3), indicating that these distinct

TCA reactions were uncoupled in hypoxic Mtb. These observations are generally

consistent with the bifurcated TCA pathway that has been previously described in

hypoxic Mtb, in which the oxidation of acetyl-CoA to 2-ketoglytarate occurs

independently from the reduction of malate to succinate (Watanabe et al., 2011;

Eoh and Rhee, 2013). Together, both carbon storage and TCA remodeling

observed in hypoxia correlate with growth arrest and redox maintenance.

This remodeling of metabolic state was accompanied by a five-fold increase in

the abundance of 3',5'-cyclic-AMP (cAMP) in hypoxic Mtb (Figure 2.4). cAMP is a

second messenger that is synthesized by adenylate cyclase enzymes and

involved in regulation of carbon catabolism in many systems in response to

extra- or intra-cellular stimuli. While cAMP was relatively increased in hypoxic

cells, the abundance of adenosine and AMP were similar in aerobic and hypoxic

conditions suggesting that the increase in abundance of cAMP is not a byproduct

of altered of precursor pools, but likely reflected an increased rate of production.

These results confirmed and extended previous characterizations of the

metabolic adaptation to hypoxia and implicated cAMP as a possible regulator of

this response.

Figure 2.1. Metabolite abundance in hypoxic vs. aerobic Mtb.

M. tuberculosis was grown in either hypoxic or aerobic conditions and GC/MS and LC/MS were used to quantify the relative abundance of each metabolite. A fold-change ratio of 1 indicates no chance in metabolite abundance. A dotted line representing statistical significance ($p \leq 0.05$) was determined using student's t test on quadruplicate replicates. A complete list of metabolites profiled is included in Table 4.1.

Metabolite Abundance

Legend:
- Amino Acid (green)
- Oxidative TCA (red)
- Reductive TCA (yellow)
- Free Fatty Acid (blue)
- Sugar Alcohol (magenta)
- cAMP (cyan)
- Other (black)

Y-axis: p value (Increasing significance); 10^0, 10^{-1}, 10^{-2}, 10^{-3}, 10^{-4}, 10^{-5}, 10^{-6}, 10^{-7}, 10^{-8}, 10^{-9}, 10^{-10}

X-axis: Fold Change; 0.01, 0.1, 1, 10, 100

Decreased in Hypoxia ← → Increased in Hypoxia
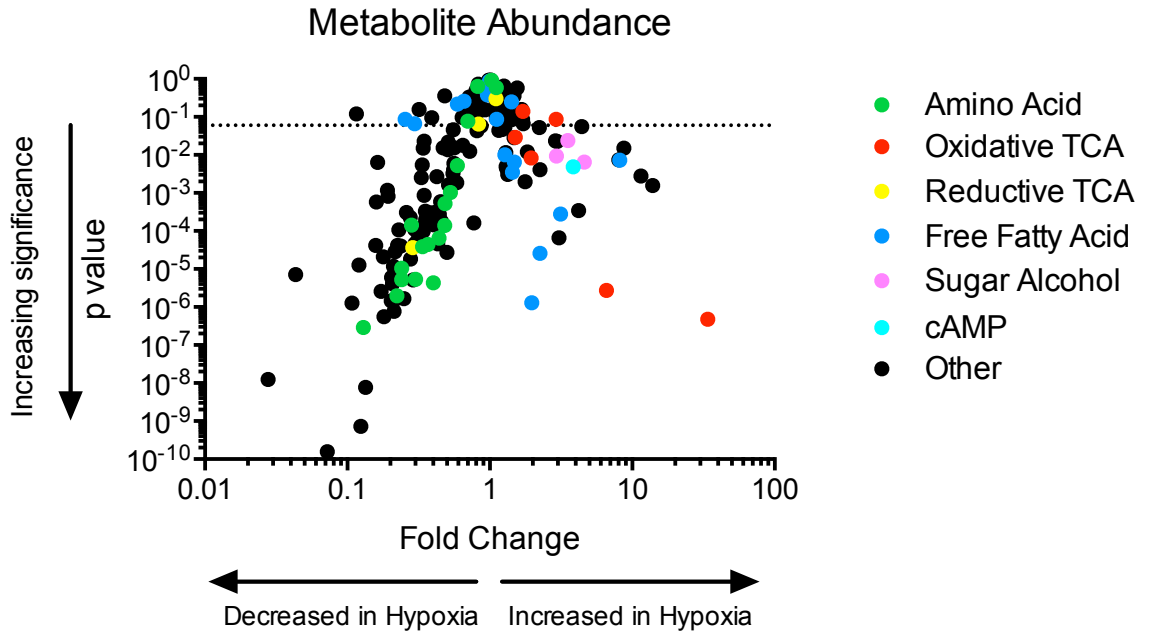
Figure 2.2. Abundances of free fatty acids increase in hypoxic Mtb.

Condition-specific abundances of free fatty acids (highlighted in Figure 2.1). *M. tuberculosis* was grown in hypoxic and aerobic conditions and metabolite abundance was determined by GC/MS and LC/MS. Metabolites were measured in quadruplicate.
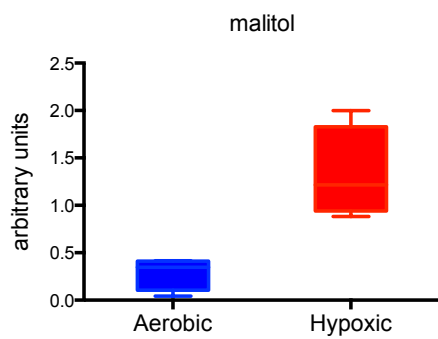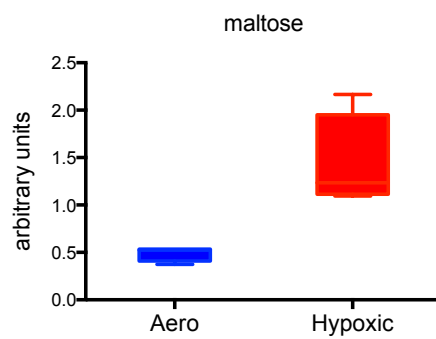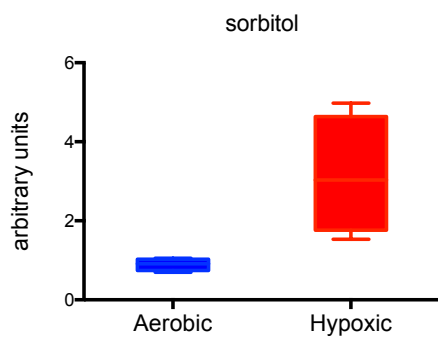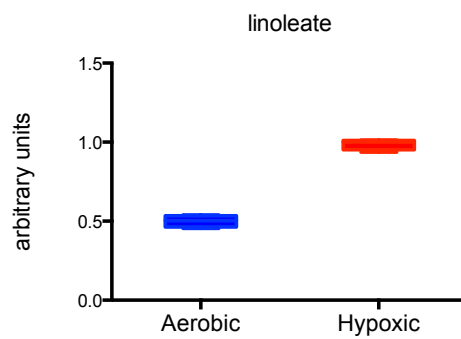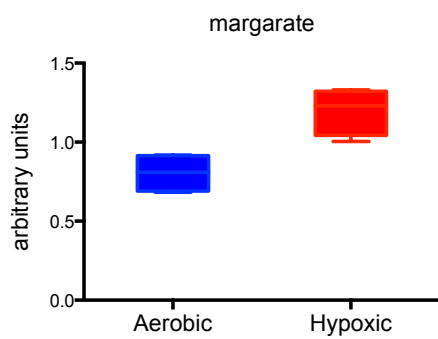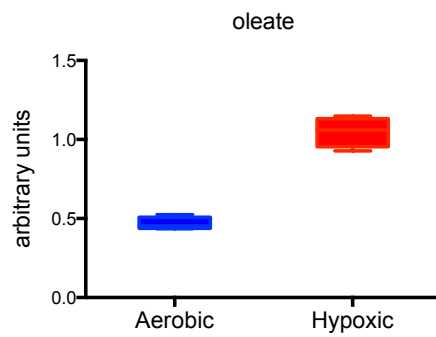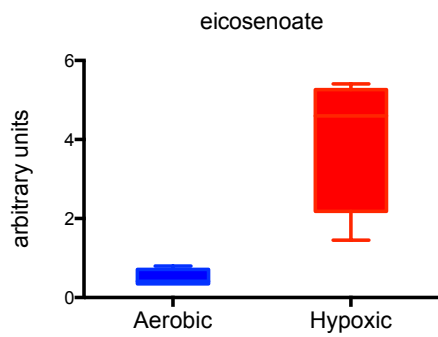
Figure 2.3. Abundance of TCA metabolites in hypoxic and aerobic Mtb.

Condition-specific abundances of TCA cycle intermediates (highlighted in

Figure 2.1). *M. tuberculosis* was grown in hypoxic and aerobic conditions and

metabolite abundance was determined by GC/MS and LC/MS. Metabolites

were measured in quadruplicate. Oxidative (Ox.) and reductive (Red.)

branches of the TCA cycle are indicated.
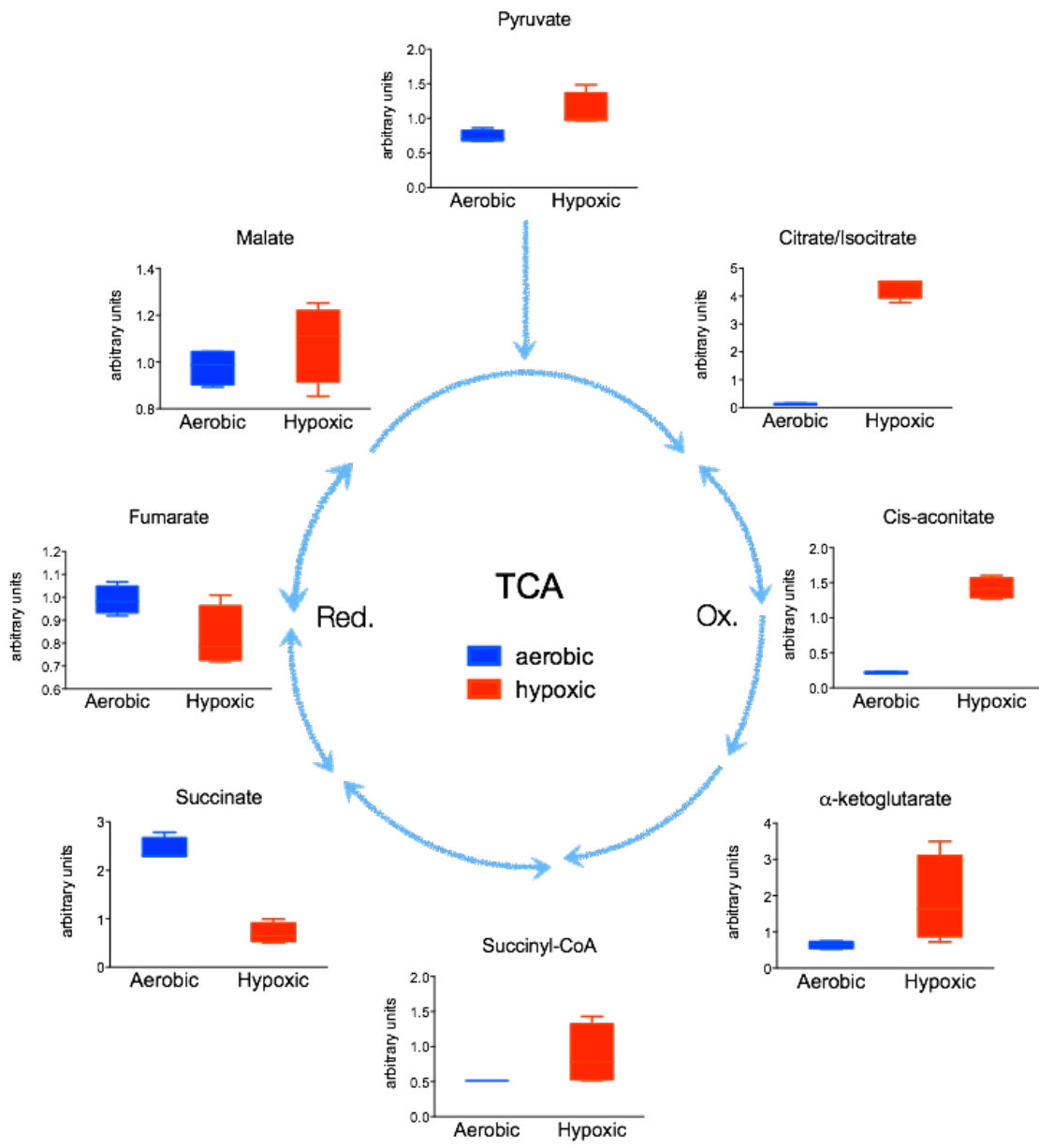
Figure 2.4. Abundance of 3',5'-cAMP increases in hypoxic Mtb.

Condition-specific abundance of 3',5'-cAMP (highlighted in Figure 2.1). *M. tuberculosis* was grown in hypoxic and aerobic conditions and metabolite abundance was determined by GC/MS and LC/MS. Metabolites were measured in quadruplicate. Ratio p value < 0.005 (Table 4.1).

3',5'-cyclic-AMP (cAMP)
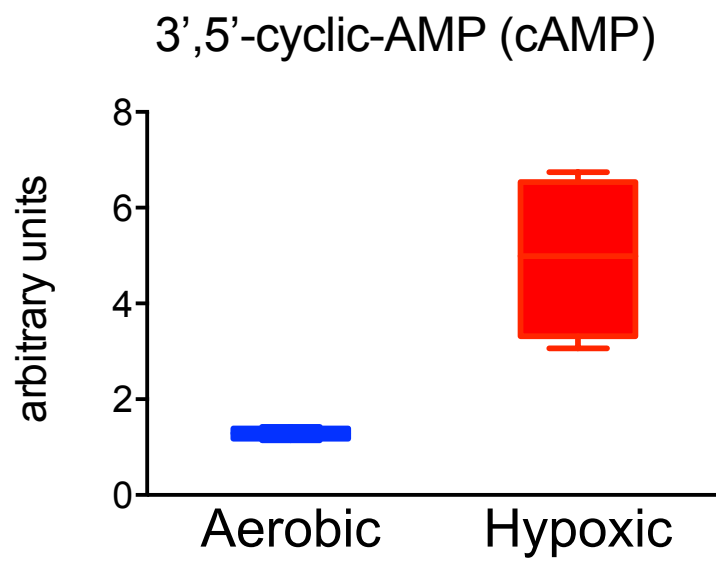
Genome-wide mutant fitness profiling identifies redox maintenance and cAMP pathways that are essential for the adaptation to hypoxia

To associate the observed metabolic changes with the responsible bacterial genes, we quantified the relative fitness of Mtb mutants under hypoxic conditions. A highly saturated library of random transposon mutants was generated, in which 55,000 of the possible 76,000 TA dinucleotide insertion sites were represented. In this complex library, an insertion is present every 80 bases on average and virutally every nonessential gene is represented by multiple individual clones (Sassetti et al., 2003; Griffin et al., 2011). The transposon library was subjected to hypoxic culture for either three or six weeks, and the relative abundance of each mutant in the input pool and selected pools was compared using next generation sequencing (Figure 2.5). This "transposon sequencing" (TNseq) strategy allows relative fitness of each Mtb mutant to be estimated over the period of selection. The multiple time points included in this experimental design allowed us to differentiate between three distinct phenotype classes (Figure 2.6). 30 mutants were found to be relatively underrepresented after three weeks of hypoxia ("early hypoxia"), when compared to the input library. These mutants likely include both those with defects in growth during the period of oxygen depletion and in initial survival in hypoxia. All but two of these mutants were among the 101 that were significantly underrepresented when the input was compared to the libraries selected for 6 weeks ("late hypoxia"). To specifically

define the mutants that were unable to survive in the quiescent state, we compared the composition of libraries that were selected for 3 versus 6 weeks of hypoxia. This latter set of 32 mutants represents genes that are specifically required for maintaining viability in the absence of replication (Figure 2.7, Table 4.2 – 4.7).

While the majority of genes found to be conditionally essential in hypoxia had no annotated function, a number of known pathways were identified. As expected, a number of the conditionally essential genes are part of the DosR dormancy regulon, including dosR (rv3133c) and acr/hspX (rv2031c), which were essential in both early and late hypoxia. Other DosR regulon genes dosS (rv3132c), otsB1 (rv2006) and unknown genes rv2030c, and rv2623 were found to be conditionally essential in late hypoxia. The DosR regulon consists of 48 genes that are transcriptionally upregulated upon exposure to hypoxic conditions and, furthermore, acr/hspX has been shown to be the most strongly upregulated transcript by DosR in hypoxic conditions (Sherman *et al*., 2001; Voskuil et al., 2003). The activity of DosR is involved in maintaining the redox state of the cell in the absence of oxygen (Leistikow et al., 2010) facilitated at least in part by induction of tgs1 and accumulation of triacylglyceride (Baek et al., 2011). Consistent with a redox regulation as a critical adaptation to hypoxia, a number of genes predicted to be involved in F_{420} biosynthesis/metabolism were identified as conditionally essential: fbiA (rv3261) and fgd1 (rv0407). F_{420} is a rare

prokaryotic coenzyme present in Mycobacterial species that is involved in protecting the bacterium from nitrosative damage (Purwantini and Mukhopadhyay, 2009) and has a role in maintaining viability in hypoxia (Gurumurthy et al., 2013). Indeed, the mycobacterial Fgd1, an F_{420}-dependent glucose-6-phosphate dehydrogenase, has been shown to respond to oxidative stress by metabolizing glucose-6-phosphate (G6P) in order to maintain redox balance (Hasan et al., 2010). Thus, our hypoxic genetic screen confirms maintenance of redox balance as a central theme in the adaptive response to hypoxia.

The observed increase in cAMP during the adaptation to hypoxia (Figure 2.4) led us to investigate the behavior of mutants lacking predicted cAMP-associated genes under these conditions. The Mtb genome encodes sixteen proteins with predicted adenylate cyclase (AC) domains; of which ten have been biochemically characterized as active cAMP producing enzymes (Shenoy and Visweswariah, 2006). Only one of these adenylate cyclases met our significance threshold in the hypoxic transposon mutant library screen, Rv1625c/Cya (Figure 2.8). Despite the statistical significance of this phenotype, mutants lacking this enzyme displayed a modest fitness defect and were underrepresented by 1.5-fold after 6 weeks of hypoxia.

cAMP acts by interacting with effector proteins that contain nucleotide binding

domains (NBD). To identify potential the downstream targets of cAMP signals in

Mtb, we specifically assessed the relative fitness of mutants lacking each of the

nine predicted cAMP-binding proteins encoded in the genome. Only one of these

mutants, lacking the *rv0998* gene, was significantly underrepresented in our

hypoxic transposon library screen (Figure 2.9). Indeed, the abundance of this

mutant decreased by more than 20-fold between 3 and 6 weeks of hypoxia,

representing the most profound survival defect identified during this period of

quiescence. *rv0998* encodes a cAMP-regulated protein lysine acetyltransferase,

known as MtPat (Nambi et al., 2010; Lee et al., 2012; Nambi et al., 2013). This

two-domain protein is homologous to a large family of protein acetyltransferase

(Pat) proteins. The mycobacterial Pat ortholog also contains an additional

nucleotide-binding domain that is structurally similar to the cAMP responsive

region of protein kinase A, and has been shown to increase acetylation activity

upon cAMP binding. To confirm the predicted essentiality of MtPat in hypoxia,

this gene was deleted in Mtb. The ΔMtPat deletion mutant grew normally in

aerobic conditions and reached a similar cell density as wild type Mtb in hypoxic

vials. However, unlike wild type Mtb or a complemented strain, the ΔMtPat

mutant progressively lost viability once hypoxia was achieved (Figure 2.10).

Notably, the ΔMtPat did not display a survival defect in starvation conditions

(Figure 2.12), but did have a hypersensitivity to streptomycin treatment (Figure

2.11), which suggests MtPat's role is specific to stress from respiration limitation.

Together, this comprehensive mutant fitness profiling confirmed the importance

of redox maintenance systems in survival under hypoxic conditions.

Furthermore, this study specifically implicated a cAMP-mediated pathway,

consisting of Cya and MtPat, in this adaptation.

Figure 2.5. Hypoxia TnSeq experimental model to predict conditionally essential genes.

A mutagenized *M. tuberculosis* transposon library was inoculated into hypoxic vials and plated for surviving mutants (CFU) at the indicated time points (zero, three and six weeks). Stable adaptaion to hypoxia occurs at approximately week one. Surviving mutants from week three and week six were compared to the input (time zero) to determine which mutants increased or decreased in abundance. The comparison of week three versus week six allows for the prediction of essential genes specifically required after the stable adaptation to hypoxia.

Hypoxic Survival
TnSeq Experimental Model
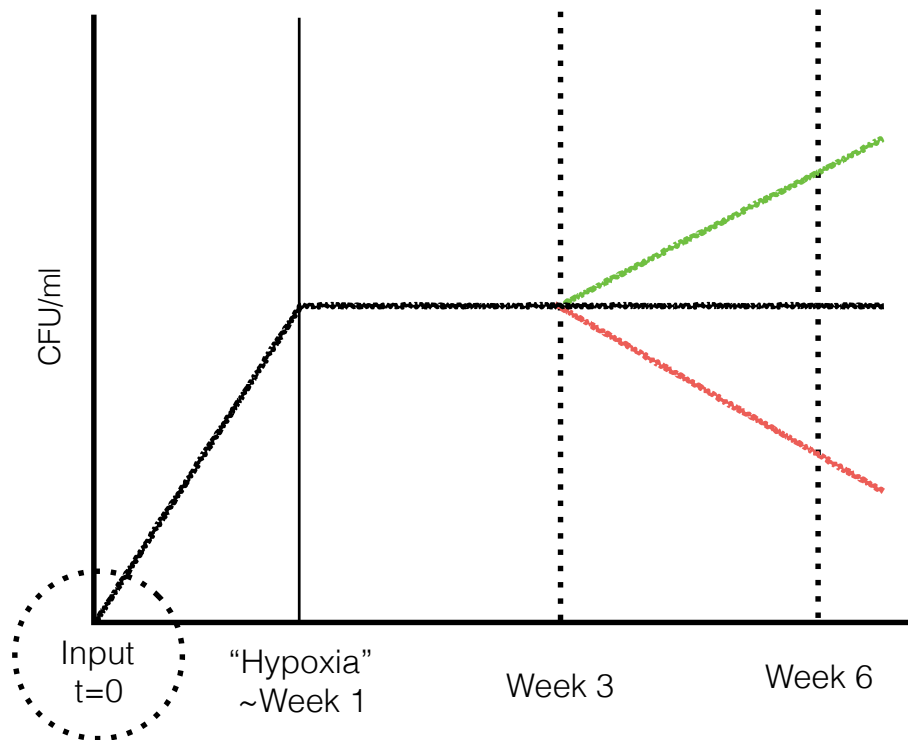
Figure 2.6. TnSeq in hypoxic Mtb identifies conditionally essential genes.

Non-essential genes with >4 TAs hit are plotted by their log2 change fold ratio

Individual genes are represented by blue dots. A ratio in the range of 1 to -1

indicates no significant change in the fitness of the transposon-interrupted

gene between the two conditions, while a ratio of |1.5| or greater (red dotted

lines) indicates a significant change in the gene in hypoxic conditions.

TnSeq Genetic Screen (Input v H3)

TnSeq Genetic Screen (Input v H6)

TnSeq Genetic Screen (H3 v H6)
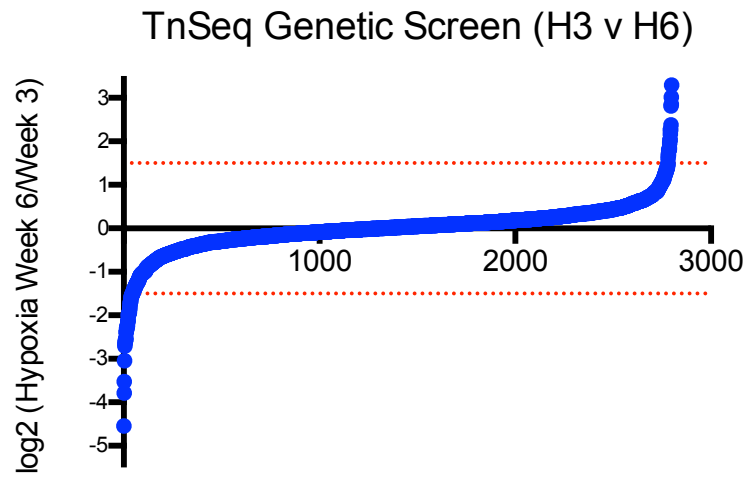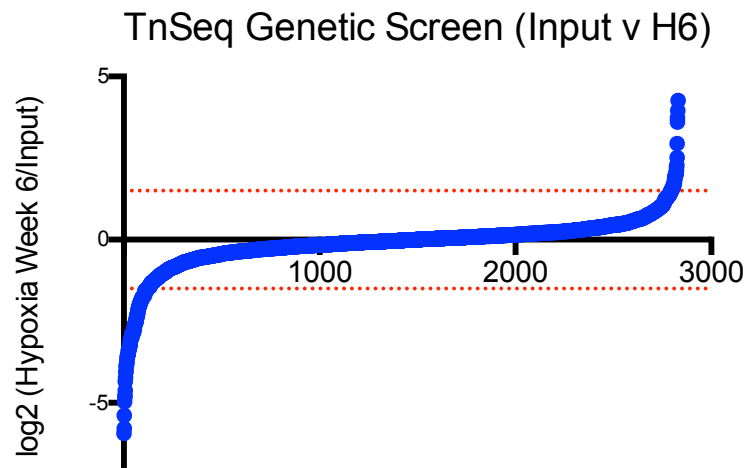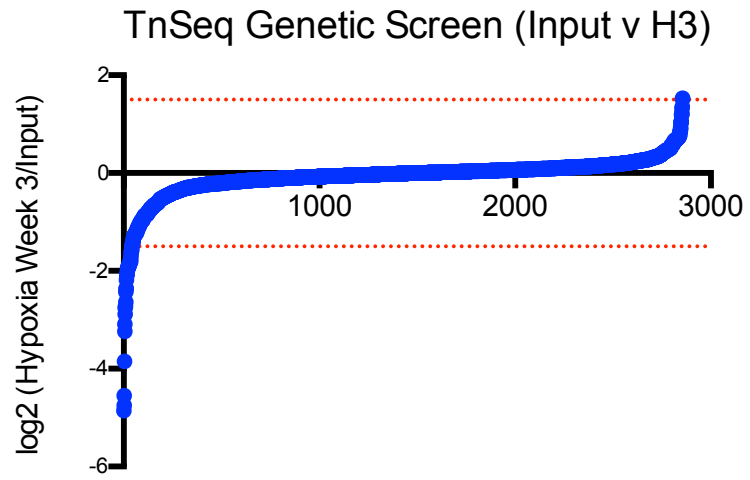
Figure 2.7. Hypoxic conditonally essential genes are consistent across timepoints.

A Venn Diagram compares the underrepresented genes identified from each time point comparison: input vs. hypoxia week 3 (IvH3), input vs. hypoxia week 6 (IvH6), and hypoxia week 3 vs. hypoxia week 6 (H3vH6). The conditionally essential underrepresented genes identified were largely consistent across datasets. Conditionally essential genes were defined as: p value ≤ 0.005, TAs hit >4, log2 fold change ≤ -1.5.
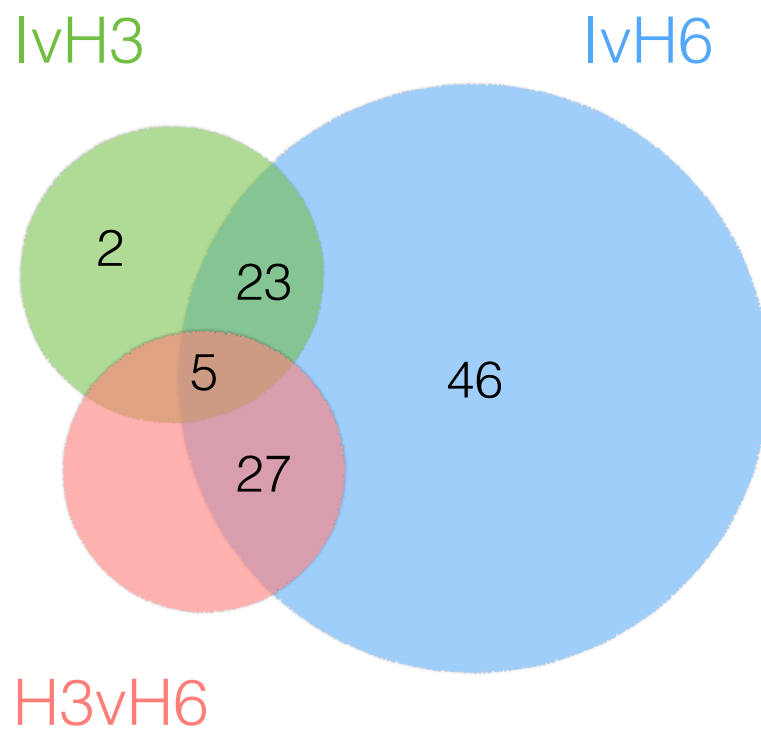
**Figure 2.8. Comparison of Mtb Adenylate Cyclase (AC) predicted
essentiality in hypoxia.**

Comparison of the log2 fold change of the predicted Adenylace Cyclase (AC)

enzymes of *M. tuberculosis* (TAs hit >4) at week three vs week six. Rv1625c is

the only AC with a p value ≤ 0.05 (denoted by asterisk), and no AC has a log2

fold change greater than |1.5|.

Predicted AC's H3vH6

*
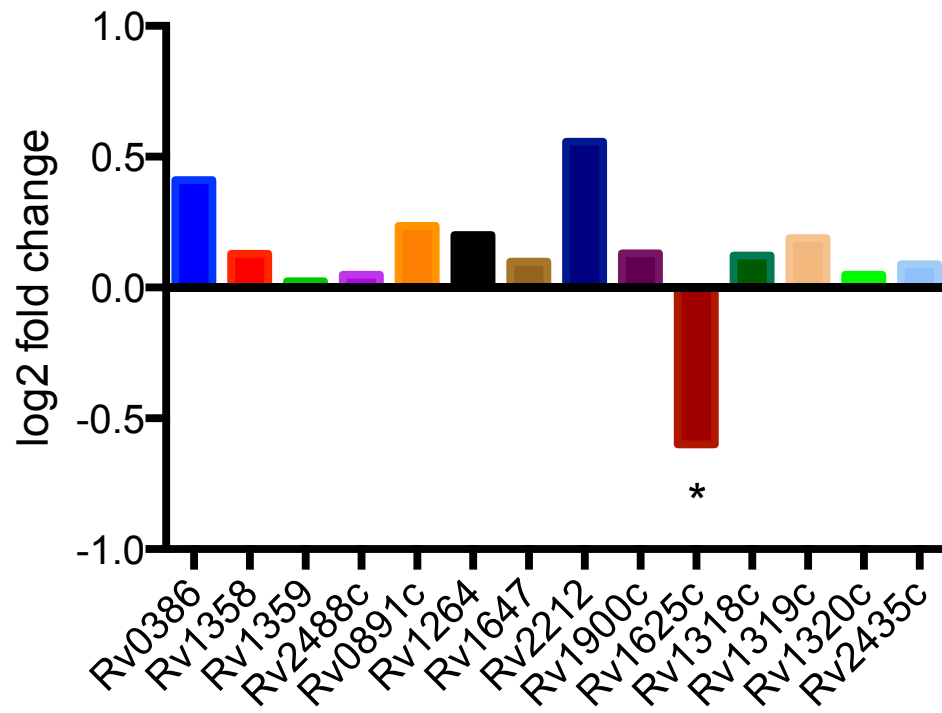
Figure 2.9. Comparison of Mtb cyclic nucleotide binding proteins (cNMP) predicts essentiality of MtPat in hypoxia.

Comparison of the log2 fold change of the predicted cyclic nucleotide binding proteins (cNMP) of *M. tuberculosis* (TAs hit >4) at week three vs week six. Rv0998 (MtPat) is the only statistically significant cNMP with a p value ≤ 0.05 (denoted by asterisk), and log2 fold change greater than |1.5|.

Predicted cNMP's H3vH6
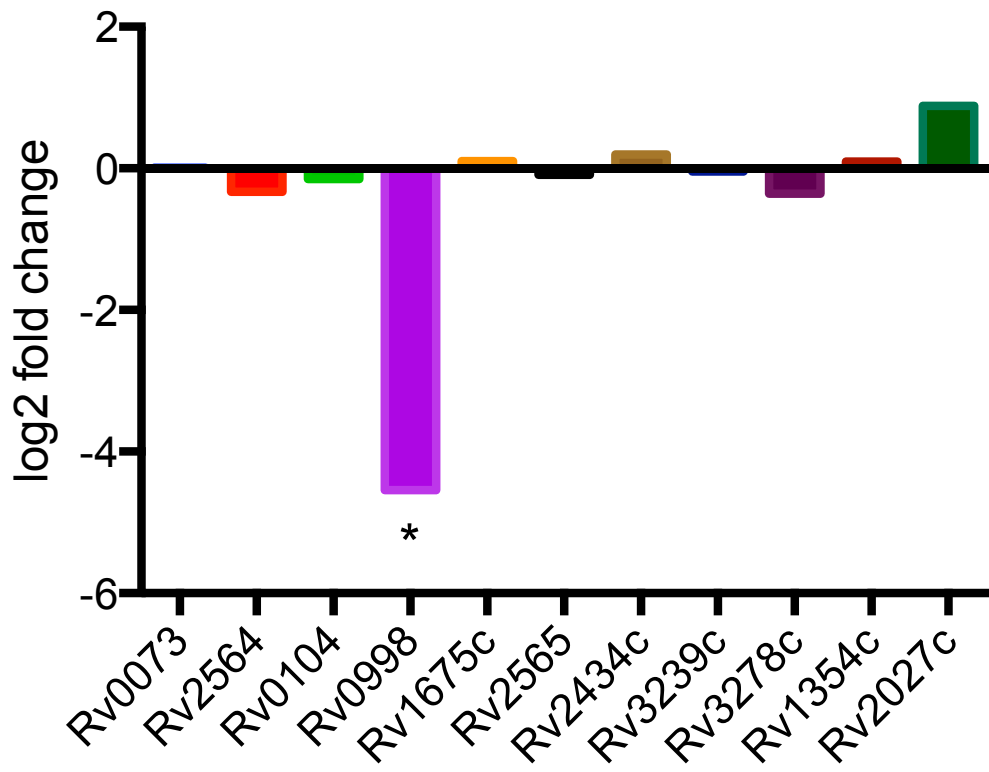
Figure 2.10. Reduced survival of ∆MtPat in hypoxia.

Hypoxic survival in an ∆MtPat deletion strain is significantly impared. Cultures were grown in triplicate in hypoxic vials. Viability was measured by CFU/mL at the indicated time points.

Hypoxia Survival
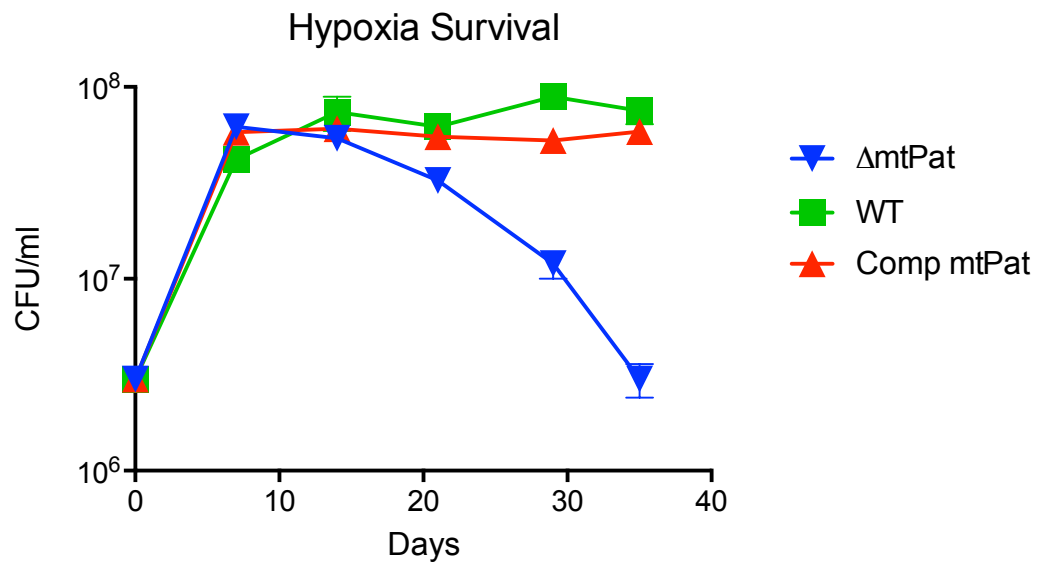
Figure 2.11. ΔMtPat is hypersensitive to streptomycin treatment.

Survival of streptomycin treatment (2µg/mL streptomycin) in an ΔMtPat

deletion strain is significantly impared. Viability was measured by CFU at the

indicated time points and percent survival was determined for each strain

based on pre-treatment CFU.

Streptomycin treatment (2μg/mL)
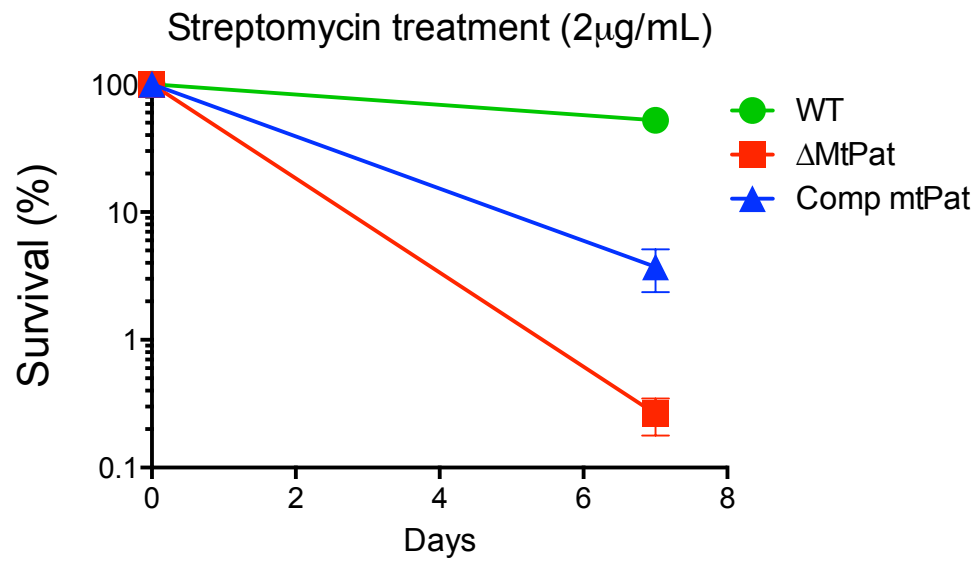
Figure 2.12. ∆MtPat survives starvation stress.

No survival defect was observed in starvation conditions (PBS+tyloxapol) in an

∆MtPat deletion strain. Viability was measured by CFU at the indicated time

points.

Starvation (PBS+tyloxapol)
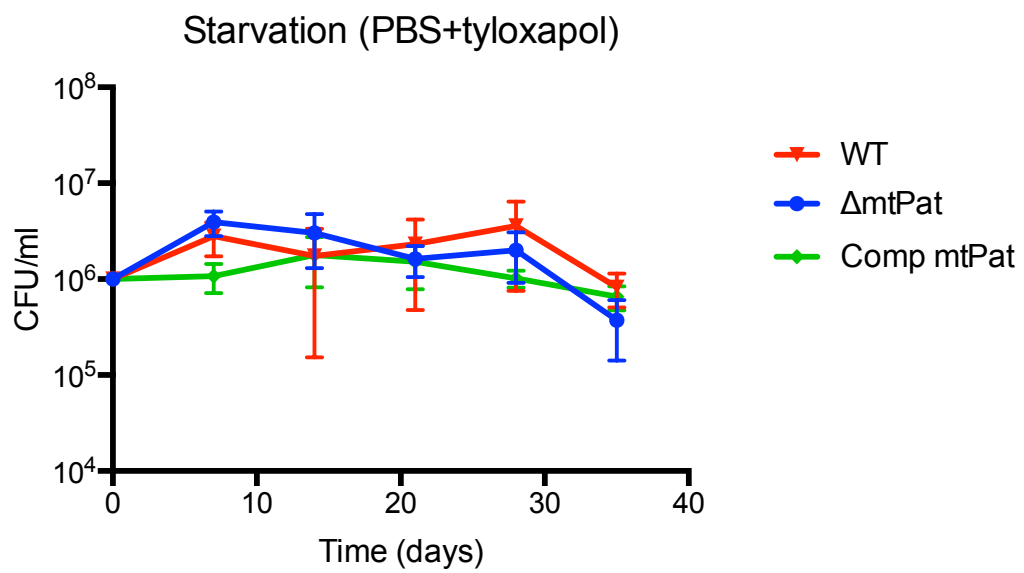
cAMP induced protein lysine acetylation is required to remodel central metabolism and maintain redox homeostasis

Because cAMP and Pat orthologs have been shown to regulate carbon metabolism in other systems (Wang et al., 2010; Castaño-Cerezo et al., 2011), we hypothesized that MtPat may be involved in regulating the pathways known to be altered in hypoxia (Watanabe et al., 2011; Eoh and Rhee, 2013). To specifically quantify the effect of MtPat on carbon metabolism, we used stable isotope labeling to measure the relative flux through each metabolite pool. Wild type, ΔMtPat, and complemented strains were independently grown on media containing a mixture of substrates for glycolysis and beta-oxidation, and 2-[^{13}C]-labeled glucose was added to track the fate of each carbon source in aerobic or hypoxic conditions. After nine days of hypoxic culture, total metabolites were extracted and analyzed via HPLC-LC/MS. Relative flux was measured via the level of conversion of each metabolite to the ^{13}C labeled form.

Under aerobic conditions wild-type incorporated 2-[^{13}C]-glucose into all TCA metabolites, consistent with the use of a canonical TCA cycle. Under hypoxic conditions, however, flux of 2-[^{13}C]-glucose indicated branched TCA metabolism (Figure 2.13). Flux of glycolytic carbon was concentrated primarily into malate and succinate, while flux through citrate/isocitrate and alpha-ketoglutarate was barely detectable. This pattern of labeling indicated that accumulation of citrate and alpha-ketoglutarate in our initial metabolomic screen was due to a reduction

in flux through these reactions. These data are consistent with branched TCA

metabolism in hypoxia, with a preferential use of reductive branch that converts

malate to succinate and an almost complete absence of activity in the oxidative

branch that converts citrate to alpha-ketoglutarate (Eoh and Rhee, 2013;

Watanabe et al., 2011).

In contrast with wild-type Mtb and the complemented ΔMtPat mutant, the ΔMtPat

strain continued to incorporate 2-[^{13}C]-glucose into the oxidative branch of TCA

under hypoxic conditions. Whereas there was no detectable flux through

citrate/isocitrate in wild type hypoxic Mtb, the mutant incorporated ^{13}C -labeled

carbon into this dedicated first step of oxidative TCA, and ultimately had ^{13}C -flux

patterns similar to aerobically growing bacteria.

The preferential use of reductive TCA reactions in hypoxia has been

hypothesized be important for the regeneration of NAD+, which is expected to

become reduced to NADH in the absence of an efficient electron acceptor, such

as oxygen (Eoh and Rhee, 2013; Watanabe et al., 2011). As a result, the

continued flux through the oxidative branch of TCA in ΔMtPat might impair

survival in hypoxia by limiting NAD+ regeneration from NADH. To test this

hypothesis, we measured the redox state of the NAD+/NADH pool (Figure 2.14).

Under aerobic conditions, both wild type and the ΔMtPat mutant maintained a

balance of NADH and NAD+, with this cofactor primarily in the oxidized form.

While wild type bacteria were able to maintain NADH/NAD+ balance in hypoxia, the ratio of NADH/NAD+ increased by more than 10-fold in the ΔMtPat deletion mutant upon oxygen limitation. The observed redox imbalance in the mutant is consistent with the increased flux through oxidative reactions inferred by ^{13}C-carbon tracing, and implies that depletion of NAD+ could underlie the impaired survival of this strain in hypoxia.

Figure 2.13. Hypoxic metabolism utilizes reductive TCA, while ∆MtPat continues oxidative TCA flux.

M. tuberculosis grown on 2-[^{13}C] glucose in aerobic conditions incorporates ^{13}C into all metabolites of the TCA cycle (blue bars) as measured by HPLC/MS. Anaylsis of *M. tuberculosis* in hypoxic conditions (red bars) identifies a reduction in flux through oxidative TCA metabolites (citrate/isocitrate, α-ketoglutarate), while maintaining flux through reductive TCA metabolites (malate, succinate). Unlike hypoxic WT, hypoxic ∆MtPat continues to incorporate ^{13}C into oxidative branch metabolites (green bars). Metabolites were quantitated by HPLC/MS and flux was determined by the change (∆) in peak area of M (metabolite mass) to M+1 (metabolite mass + 1, i.e. ^{13}C-labeled).

^{13}C-Glucose

^{13}C malate

^{13}C citrate/isocitrate

^{13}C succinate

^{13}C α-ketoglutarate

TCA

WT Aerobic
WT Hypoxic
ΔmtPat Hypoxic

ΔM+1
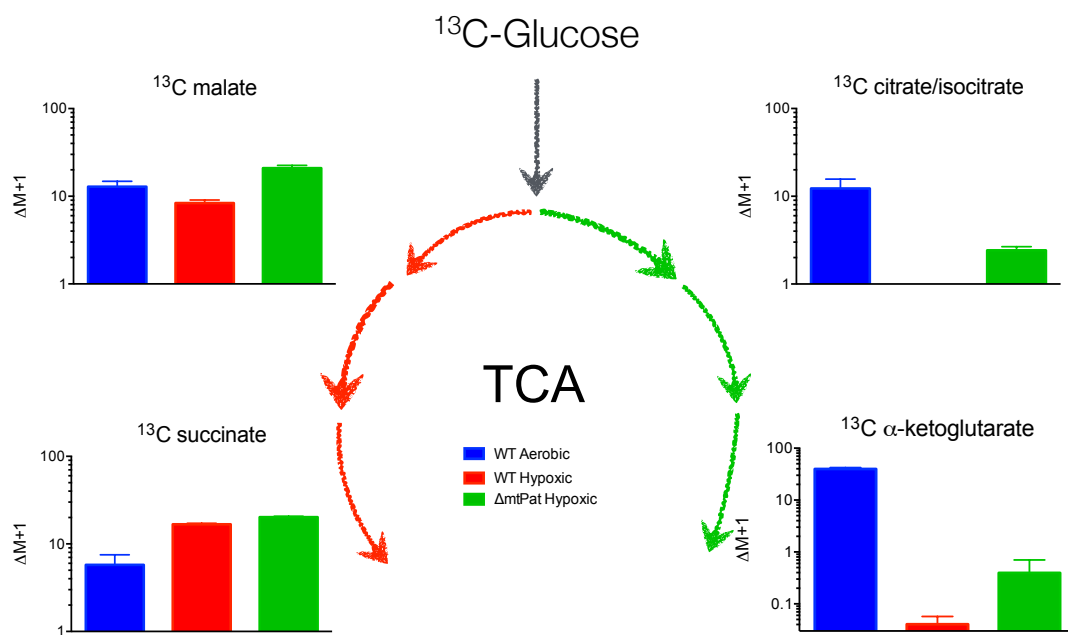
Figure 2.14. ∆MtPat is overreduced in hypoxia.

The ratio of NADH and NAD+ was quantified for each strain in aerobic and

hypoxic conditions. Values were normalized to CFU for each strain in each

condition.
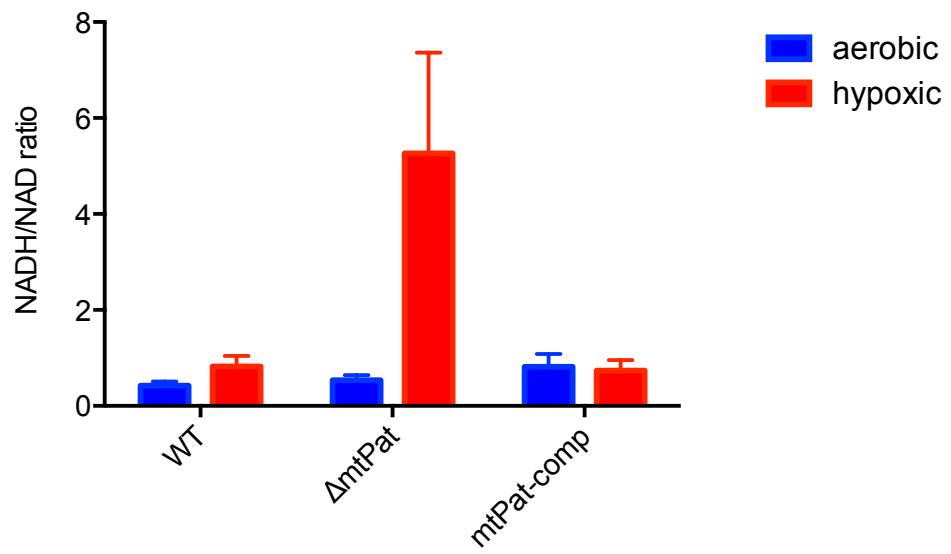
Coordinated regulation of oxidative metabolic reactions via MtPat is necessary for hypoxic survival

While many substrates have been proposed for Pat orthologs, based largely on acetyl-proteomic approaches, biochemical studies have implicated predominantly acetyl- and acyl-CoA ligases as targets of Pat-mediated regulation (Crosby et al, 2012). Indeed, MtPat acetylates both the acetyl-CoA ligase (Acs) and 10 different acyl-CoA ligases (FadD paralogs) in a cAMP-dependent manner (Xu et al., 2011; Nambi et al., 2013). These FadD proteins are involved in fatty acid catabolism through beta-oxidation. Like the oxidative branch of TCA, beta-oxidation consumes NAD+ and produces NADH. Furthermore, catabolism of fatty acids ultimately ends in the production of acetyl-CoA, which is readily incorporated the oxidative branch of the TCA cycle. Based on these similarities between beta-oxidation and oxidative TCA cycle reactions and the known effect of MtPat on acyl-CoA ligase activity, we hypothesized that coordinated repression of these pathways may be important for survival in hypoxia.

To test whether the MtPat-mediated inhibition of fatty acid catabolism to acetyl-CoA is important for hypoxic survival, we determined whether the survival of the ΔMtPat mutant was altered by abundance of fatty acid in the medium. While the presence of oleate had no effect on the viability of wild type Mtb or the ΔMtPat complemented strain, the omission of fatty acid from the medium effectively

ameliorated the viability defect of the ΔMtPat mutant (Figure 2.15). Together

these results indicate that the coordinated inhibition of fatty acid catabolism and

oxidative TCA reactions by MtPat contributes to the survival of Mtb in hypoxia.

Figure 2.15. Fatty Acid-free media rescues hypoxic ∆MtPat.

Hypoxic ∆MtPat has a survival defect in standard 7H9 media (mixed carbon including glucose, oleate and glycerol). Survival of hypoxic ∆MtPat is no longer impared in fatty-acid free (glucose and glycerol) media. Viability was measured by CFU at indicated time points.

Glucose + glycerol + oleate

Glucose + glycerol

WT
ΔmtPat
mtPat-Comp
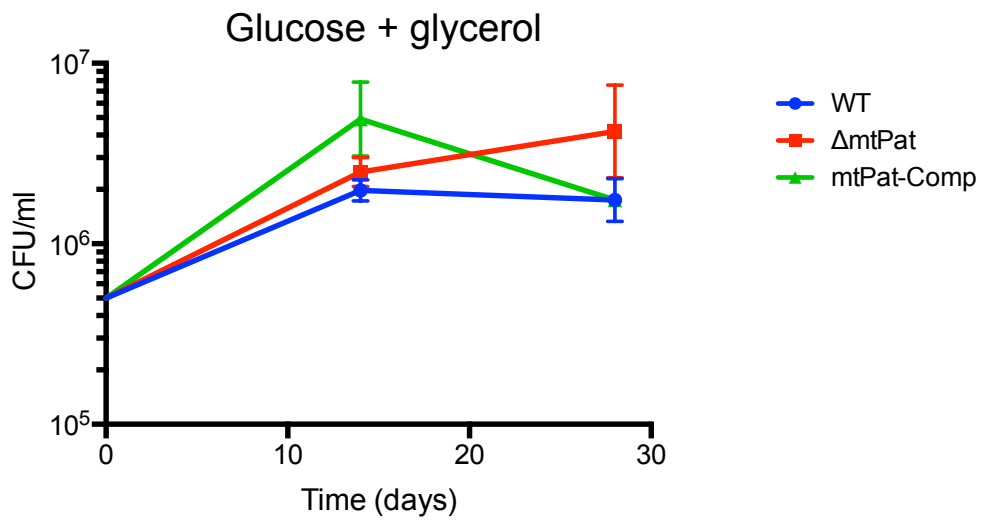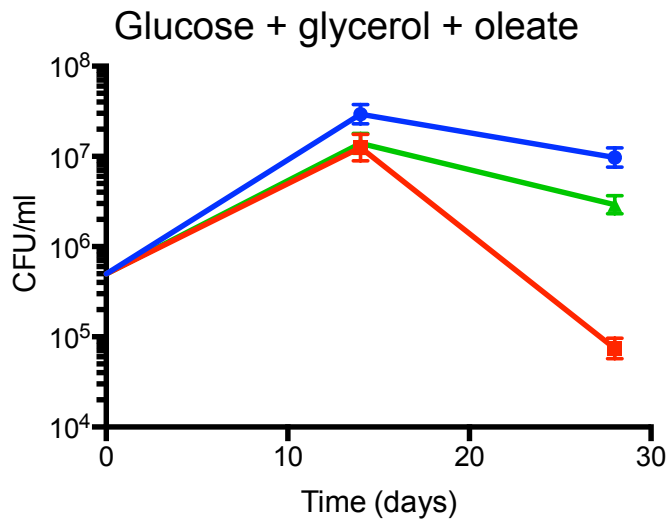
Targeting components of the reductive branch of the TCA cycle in quiescent *M. tuberculosis* increases the efficacy of existing drug therapies

The redox state of the cell correlates with antibiotic sensitivity (Dwyer et al., 2014). Since the reductive branch of the TCA cycle is actively utilized during the hypoxic state, we hypothesized that targeting components of this branch would make effective targets for drug treatment in vivo. C57BL/6 mice were infected with ΔMtPat and treated with isoniazid (INH) starting at four weeks post infection. After eight weeks of treatment, the bacterial burden in mice infected with the ΔMtPat deletion strain was significantly reduced in the lung and complete sterilization achieved in the spleen (Figure 2.16). Thus, targeting an enzyme involved in metabolic switch to the reductive branch of the TCA cycle is effective in sensitizing quiescent *M. tuberculosis* to INH in vivo.

Figure 2.16. ∆MtPat is hypersensitive to INH treatment *in vivo*.

Aerosol mouse (C57BL/6) infection with WT (H37Rv) and ∆MtPat strains. Mice

were started on isoniazid (INH) treatment at week four (pre-treatment, blue

bars) and treatment was continued for eight weeks (week twelve, red bars).

Mouse lungs and spleen were plated on 7H10 agar for CFU at weeks four and

eight. Limit of detection = 100 CFU.

Mouse Infection CFU/Lung +/- INH
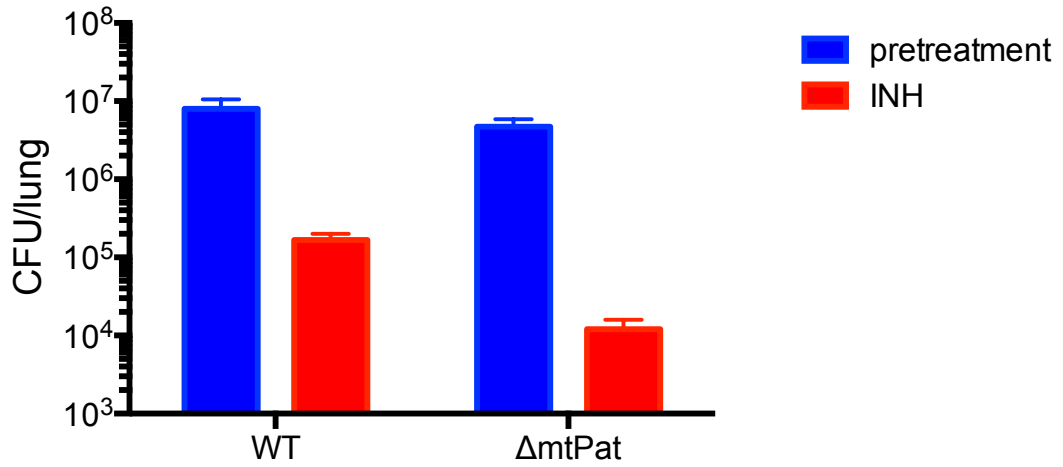
Mouse Infection CFU/Spleen +/- INH
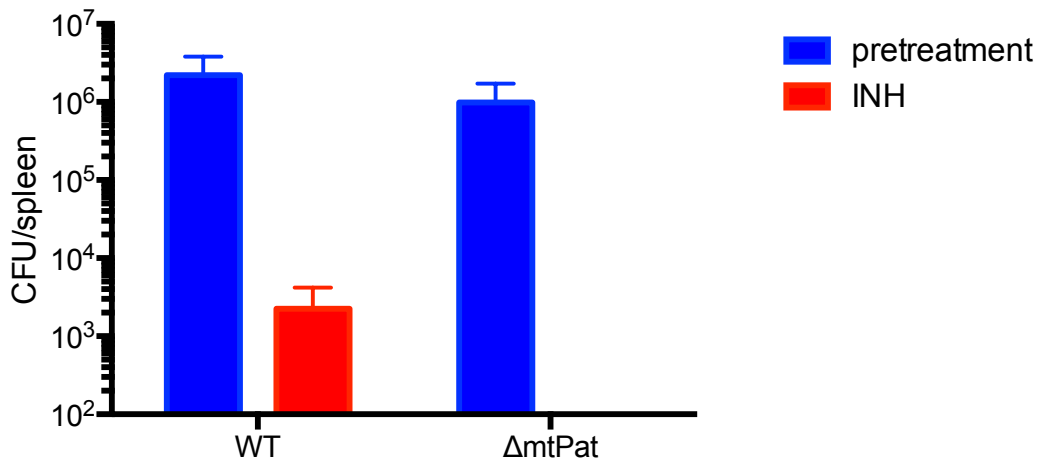
Utilization of the reductive branch of the TCA cycle is critical for survival of quiescent *M. tuberculosis in vitro* and *in vivo*

The impaired survival of the ΔMtPat mutant in hypoxia indicated that preferential utilization of reductive TCA reactions was important for maintaining viability in hypoxia. In order to directly assess the importance of these reactions, we constructed a mutant in which the only non-redundant step in the predicted reductive pathway, malate dehydrogenase (Mdh), could be inducibly depleted. The *mdh* gene was fused *in situ* with a DAS+4 tag. This tag directs the proteolysis of the fusion protein by the ClpXP system upon the induction of the SspB adapter by anhydrotetracycline (ATc) addition. To verify that protein depletion was efficient in quiescent cells, ATc was added to the Mdh-DAS mutant after ten days of hypoxic culture. Eight days later, 97.83 % depletion of Mdh was confirmed by targeted mass spectrometry (Figure 2.17).

To assess the relative contribution of Mdh to Mtb survival, the protein was depleted in either aerobic or hypoxic cultures and viability was assessed over time (Figure 2.18). Mdh depletion arrested the growth of the Mdh-DAS mutant when ATc was added to exponentially growing aerobic cultures, confirming the predicted essentiality of this gene under these conditions. When Mdh was depleted in non-growing cells, the relative effect depended on the presence of oxygen. In stationary phase aerobic cultures, Mdh depletion only modestly

increased the rate of cell death (Figure 2.19). In contrast, Mdh depletion in

hypoxia resulted in a significant increase in cell death. Within four weeks of ATc

addition, the viability of Mdh-DAS mutant cultures had fallen below the limit of

detection (Figure 2.19). To determine if Mdh depletion had a similar effect on

central carbon metabolism as ΔMtPat deletion, we traced the fate of 2-[^{13}C]-

glucose in the Mdh-DAS mutant in the presence and absence of ATc. Under

hypoxic conditions, we found that inhibiting reductive TCA activity via Mdh

depletion increased flux through the oxidative branch of TCA, as measured by

the increased conversion of citrate/isocitrate to the ^{13}C-labeled form (Figure

2.20). These data further support the conclusion that the preferential utilization of

reductive TCA reactions is critical for survival during hypoxia-induced

quiescence.

While the induction of the DosR regulon during growth in the lungs of C57BL/6

mice (Voskuil et al., 2003; Rustad et al., 2008) suggests that respiration is limited

at this site, overtly hypoxic lesions are not observed in this model. To determine if

Mdh is necessary for Mtb survival in the mouse lung despite the absence of

hypoxic lesions, we infected mice with a mixture of wild type Mtb and the Mdh-

DAS mutant, and the relative abundance of these strains was quantified in lung

homogenates by quantitative PCR (Blumenthal et al., 2010). Depletion of Mdh

was initiated either 1 week or 6 weeks after infection by the administration of

doxycycline. In either treatment regime, the viability of the Mdh-DAS strain was

reduced 10^5-10^6 fold upon protein depletion (Figure 2.21).

Figure 2.17. Depletion of targeted knockdown constructs in hypoxia.

Conditional depletion of Mdh and SucD was initiated at day ten of hypoxia using anhydrotetracycline (ATc), and lysates obtained at day eighteen of hypoxia were analyzed via MS multiple-reaction-monitoring (MRM) mode. Abundance of target peptides from Mdh (knockdown), SucD (knockdown) and Icd2 (knockout) strains at day eighteen were normalized to SigA levels and expressed as a percentage of peptide abundance in a control sample.

Target Peptide Abundance (MS)
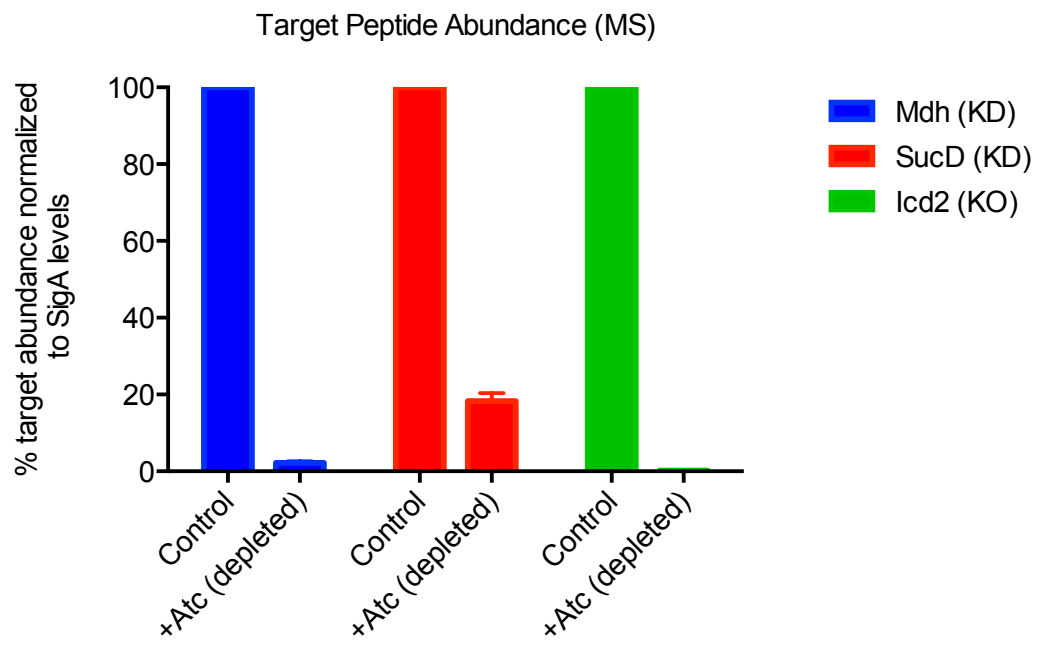
Figure 2.18. Inducible depletion of knockdown targets is sufficient to inhibit the essential activity of the enzymes.

Growth inhibition of induced delpletion of target enzymes was measured by optical density (OD) over eight days. Depletion was initiated by addition of ATc (1 µg/mL) to culture media at day zero. Cultures were grown and measured in triplicate.
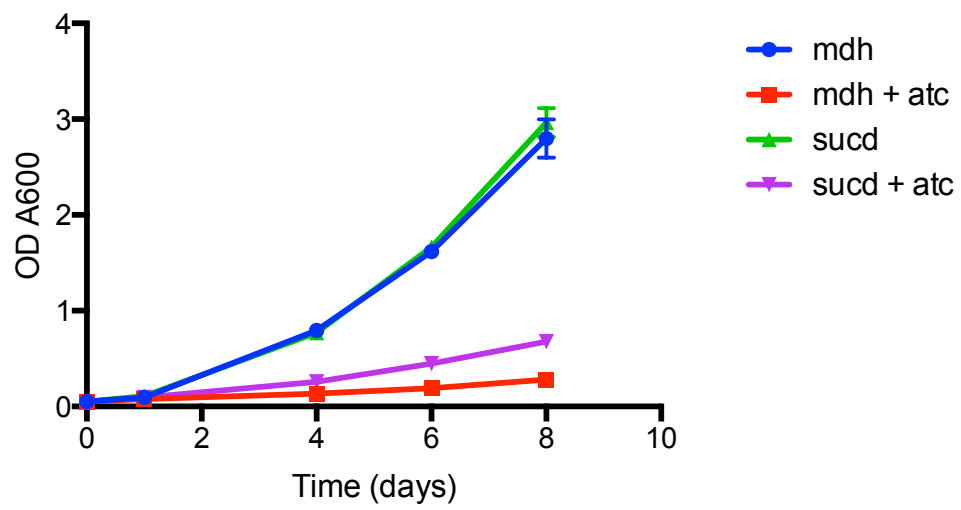
Figure 2.19. Mdh is required for survival in hypoxia.

Knockdown of target enzymes was induced at day ten in hypoxic and aerobic conditions. CFU was enumerated at indicated time points. Limit of detection = 100 CFU (dotted line). Cultures were grown and plated in triplicate for each strain and condition.

Hypoxic

Aerobic/Stationary
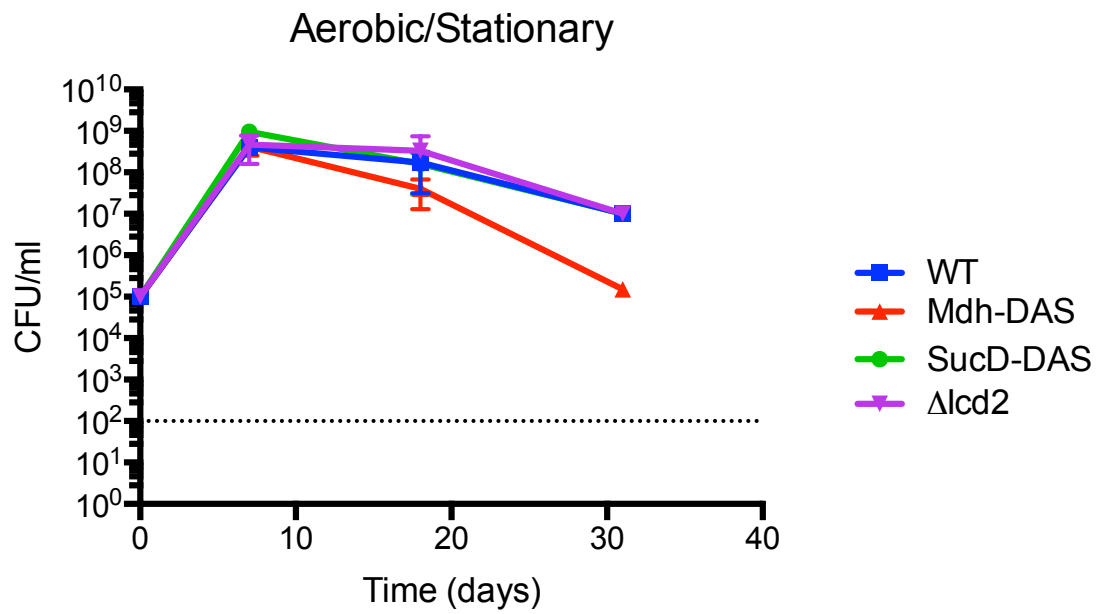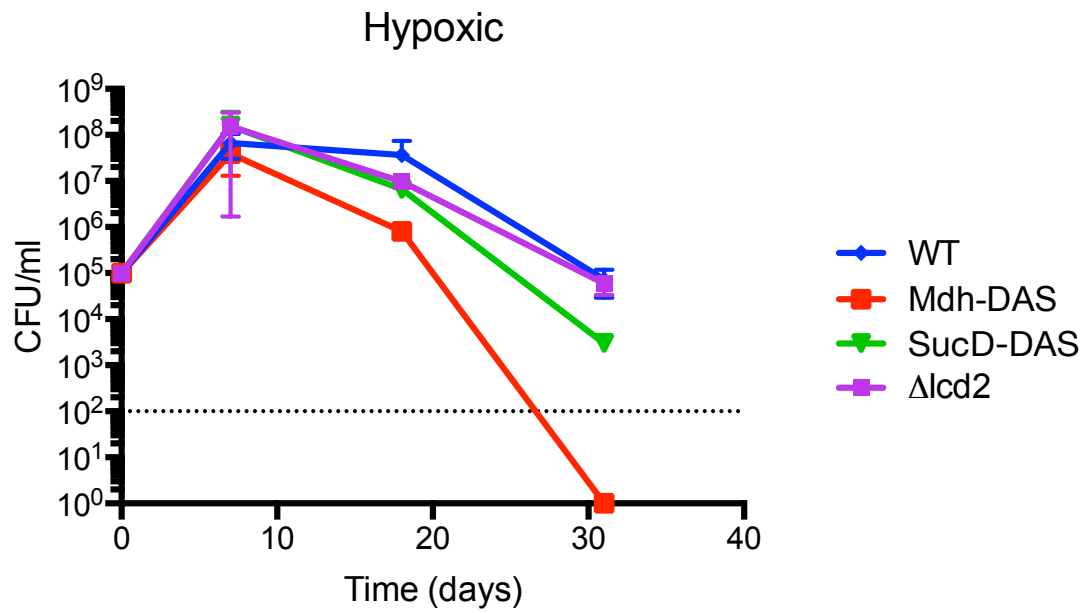
Figure 2.20. Mdh-DAS exhibits oxidative branch cycling in hypoxia.

Metabolic flux tracing of ^{13}C-labeled glucose is incorporated into oxidative

branch metabolites (citrate/isocitrate) in hypoxic Mdh-DAS. Ratio is

determined by percent of ^{13}C labeled carbon (natural abundance of ^{13}C-

citrate/isocitrate is approximately 6%).

^{13}C citrate/isocitrate
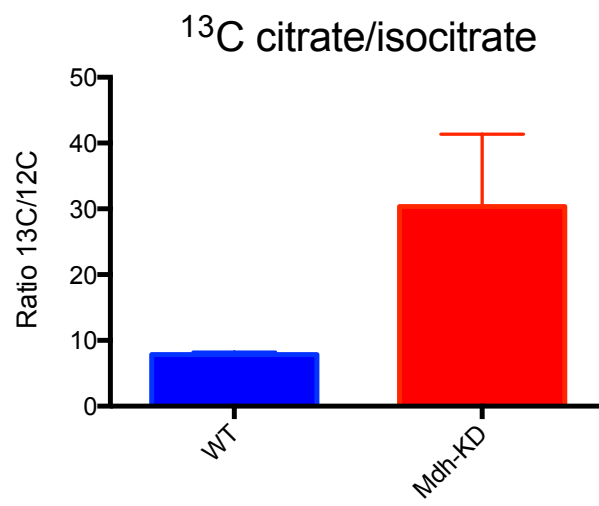
Figure 2.21. Mdh is required in *in vivo* mouse infection.

Aerosol mouse infection (C57BL/6) of pooled, barcoded ("qtag") *M. tuberculosis* strains. Induced depletion of knockdown strains (Mdh-DAS, SucD-DAS) was initiated at week one and week six via doxy chow. For delpletion initiated at week one, lungs were harvested at week three, plated for CFU, and abundance was determined for each strain (WT1, WT2, Mdh-DAS, SucdD-DAS) via qPCR of unique "qtag" barcoded regions (constant:variable). For delpletion initiated at week six, lungs were harvested at week fourteen, plated for CFU, and abundance was determined for each strain (WT1, WT2, Mdh-DAS, SucdD-DAS) via qPCR of unique "qtag" barcoded regions (constant:variable).

Pooled strains infection (C57BL/6)

Week 3

Legend:
- qtag 22 (wt) — blue
- qtag 24 (wt) — red
- qtag 28 (mdh) — green
- qtag 29 (sucD) — purple

Pooled strains infection (C57BL/6)

Week 14

Legend:
- qtag 22 (wt) — blue
- qtag 24 (wt) — red
- qtag 28 (mdh) — green
- qtag 29 (sucD) — purple
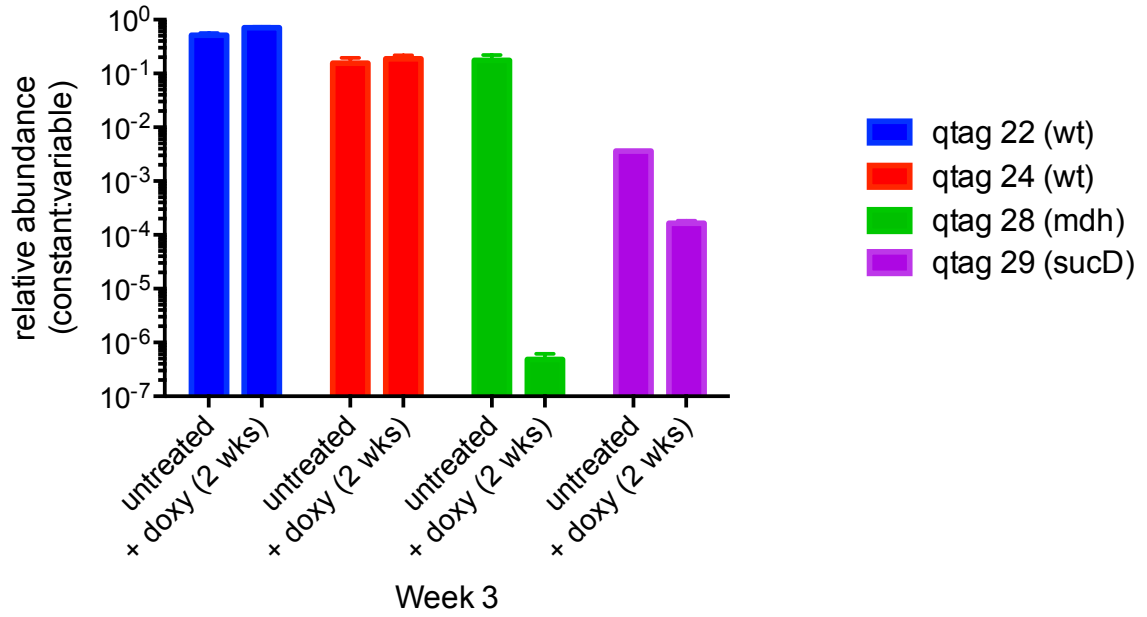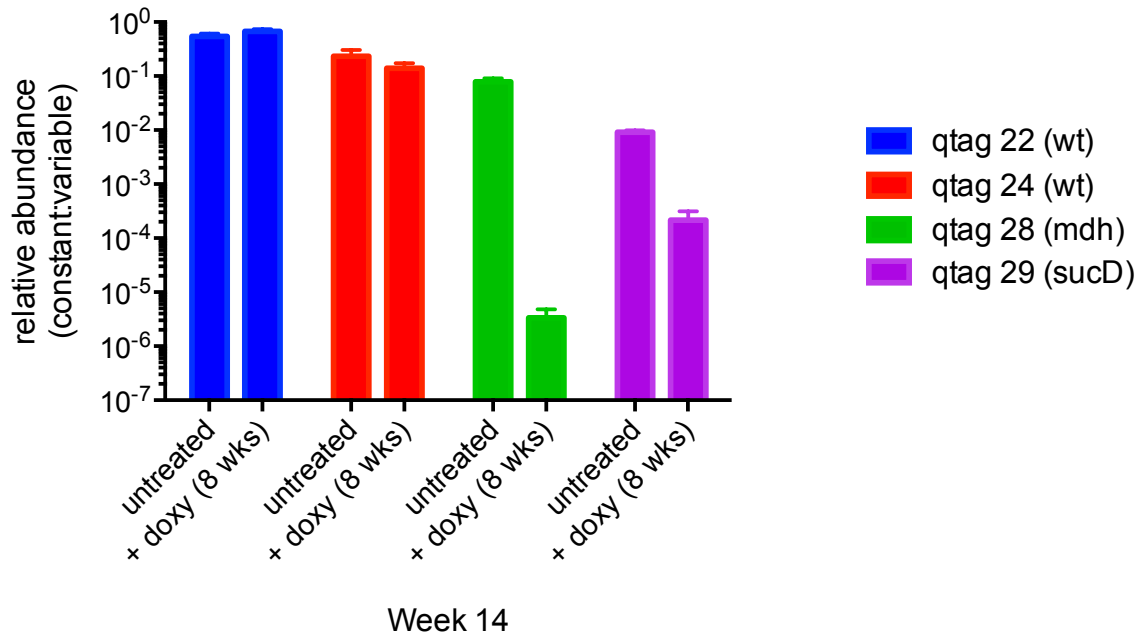
Chemical inhibition of Mdh kills hypoxic *M. tuberculosis*

While the requirement for Mdh in quiescent cells in vitro and in the mouse lung suggest that Mdh inhibition could be therapeutically useful, chemical inhibition of TCA enzymes has proven difficult (Lee et al., 2015). To determine if the Mtb Mdh enzyme is 'druggable' we performed a high-throughput screen for inhibitors. To focus the screen on compounds that are likely to have access to the mycobacterial cytosol, we used a curated library of 3600 compounds that have been shown to inhibit mycobacterial growth in a variety of high-throughput screening efforts (Figure 2.22). We identified three Mdh inhibitors with the properties listed in Table 2.1. The most potent Mdh inhibitor, Compound A (CHEM ID # 5104073), was selected for further testing in intact Mtb (Figure 2.23).

To determine if this compound's growth inhibitory activity was related to Mdh inhibition in the intact cell, we determined if genetic depletion of Mdh altered susceptibility to this compound (Franzblau et al., 1998). Since Mdh knockdown is lethal by itself, we performed a 'checkerboard' analysis in which doses of the putative Mdh inhibitor and ATc were cross-titered to allow the effect of partial inhibition to be assessed. Using this scheme, we identified synergy between ATc and the Mdh inhibitor, such that the Mdh-depleted strain was hypersensitive to a

0.5x MIC concentration of Mdh inhibitor (Figure 2.24). Both the in vitro inhibition

of Mdh by this compound and the chemical-genetic synergy observed between it

and Mdh-depletion, suggest that Mtb growth inhibition is at least partially

dependent upon Mdh inhibition.

To determine if chemical Mdh inhibition could mimic genetic Mdh depletion we

compared the activity of the Mdh inhibitor with the mycolic acid inhibitor,

isoniazid, in hypoxic culture. Each compound was added after 10 days of hypoxic

culture and every seven days thereafter. Over the treatment period, isoniazid had

a minimal effect on the viability of quiescent Mtb, as previously shown for this

compound and other cell wall inhibitors. In contrast, Mdh inhibition had a similar

effect as Mdh protein depletion, killing 99% of Mtb after 21 days of treatment and

reducing viability beyond the limit of detection after 35 days (Figure 2.25).

Furthermore, compound treated cells were overreduced (Figure 2.26). These

data indicate that chemical inhibition of reductive TCA in general, and Mdh in

particular, may be an effective strategy for killing quiescent bacteria and

accelerating TB therapy (Figure 2.27).

Figure 2.22. High throughput screen for Mdh inhibition assay.

Assay condition: 100mM HEPES, 50mM KCl, pH7.5, 100 µM OAA, 250 µM

NADH and 0.25nM Mdh. Read fluorescent decrease of NADH (Ex: 340nm Em:

460nm). Screened compounds: 3653 (i3321 of them have showed in vitro

whole cell activity). Active compounds identified: 3.

s-malate   NAD$^+$ NADH+ H$^+$ oxaloaceteate
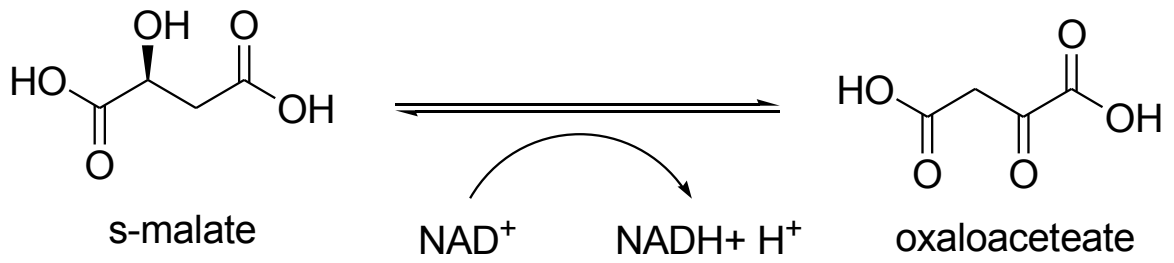
K_m of OAA=49μM; K_m of NADH=48.8 μM

Table 2.1. Potential inhibitors of Mdh

Compound	A	B	C
IC_{50} (uM)	15	15	37.5
MIC_{99} for *M. Smegmatis* in 7H9 dextrose (uM)	ND	>100	>100
MIC_{99} for *M. Smegmatis* in 7H9 acetate (uM)	ND	25	>100
MIC_{99} for *mc^2 7000* in 7H9 dextrose (uM)	ND	ND	>100
MIC_{99} for *mc^2 7000* in M9 acetate (uM)	20*	25	>100

* Dual carbon sources: acetate and dextrose

Figure 2.23. Structure of "Compound A" (CHEM ID #5104073).
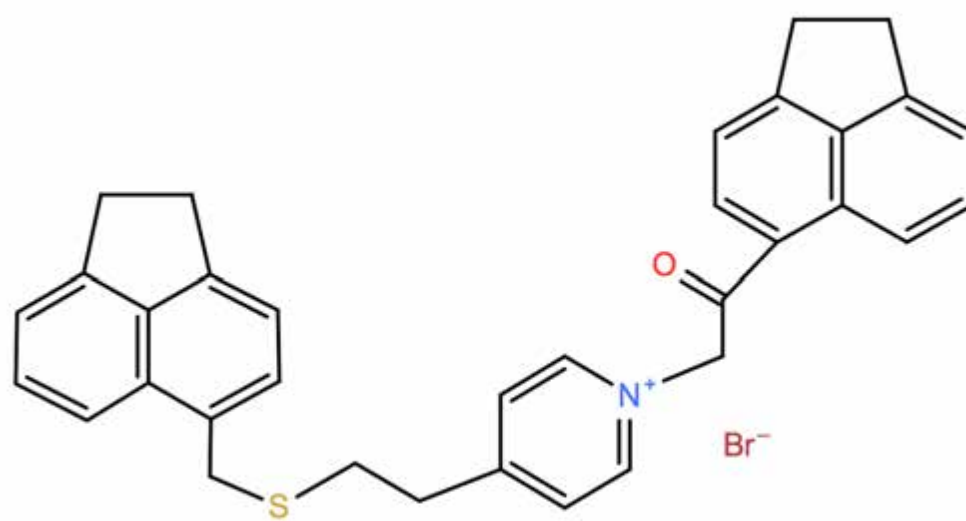
Figure 2.24. Mdh-DAS is hypersensitive to sub-MIC "Compound A".

WT, Mdh-DAS, and SucD-DAS strains were treated with 0 µM, 10 µM (0.5x

MIC), 20 µM (1x MIC), or 40 µM (2x MIC) in the presence of ATc in triplicate.

Viability was determined by reduction of alamarBlue measured via

fluorescence intensity.
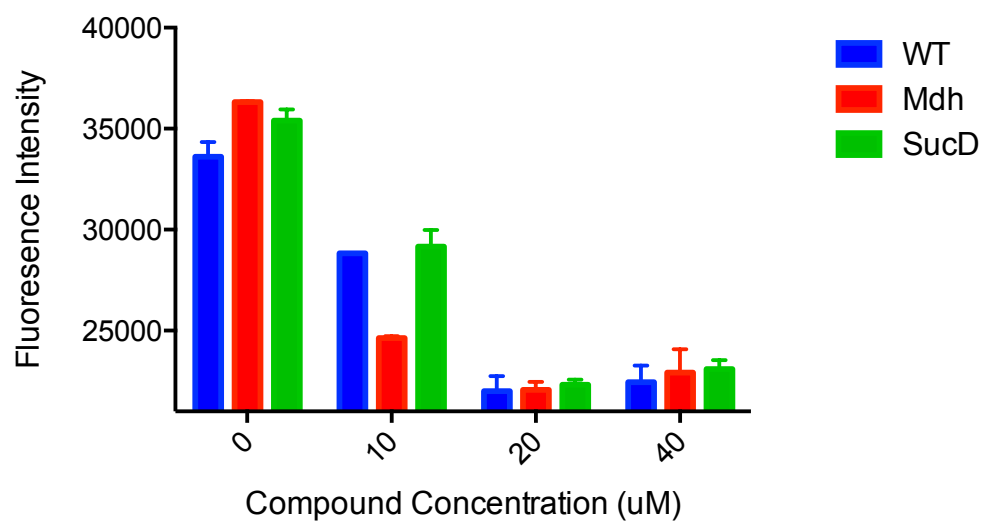
Figure 2.25. "Compound A" reduces hypoxic CFU *in vitro*.

Compound A (40 µM), isoniazid (INH) (2 µg/mL), and Compound A and INH in combination were added to hypoxic cultures of WT H37Rv every seven days starting at day ten as indicated. Cultures were grown in triplicate and CFU were enumerated at indicated time points. Limit of detection = 100 CFU (dotted line).

Hypoxia Survival
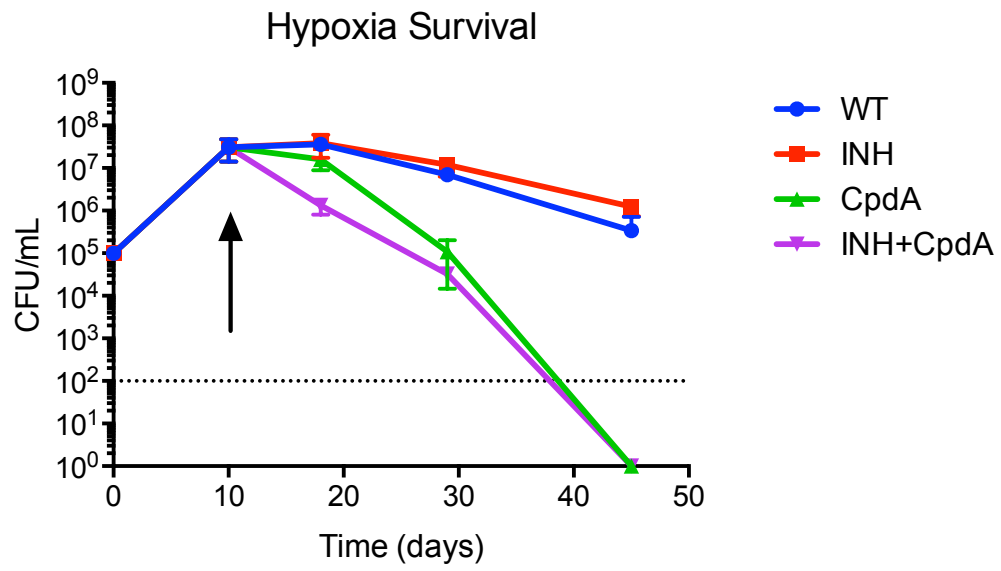
Figure 2.26. "Compound A" treated hypoxic cells are overreduced.

NADH was quantified from WT and treated lysates at day twenty-four of hypoxia (i.e. fourteen days of drug treatment). Cultures were measured in triplicate and values were normalized to CFU at the indicated time point.

NADH in hypoxia

Acknowledgements

Chapter III. Discussion

Our study confirms and extends the metabolic changes that occur as Mtb adapts to the quiescent state under hypoxic conditions. We show that MtPat is responsible for the coordinated inhibition of both oxidative TCA and beta-oxidation, and that this is critical for regeneration of NAD+ in the absence of oxidative phosphorylation. In conjunction with previous studies, these results suggest the presence of a multi-step metabolic adaption that is necessary for long-term survival in hypoxia (Figure 3.1).

The immediate response to hypoxia is DosR induction and triglyceride (TG) synthesis, which was shown to be important for the initial growth arrest of the bacterium. Inhibiting TG synthesis by deleting Tgs1 resulted in continued growth and metabolic activity in hypoxia and increased sensitivity to a number of antibiotics (Baek et al., 2011). In this study, we found a number of metabolites accumulate in hypoxia that suggest additional carbon storage pathways. The accumulated fatty acids may be a component of the same cytosolic lipid bodies that harbor TG, and the maltose oligomers indicate the accumulation of glycogen. While inhibiting Tgs1 does potentiate antibiotic activity somewhat (Baek et al., 2011), the presence of multiple carbon storage pathways may undermine efforts to target characterized carbon storage pathways to accelerate drug treatment.

Both DosR activation and Tgs1 expression is transient, and the subsequent adaptation to hypoxia depends, at least in part, on cAMP. The cAMP system in mycobacteria is complex and poorly understood (McDonough and Rodriguez, 2011). *M. tuberculosis* is predicted to encode sixteen adenylate cyclases in its genome, while *E. coli*, for comparison, only has one (Shenoy and Visweswariah, 2006). Additionally, *M. tuberculosis* is predicted to have ten cNMP-binding proteins, and a recent report suggests even more may exist that contain non-canonical cNMP-binding domains (Bai et al., 2011; Banerjee et al., 2015). In this study, we identified one cAMP-binding protein, MtPat that was important for surviving the hypoxic state. It is likely that *M. tuberculosis* relies on its abundance of adenylate cyclases to sense and produce a cAMP signal depending on a variety of stresses encountered in the host, such as hypoxia, pH, low iron, nutritional limitation, etc. For example, one characterized adenylate cyclase, Rv1626, is activated by low pH (Tews et al., 2005). Mutations in one AC, Rv1625c/Cya caused a significant survival defect, but this phenotype was much less severe than that seen for MtPat. We speculate that the multitude of ACs encoded by *M. tuberculosis* may be able to compensate for one another. Alternatively, alterations in free cAMP levels may also be controlled by the amount of cAMP bound to or released by Rv1636, a recently described cAMP "buffer" protein (Banerjee et al., 2015).

MtPat has previously been shown to acetylate acetyl-CoA synthase (Acs) and ten beta-oxidative fatty acid ligases (FadDs) *in vitro* (Xu et al., 2011; Nambi et al., 2013). Both Acs and beta-oxidative FadDs produce acetyl-CoA as end products, which suggest a cohesive role for MtPat in regulating acetyl-CoA availability and metabolism. Furthermore, we have shown that restricting fatty acid metabolism rescues hypoxic ΔMtPat, which suggests MtPat inhibits beta-oxidation in hypoxia and that the maintenance of NAD+/NADH homeostasis via the coordinated control of oxidative reactions is important for survival. While MtPat mediated inhibition of fatty acid catabolism can be attributed to known targets, such as FadD proteins and Acs, the mechanism by which it controls oxidative TCA activity remains unclear. Acetyl-proteomic studies in other bacteria have identified a number of potential targets for regulatory acetylation that could mediate these effects, such as pyruvate dehydrogenase complex, isocitrate dehydrogenase and alpha-ketoglutarate dehydrogenase (Zhang et al., 2009).

The result of MtPat activation is an inhibition of oxidative carbon metabolism, and preferential use of the reductive TCA reactions described previously (Watanabe et al., 2011; Eoh and Rhee, 2013). While all of the enzymes necessary for the conversion of glycolytic carbon to succinate via this fermentation pathway have not been defined, the one clearly non-redundant reaction is mediated by Mdh. Depletion of Mdh killed Mtb within hypoxia and mouse lung. While there is no hypoxia in mouse lung, we think the combination of NO, CO, low pH, and low

iron is likely creating a similarly respiratory limited environment.

We were able to show that a small molecule compound could chemically inhibit Mdh and this inhibition led to robust depletion of CFU. These studies provide proof of the concept that interfering with the pathways necessary for survival in the absence of replication could accelerate the eradication of Mtb. The structure for *M. tuberculosis* Mdh has been solved (Ferraris et al., 2015), and while it is similar to the human Mdh ortholog, there are sufficient structural differences that can be exploited in order to engineer a compound that is specific to *M. tuberculosis* Mdh (Figure 3.2). Therefore, we have shown that understanding active components of quiescence metabolism -- MtPat, Mdh -- are effective targets for treating this heretofore difficult to treat disease state.

Figure 3.1. Summary.

An increase in cAMP in hypoxic *M. tuberculosis* activates a cAMP-protein

lysine acetyltransferase, MtPat (Rv0998), which inhibits fatty acid catabolism

resulting in reduced availability of acetyl-CoA to oxidative TCA. Flux through

the reductive branch of TCA is essential in hypoxia, and genetic and chemical

inhibition of Mdh in hypoxia results in cell death.

Hypoxic Metabolic Remodeling
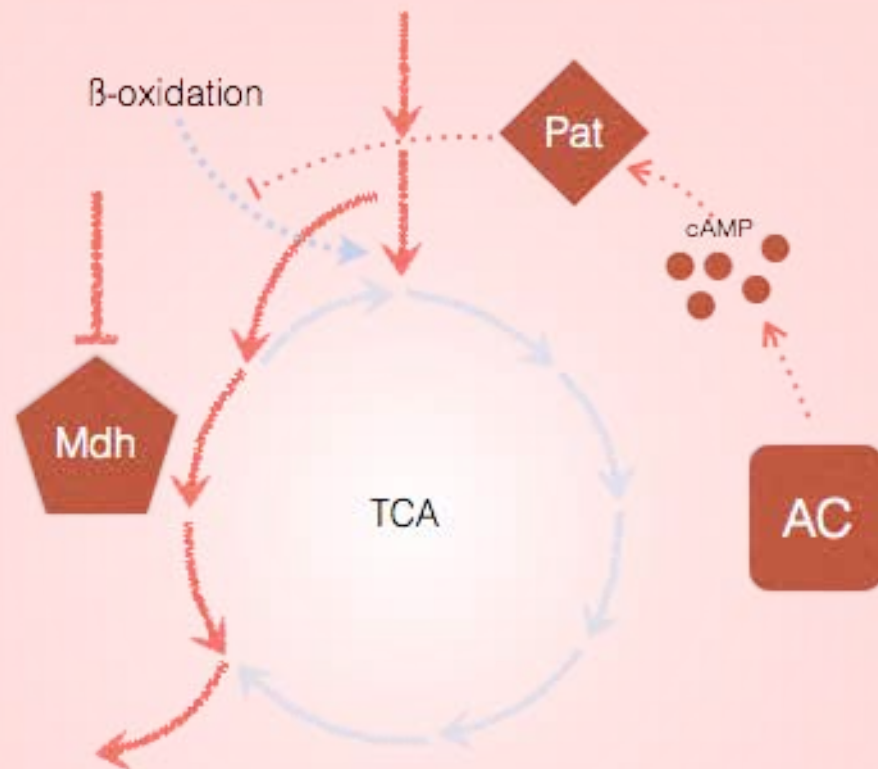
Figure 3.2. Structural comparison of Mtb Mdh and Human Mdh.

M. tuberculosis Mdh (top query) and human Mdh (bottom query) share a

17.56% structural identity and 27.98% structural similarity. Alignment based on

the jFATCAT_rigid algorithm (Ye and Godzik, 2003; Prlić et al., 2010).

```
P-value: 6.66e-15
Equ: 302
RMSD: 2.48
Score: 609.33
Align-len: 336
Gaps: 34 (10.12%)

Identity: 17.56%
Similarity: 27.98%

5:A              20:A                    40:A               60:A
 |      |     .     |      .     |      .     |      .     |      .     |
PLKVAVTGAAGQIGYSLLFRLASGSLLGPDRPIELRLLEIEPALQALEGVVMELDDCAFPLLSGVEIGSD
..||||.||.|.||..|...|...        .....|.|.:|    ....||..:|. .............
NAKVAVLGASGGIGQPLSLLLKNS------PLVSRLTLYDI-----AHTPGVAADLS-HIETKAAVKGYLGP
 |      |     .     |      .           |      .     |      .     |      .
6:A              20:A                       40:A               60:A


      80:A              100:A              120:A              140:A
  .      |     .     |      .     |      .     |      .     |      .     |
--PQKIFDGVSLALLVGARPRGAGMERSDLLEANGAIFTAQGKALNAVAADDVRVGVTGNPANTNALIAM
......|.....:....||..||.|.|.||...|..|......|......:  ..:.|..||.|....|..
EQLPDCLKGCDVVVIPAGVPRKPGMTRDDLFNTNATIVATLTAACAQHCPE-AMICVIANPVNSTIPITA
    |      .     |      .     |      .     |      .     |      .     |
            80:A              100:A              120:A


              160:A              180:A              200:A
  .      |     .     |      .     |      .     |      .     |      .
TNAP---DIPRERFSALTRLDHNRAISQLAAKTGAAVTDIKKMTIWGNHSAT-QYPDLFHAEVAGKNAAE
....    .....:....|.||..||....|...|....:. ..:.|.|... ..|.:......      .
EVFKKHGVYNPNKIFGVTTLDIVRANTFVAELKGLDPARVN-VPVIGGHAGKTIIPLISQCTP------K
 .      |     .     |      .     |      .     |      .     |      .
       140:A              160:A              180:A


          220:A              240:A              260:A
  |      .     |      .     |      .     |      .     |      .     |
VVNDQAWIEDEFIPTVAKRGAAIIDARG--ASSAASAASATIDAARDWLLG--TPADDWVSMAVVSDGSY
|...|..:.  .....:...|..::.|:.  .|...|.|.|..........  ...........|.|..
VDFPQDQLT-ALTGRIQEAGTEVVKAKAGAGSATLSMAYAGARFVFSLVDAMNGKEGVVECSFVKSQE--
 |      .     |      .     |      .     |      .     |      .     |
  200:A              220:A              240:A              260:A


   280:A              300:A              320:A
  .     |      .     |      .     |      .     |      .
GVPEGLISSFPVTTKGGNW-TIVSGLEIDEFSRGRIDKSTAELADERSAVTELGLI
.....  .|.|..........  .......:..|....|.....||............
-TECTY-FSTPLLLGKKGIEKNLGIGKVSSFEEKMISDAIPELKASIKKGEDFVKT
 .      |     .     |      .     |      .     |      .
          280:A              300:A


        | ... Structurally equivalent and identical residues
        : ... Structurally equivalent and similar residues
        . ... Structurally equivalent, but not similar residues.
```

Appendix

Table 4.1. Hypoxic-dependent metabolomic profiling.

"Ratio Hypoxic/Aerobic" = relative abundance of metabolite in hypoxia / relative abundance of metabolite in aerobic conditions
"P-Value" = calculated using student t-test on quadruplicate samples

BIOCHEMICAL	Ratio Hypoxic/Aerobic	P-Value
1-octadecanol	1.2750	0.010004593
1-palmitoylglycerophosphoinositol*	0.1927	0.000813584
1-stearoylglycerol (1-monostearin)	1.2555	0.645006280
2-aminoadipate	1.2373	0.162577251
2-aminobutyrate	1.1605	0.429311377
2-isopropylmalate	0.1075	0.000001267
2-pyrrolidinone	0.7050	0.092559601
2'-deoxyadenosine	1.0000	
3-phosphoglycerate	4.4313	0.055642110
4-acetamidobutanoate	2.2282	0.053012805
4-hydroxybutyrate (GHB)	8.0364	0.007474693
5-methylthioadenosine (MTA)	0.2077	0.000004099
5-oxoproline	0.4524	0.000586128
7-alpha-hydroxycholesterol	1.0745	0.141148658
7-beta-hydroxycholesterol	1.0000	
acetyl CoA	1.9494	0.008398702
adenine	0.3450	0.000858261
adenosine	0.1596	0.000573986
adenosine 3'-monophosphate (3'-AMP)	0.6697	0.103490198
adenosine 3',5'-cyclic monophosphate (cAMP)	3.8423	0.004831917
adenosine 5'-monophosphate (AMP)	0.3167	0.000115237
adenosine 5'diphosphoribose	1.0000	
adenosine-5'-diphosphoglucose	0.3467	0.023085001
alanine	0.4819	0.000138738
alanylalanine	1.2840	0.387935532
alpha-ketoglutarate	2.9152	0.086027272
alpha-tocopherol	1.3516	0.335355311
arachidate (20:0)	1.4392	0.003514474
arginine	0.2404	0.000010581
asparagine	1.0000	
aspartate	0.4004	0.000004328
beta-alanine	0.7247	0.278815341

beta-hydroxyisovalerate	1.1444	0.278244812
beta-methyllevulinate	1.1392	0.294965515
betaine	0.1241	0.000000001
cadaverine	1.0000	
caproate (6:0)	1.4186	0.248645108
caprylate (8:0)	1.0195	0.905932890
cholesterol	1.0000	
cis-aconitate	6.5739	0.000002728
citrate	33.7999	0.000000473
citrulline	0.2886	0.000005208
cysteine	0.8226	0.639627073
diaminopimelate	0.2369	0.000040453
dihydroxyacetone phosphate (DHAP)	0.3184	0.157122942
diisopropanolamine	1.6753	0.158475072
eicosenoate (20:1n9 or 11)	8.1845	0.007320390
flavin adenine dinucleotide (FAD)	0.2979	0.000046093
flavin mononucleotide (FMN)	0.7714	0.000164632
fructose	0.7926	0.415201016
fructose-6-phosphate	0.4033	0.000146366
fumarate	0.8344	0.064609902
gamma-aminobutyrate (GABA)	0.7544	0.139379235
gamma-glutamyl-2-aminobutyrate	0.3569	0.000186826
gamma-glutamylalanine	0.3720	0.000189911
gamma-glutamylglutamate	1.1399	0.445853510
gamma-glutamylglutamine	0.2965	0.000112181
gamma-glutamylisoleucine*	0.3167	0.000088186
gamma-glutamylleucine	0.3550	0.000202000
gamma-glutamylmethionine	0.1724	0.000002573
gamma-glutamylphenylalanine	0.5084	0.013786352
gamma-glutamylthreonine*	0.2777	0.000018177
gamma-glutamyltyrosine	0.6930	0.114399161
gamma-glutamylvaline	0.1807	0.000000561
GDP-mannose	2.9603	0.022401943
glucose	1.1367	0.218631151
glucose 1-phosphate	0.5113	0.021943436
glucose-6-phosphate (G6P)	0.3128	0.000057624
glutamate	0.2231	0.000001958
glutamate, gamma-methyl ester	0.4239	0.002668751
glutamine	0.3374	0.000038355
glycerate	0.9804	0.917806752
glycerol	1.4817	0.028428205
glycerol 2-phosphate	0.2149	0.000001564
glycerol 3-phosphate (G3P)	0.1340	0.000000008
glycerophosphorylcholine (GPC)	0.2254	0.000042091
glycine	0.2814	0.000143861

glycolate (hydroxyacetate)	1.1467	0.409844006
guanosine	1.3437	0.212345834
guanosine 5'- monophosphate (GMP)	0.3916	0.095694729
histidine	1.0264	0.916443983
homoserine	0.3413	0.015010320
inosine	1.0845	0.588772492
inositol 1-phosphate (I1P)	0.5126	0.001615975
Isobar: fructose 1,6-diphosphate, glucose 1,6-diphosphate	1.0127	0.938953105
Isobar: ribulose 5-phosphate, xylulose 5-phosphate	0.3295	0.002534627
isoleucine	0.4402	0.000064794
leucine	0.4848	0.000528007
linoleamide (18:2n6)	0.2548	0.086201203
linoleate (18:2n6)	1.9745	0.000001287
lysine	0.5299	0.001020144
malate	1.1058	0.302271196
malitol	4.6168	0.006547860
maltose	2.9322	0.009397942
maltotetraose	0.5551	0.046188245
maltotriose	1.1812	0.414358832
mannose	0.3816	0.000299511
mannose-1-phosphate	0.2129	0.000000773
mannose-6-phosphate	0.3399	0.000099249
margarate (17:0)	1.4893	0.006515264
methylphosphate	0.1155	0.119725771
methylsuccinate	0.4694	0.015492167
mycothione (MSSM)*	0.4294	0.000284995
myo-inositol	0.4310	0.000046217
myristate (14:0)	0.9411	0.502310756
N-6-trimethyllysine	1.6970	0.086106062
N-acetylglutamate	0.1915	0.001173212
N-acetylornithine	13.9076	0.001563377
n-Butyl Oleate	0.6577	0.258382263
N2-acetyllysine	1.4292	0.084569726
N6-acetyllysine	1.0263	0.866137067
nicotinamide adenine dinucleotide (NAD+)	0.2486	0.000001676
nicotinate	0.2762	0.000224946
nicotinate ribonucleoside*	0.3350	0.005414823
nicotinic acid mononucleotide (NaMN)	0.2110	0.000011843
O-acetylhomoserine	0.4415	0.000274634
oleamide	0.2969	0.066537598
oleate (18:1n9)	2.2505	0.000025901
ornithine	0.5867	0.001865578
palmitate (16:0)	0.9616	0.377259423
pantothenate	0.2161	0.000028308

pentadecanoate (15:0)	1.1171	0.086609671
phenylalanine	1.1129	0.592178077
phosphate	1.7699	0.001973597
pipecolate	0.7986	0.494987747
proline	0.2410	0.000005216
pyruvate	1.5097	0.028969869
ribose 5-phosphate	1.4781	0.355917684
S-adenosylhomocysteine (SAH)	0.2035	0.000001464
sedoheptulose-7-phosphate	0.4571	0.000177267
serine	0.3686	0.000044288
sorbitol	3.5214	0.023860615
stearate (18:0)	0.9900	0.865386426
succinate	0.2874	0.000036198
succinyl CoA	1.7079	0.140596777
threonine	0.1294	0.000000291
thymidine 5'-monophosphate	0.2599	0.000308292
trehalose	1.0891	0.541711278
trehalose 6-phosphate	0.1628	0.006365764
triethyleneglycol	0.9731	0.789545082
tryptophan	0.5933	0.005209362
tyrosine	0.6995	0.077677710
valine	0.3018	0.000005388
X - 02973	0.5506	0.003283806
X - 03094	0.8145	0.043294197
X - 04033	8.7237	0.015157693
X - 04044	0.8697	0.058128617
X - 04768	1.8307	0.012026906
X - 05407 - retired for 2,3-dihydroxyisovalerate	1.2072	0.086218191
X - 05437	0.5604	0.005968419
X - 06346 - retired for isoproturon	1.2426	0.346685166
X - 07887- retired for p-toluic acid	1.0585	0.573374023
X - 08754	0.2044	0.000006017
X - 08889	1.2427	0.485254859
X - 08988	0.8283	0.734434555
X - 10821 - retired for gamma-glutamylmethionine	0.0433	0.000007111
X - 10889	0.2303	0.000107866
X - 11011 - retired for 2-methylcitrate	0.7148	0.330074809
X - 11251	1.2961	0.011463773
X - 11297	0.6385	0.097424806
X - 11391	1.1097	0.092179609
X - 11394	1.0339	0.378431842
X - 11395	0.9593	0.689867241
X - 11404	1.0246	0.712704435
X - 11406_200	0.4812	0.355917684
X - 11453	1.2121	0.314669108

X - 11455	1.3597	0.112664688
X - 11456 - retired for tetraethylene glycol	1.1740	0.184916742
X - 11457	1.1592	0.044274550
X - 11461	1.3061	0.004517783
X - 11509	3.0601	0.000066355
X - 11533	0.9282	0.153747050
X - 11550	0.5011	0.000027172
X - 11568 - retired for ergothioneine	0.0278	0.000000013
X - 11687_200	2.8933	0.023689277
X - 11730- retired for 17-methylstearate	3.1402	0.000279737
X - 11795	11.5222	0.002818278
X - 11809	0.5619	0.015358099
X - 11840	0.9875	0.918523786
X - 11875	0.8357	0.139495515
X - 11910	1.1954	0.081907611
X - 12051	0.1579	0.000041817
X - 12660	0.1208	0.000012793
X - 12776	1.2209	0.046586001
X - 12805	0.9535	0.667743217
X - 12889_201	0.0722	0.000000000
X - 13005	0.6470	0.017832251
X - 13093	1.5596	0.574092317
X - 13149	1.3345	0.003093639
X - 13168	1.0000	
X - 13183 - retired for stearamide	0.5912	0.217364956
X - 13548	1.0990	0.285006083
X - 13549	1.0507	0.609667748
X - 13645	1.0000	
X - 13672	1.2742	0.053370122
X - 13737	0.4223	0.000321245
X - 13828	0.8855	0.495973254
X - 13872	0.5563	0.004082046
X - 14318	1.0000	
X - 14359	0.1788	0.000020884
X - 14568	1.3020	0.004982376
X - 14575	4.1950	0.000343660
X - 14588	2.2485	0.004081221
X - 14955	1.7146	0.066359291
X - 15138	0.7239	0.012575161
X - 15177	0.3538	0.000331370
X - 15261 - retired for 2-methylcitrate	1.0000	
X - 15279	0.8442	0.235179536

Table 4.2. Conditionally Essential Genes Underrepresented at Week Three of Hypoxia Versus Input Library (IvH3).

Gene Number	Gene Name	Log2 Fold Change	P Val. (resampling)
Rv1069c	-	-4.8575	0.0004
Rv3680	-	-4.7476	0.0004
Rv3133c	dosR	-4.5473	0.0004
Rv2179c	-	-3.8493	0.0004
Rv3720	-	-3.0884	0.0004
Rv0204c	-	-2.7567	0.0004
Rv2869c	rip	-2.7228	0.0004
Rv3849	espR	-2.6390	0.0004
Rv3270	ctpC	-2.4333	0.0004
Rv1432	-	-2.3675	0.0004
Rv2381c	mbtD	-2.1842	0.0004
Rv3810	pirG	-2.0850	0.0004
Rv2386c	mbtI	-2.0843	0.0032
Rv2535c	pepQ	-2.0603	0.0004
Rv3210c	-	-1.9555	0.0004
Rv3024c	trmU	-1.9549	0.0004
Rv1170	mshB	-1.9153	0.0004
Rv0135c	-	-1.8953	0.0004
Rv2115c	mpa	-1.8819	0.0032
Rv2384	mbtA	-1.8679	0.0004
Rv0821c	phoY2	-1.8580	0.0004
Rv2383c	mbtB	-1.8315	0.0004
Rv0361	-	-1.8253	0.0004
Rv2379c	mbtF	-1.8236	0.0004
Rv0470c	pcaA	-1.8152	0.0004
Rv2031c	hspX	-1.8005	0.0004
Rv2380c	mbtE	-1.6252	0.0004
Rv2051c	ppm1	-1.6009	0.0004
Rv1178	-	-1.5796	0.0004
Rv0344c	lpqJ	-1.5436	0.0004

Table 4.3. Conditionally Essential Genes Overrepresented at Week Three of Hypoxia Versus Input Library (IvH3).

Gene Number	Gene Name	Log2 Fold Change	P Val. (resampling)
Rv3484	cpsA	1.5272	0.0004

Table 4.4. Conditionally Essential Genes Underrepresented at Week Six of Hypoxia Versus Input Library (IvH6).

Gene Number	Gene Name	Log2 Fold Change	P Val. (resampling)
Rv1069c	-	-5.9379	0.0002
Rv0361	-	-5.7894	0.0002
Rv2031c	hspX	-5.3831	0.0002
Rv2869c	rip	-4.9620	0.0002
Rv3133c	dosR	-4.8122	0.0002
Rv1712	cmk	-4.7855	0.0002
Rv2384	mbtA	-4.6212	0.0002
Rv3261	fbiA	-4.3418	0.0002
Rv2179c	-	-4.2293	0.0002
Rv2383c	mbtB	-4.0530	0.0002
Rv2115c	mpa	-4.0384	0.0002
Rv1432	-	-3.8820	0.0002
Rv0561c	-	-3.8623	0.0002
Rv0007	-	-3.8120	0.0002
Rv3274c	fadE25	-3.7889	0.0002
Rv2379c	mbtF	-3.7030	0.0002
Rv3193c	-	-3.6257	0.0002
Rv3849	espR	-3.5857	0.0017
Rv2381c	mbtD	-3.5797	0.0002
Rv2563	-	-3.5323	0.0002
Rv2382c	mbtC	-3.5236	0.0002
Rv0248c	-	-3.4902	0.0002
Rv0127	mak	-3.4007	0.0002
Rv0204c	-	-3.3985	0.0002
Rv0998	MtPat	-3.3748	0.0002
Rv2623	TB31.7	-3.3700	0.0002
Rv3160c	-	-3.3584	0.0002
Rv1791	PE19	-3.3413	0.0002
Rv3283	sseA	-3.2967	0.0002
Rv0247c	-	-3.2641	0.0002
Rv3574	kstR	-3.2366	0.0002
Rv0407	fgd1	-3.2079	0.0002
Rv2241	aceE	-3.0503	0.0002
Rv0470c	pcaA	-3.0423	0.0002
Rv3680	-	-3.0312	0.0002
Rv1626	-	-3.0307	0.0002

Rv2553c	-	-3.0126	0.0017
Rv3270	ctpC	-3.0037	0.0002
Rv2386c	mbtI	-2.9984	0.0002
Rv2989	-	-2.8756	0.0002
Rv2140c	TB18.6	-2.8731	0.0002
Rv0436c	pssA	-2.8724	0.0002
Rv2380c	mbtE	-2.8710	0.0002
Rv3720	-	-2.8691	0.0002
Rv1823	-	-2.8633	0.0002
Rv0757	phoP	-2.8460	0.0002
Rv2170	-	-2.8368	0.0002
Rv3810	pirG	-2.8106	0.0002
Rv2051c	ppm1	-2.7740	0.0002
Rv3220c	-	-2.7419	0.0002
Rv0249c	-	-2.7103	0.0002
Rv1287	-	-2.6170	0.0002
Rv1592c	-	-2.6134	0.0002
Rv2091c	-	-2.5880	0.0002
Rv0821c	phoY2	-2.5782	0.0002
Rv1212c	glgA	-2.5432	0.0002
Rv1908c	katG	-2.5380	0.0002
Rv2535c	pepQ	-2.5360	0.0002
Rv0554	bpoC	-2.5128	0.0002
Rv0994	moeA1	-2.4421	0.0002
Rv1824	-	-2.4131	0.0002
Rv3433c	-	-2.4048	0.0002
Rv3256c	-	-2.3736	0.0002
Rv3207c	-	-2.3405	0.0002
Rv0758	phoR	-2.3014	0.0002
Rv2030c	-	-2.2870	0.0002
Rv0135c	-	-2.2643	0.0002
Rv2404c	lepA	-2.1605	0.0002
Rv1860	apa	-2.1522	0.0002
Rv3024c	iscS	-2.1400	0.0002
Rv1345	mbtM	-2.0732	0.0002
Rv3600c	-	-2.0541	0.0002
Rv2859c	-	-2.0054	0.0002
Rv1473	-	-1.9806	0.0002
Rv2378c	mbtG	-1.9773	0.0031
Rv3236c	kefB	-1.9225	0.0002
Rv1078	pra	-1.8989	0.0002

Rv0324	-	-1.8914	0.0002
Rv2171	lppM	-1.8815	0.0002
Rv3132c	dosS	-1.8678	0.0002
Rv3664c	dppC	-1.8552	0.0002
Rv0066c	icd2	-1.8224	0.0031
Rv2672	-	-1.7974	0.0002
Rv1170	mshB	-1.7955	0.0002
Rv1178	-	-1.7671	0.0002
Rv3068c	pgmA	-1.7581	0.0002
Rv0945	-	-1.7542	0.0017
Rv2737c	recA	-1.7461	0.0002
Rv1538c	ansA	-1.7320	0.0002
Rv1112	-	-1.7141	0.0002
Rv0472c	-	-1.7054	0.0002
Rv1013	pks16	-1.7018	0.0002
Rv1070c	echA8	-1.6732	0.0002
Rv2733c	-	-1.6574	0.0002
Rv2363	amiA2	-1.5768	0.0002
Rv2006	otsB1	-1.5561	0.0002
Rv1565c	-	-1.5550	0.0002
Rv2795c	-	-1.5277	0.0002
Rv3223c	sigH	-1.5209	0.0002
Rv2583c	relA	-1.5203	0.0002
Rv2224c	caeA	-1.5047	0.0002

Table 4.5. Conditionally Essential Genes Overrepresented at Week Six of Hypoxia Versus Input Library (IvH6).

Gene Number	Gene Name	Log2 Fold Change	P Val. (resampling)
Rv1339	-	4.2622	0.0002
Rv0019c	fhaB	3.9590	0.0002
Rv3484	cpsA	3.7325	0.0002
Rv3696c	glpK	3.6015	0.0002
Rv0018c	pstP	2.9401	0.0002
Rv0466	-	2.5168	0.0002
Rv2691	ceoB	2.2263	0.0002
Rv1421	-	2.0087	0.0017
Rv0644c	mmaA2	2.0018	0.0017
Rv1336	cysM	1.9908	0.0002
Rv0642c	mmaA4	1.9764	0.0002
Rv1244	lpqZ	1.9558	0.0002
Rv1780	-	1.7776	0.0002
Rv2694c	-	1.7487	0.0002
Rv1058	fadD14	1.6854	0.0002
Rv1543	-	1.6729	0.0002
Rv1640c	lysX	1.6584	0.0002
Rv3779	-	1.6512	0.0002
Rv3200c	-	1.6057	0.0002
Rv0199	-	1.5736	0.0002
Rv0877	-	1.5478	0.0002
Rv3130c	tgs1	1.5349	0.0002
Rv3818	-	1.5207	0.0002

Table 4.6. Conditionally Essential Genes Underrepresented at Week Six of Hypoxia Versus Week Three of Hypoxia (H3vH6).

Gene Number	Gene Name	Log2 Fold Change	P Val. (resampling)
Rv0998	MtPat	-4.5415	0.0004
Rv0361	-	-3.7876	0.0004
Rv2031c	hspX	-3.5242	0.0004
Rv3261	fbiA	-3.0411	0.0004
Rv0007	-	-2.7064	0.0004
Rv2384	mbtA	-2.6587	0.0004
Rv2170	-	-2.6194	0.0032
Rv0561c	-	-2.6041	0.0004
Rv1791	PE19	-2.5614	0.0004
Rv0248c	-	-2.5165	0.0004
Rv2241	aceE	-2.3929	0.0004
Rv0066c	icd2	-2.3862	0.0004
Rv1212c	glgA	-2.3151	0.0004
Rv0247c	-	-2.2883	0.0004
Rv2563	-	-2.2569	0.0004
Rv2383c	mbtB	-2.2311	0.0004
Rv0407	fgd1	-2.1537	0.0004
Rv1823	-	-2.1288	0.0004
Rv1908c	katG	-2.1165	0.0004
Rv3574	kstR	-1.9883	0.0032
Rv3283	sseA	-1.9553	0.0004
Rv0758	phoR	-1.9516	0.0004
Rv2379c	mbtF	-1.9279	0.0004
Rv2989	-	-1.9163	0.0004
Rv0757	phoP	-1.8225	0.0004
Rv2091c	-	-1.7524	0.0004
Rv3236c	kefB	-1.7129	0.0004
Rv0249c	-	-1.6799	0.0004
Rv2672	-	-1.5389	0.0004
Rv1626	-	-1.5278	0.0004
Rv1592c	-	-1.5179	0.0004
Rv2171	lppM	-1.5079	0.0004

Table 4.7. Conditionally Essential Genes Overrepresented at Week Six of Hypoxia Versus Week Three of Hypoxia (H3vH6).

Gene Number	Gene Name	Log2 Fold Change	P Val. (resampling)
Rv0019c	fhaB	3.2926	0.0004
Rv3696c	glpK	3.0174	0.0004
Rv2691	ceoB	2.8478	0.0004
Rv1339	-	2.8166	0.0004
Rv1099c	glpX	2.3801	0.0032
Rv2694c	-	2.2676	0.0004
Rv0018c	pstP	2.2675	0.0004
Rv3484	cpsA	2.1723	0.0004
Rv0642c	mmaA4	2.0369	0.0004
Rv0466	-	1.8434	0.0004
Rv0820	phoT	1.8234	0.0004
Rv1925	fadD31	1.8029	0.0004
Rv0668	rpoC	1.7847	0.0004
Rv1543	-	1.6703	0.0004

Chapter IV: Acetyl-proteomic profile of hypoxic and aerobic *M. tuberculosis*

Abstract

Global profiling of protein modifications in bacteria has identified a number of post-translational acetylations on enzymatic proteins. This reversible acetylation of a lysine residue is a regulatory event capable of altering the activity of the acetylated enzyme. In *Mycobacterium tuberculosis* we sought to identify acetylated enzymes that may be involved in the metabolic switch to reductive TCA. We cultured WT, ΔMtPat, and ΔCobB strains in hypoxic and normoxic conditions to identify what acetylations are dependent on hypoxia and MtPat. While a number of acetylated peptides were identified, none could be confidently attributed to the sole activity of MtPat based on proteomics alone.

Introduction

Protein lysine acetylation is a post-translational modification recently described in bacteria (Zhang et al., 2009). Reversible lysine acetylation of substrate proteins carried out by a protein acetyltransferase (Pat) enzyme and cognate deacetylase (CobB) can serve as a regulatory mechanism for controlling enzymatic activity of acetylated proteins (Crosby et al., 2010; Nambi et al., 2010). The Pat ortholog in

M. tuberculosis, MtPat (Rv0998), was shown to acetylate a number of proteins controlling acetyl-CoA availability (Nambi et al., 2013; Xu et al., 2011). Other bacterial proteomic studies have identified acetylations of central metabolic enzymes involved in the TCA cycle (Zhang et al, 2009, Wang et al., 2010). In order to identify any potential acetylations, and therefore regulations, of metabolic enzymes in *M. tuberculosis*, in both aerobic and hypoxic conditions, we utilized an acetyl-peptide enrichment technique coupled with mass spectrometry.

Materials and Methods

Acetyl-enriched peptides were obtained from WT, ΔMtPat, and ΔCobB (Rv1151 - deactylase) strains from aerobic and hypoxic conditions. Strains were grown in triplicate in each condition, and at day 18 of hypoxic or aerobic culture cells were pelleted, washed and lysed. The resulting peptide extracts were digested with Trypsin (Promega) and incubated with an anti-acetyl-lysine antibody conjugated to beads (Immunechem Pharmaceuticals, ICP0388). 4 mg of digested protein was mixed with approximately 40 μL of washed beads and incubated overnight at 4ºC. Beads were washed 4x and peptides eluted in 100 mM glycine pH 2. Eluted peptides were desalted and concentrated with ZipTips (Millipore) before MS analysis. Peptide analysis was done with the Mascot search engine (version 2.4.1) using the Tuberculist_R27_050213 database. Scaffold software analysis was used with the following specificaitons: Protein Grouping Strategy:

Experiment-wide grouping with protein cluster analysis, Peptide Thresholds: 80.0% minimum, Protein Thresholds: 90.0% minimum and 1 peptide minimum, Peptide FDR: 1.9% (Prophet), Protein FDR: 1.1% (Prophet).

Results

Acetylated peptides identified from this enrichment strategy are listed in Tables 4.8 – 4.13. As expected, deletion of the deacetylase, ∆CobB, resulted in the most acetyl-enriched peptides (153 in hypoxia, 128 in normoxia), while WT H37RV had the fewest (81 in hypoxia, 14 in normoxia). The acetyltransferase deletion strain ∆MtPat had a similar number of acetyl-enriched peptides between both coniditons (100 in hypoxia, 103 in normoxia). The increase in acetyl-peptides from normoxia to hypoxia in WT suggests that acetylation is upregulated upon sensing oxygen tension. Furthermore, a number of metabolic peptides are acetylated in hypoxic conditions in WT that are not present in normoxic conditions, such as aceE, acn, and gdh (Table 4.8, 4.9).

Discussion

A number of central metabolic enzymes were identified as acetylated (aceE, acn, gdh), however, since they were identified in ∆MtPat (hypoxic and normoxic conditions), we are unable to conclude whether their acetylation depends on

MtPat. It is possible that in the absence of MtPat another acetyltransferase is able to compensate, or that lysine acetylation occurs spontaneously when concetrations of acetyl-CoA are high. Indeed, the overall increase in acetyl-enriched peptides from the ∆MtPat strain as compared to WT would suggest that in the absence of MtPat, acetylation is increased. We were unable to obtain peptides from known acetylation substrates of MtPat (Nambi et al., 2013; Xu et al., 2011), however this may be due to an excess of acetyl-peptides available to bind to the anti-acetyl-lysine antibody, or that the anti-acetyl-lysine antibody did not have the same affinity for all lysine acetylated peptides. Because of these issues, biochemical characterization of reversible acetylations by Pat proteins is a more robust method of identifying acetylated enzymes than acetyl-enrichment studies.

Acknowledgements

Table 4.8. Peptides Identified by Anti-Acetyl-Lysine Enrichment from WT (H37Rv) Normoxia Trypsinized Lysate.

Protein name	Total spectrum count	Peptide sequence	Variable modifications identified by spectrum
Rv3800c_pks13	1	GGYLkDIK	k5: Acetyl (+42.01)
Rv0860_fadB	2	GYSEkLEAK	k5: Acetyl (+42.01)
Rv0860_fadB	2	LEAkALER	k4: Acetyl (+42.01)
Rv0685_tuf	1	TTLTAAITK	
Rv1827_garA	1	LVFLTGPK	
Rv0440_groEL2	3	GLNALADAVK	
Rv0440_groEL2	3	LAGGVAVIK	
Rv0440_groEL2	3	VALEAPLK	
Rv2031c_hspX	1	DGQLTIkAER	k7: Acetyl (+42.01)
Rv3520c_Rv3520c	1	ALkPITHPLR	k3: Acetyl (+42.01)
Rv2605c_tesB2	1	ASQQQVWLR	
Rv2241_aceE	1	TFkEVLR	k3: Acetyl (+42.01)
Rv0815c_cysA2	1	VkLLDGGR	k2: Acetyl (+42.01)
Rv3418c_groES	1	DVLAVVSK	
Rv3131_Rv3131	1	TVLTLAVR	
Rv3274c_fadE25	1	DDEGFTVGPkER	k10: Acetyl (+42.01)
Rv3417c_groEL1	1	LAGGVAVIK	

Table 4.9. Peptides Identified by Anti-Acetyl-Lysine Enrichment from WT (H37Rv) Hypoxia Trypsinized Lysate.

Protein name	Total spectrum count	Peptide sequence	Variable modifications identified by spectrum
Rv3569c_hsaD	1	LSkFSVAPTR	k3: Acetyl (+42.01)
Rv2145c_wag31	1	TYLESQLEELGQR	
Rv2220_glnA1	1	DEkVEYVDVR	k3: Acetyl (+42.01)
Rv0384c_clpB	2	HIEkDAALER	k4: Acetyl (+42.01)
Rv0384c_clpB	2	HIEkDAALER	k4: Acetyl (+42.01)
Rv0566c_Rv0566c	1	AAVDVFKEk	k9: Acetyl (+42.01)
Rv1636_TB15.3	1	AADILkDESYK	k6: Acetyl (+42.01)
Rv3800c_pks13	2	GGYLkDIK	k5: Acetyl (+42.01)
Rv3800c_pks13	2	HSVYFTHGIR	
Rv1390_rpoZ	1	YALVIYAAK	
Rv2416c_eis	1	VDRTDLkLAR	k7: Acetyl (+42.01)
Rv1310_atpD	2	TISLQPTDGLVR	
Rv1310_atpD	2	TVLIQEmINR	m7: Oxidation (+15.99)
Rv0707_rpsC	1	ADLEkLTGK	k5: Acetyl (+42.01)
Rv1144_Rv1144	1	DLASkLIR	k5: Acetyl (+42.01)
Rv3418c_groES	4	EKPQEGTVVAVGPGR	
Rv3418c_groES	4	ILVQANEAETTTASGLVIPDTAK	
Rv3418c_groES	4	VNIkPLEDK	k4: Acetyl (+42.01)
Rv3418c_groES	4	YNGEEYLILSAR	
Rv0350_dnaK	4	DAGQIAGLNVLR	
Rv0350_dnaK	4	IQEGSGLSkEDIDR	k9: Acetyl (+42.01)
Rv0350_dnaK	4	kYTAPEISAR	k1: Acetyl (+42.01)
Rv0350_dnaK	4	NQAETLVYQTEK	
Rv2429_ahpD	2	AALPEYAkDIK	k8: Acetyl (+42.01)
Rv2429_ahpD	2	DIkLNLSSITR	k3: Acetyl (+42.01)
Rv0503c_cmaA2	1	SHYDkSNEFFK	k5: Acetyl (+42.01)
Rv0860_fadB	3	GAGFYEYADGkR	k11: Acetyl (+42.01)
Rv0860_fadB	3	LEAkALER	k4: Acetyl (+42.01)
Rv0860_fadB	3	LVAEkDSITGVVVASAK	k5: Acetyl (+42.01)
Rv0282_eccA3	1	LVVIIAGYR	
Rv0247c_Rv0247c	1	LQQTQTPDLAVR	
Rv0569_Rv0569	1	FGAVQSAILHAR	
Rv0652_rplL	1	EAkDLVDGAPKPLLEK	k3: Acetyl (+42.01)
Rv1133c_metE	1	mRQEITEVIALQER	m1: Oxidation (+15.99)
Rv1630_rpsA	1	DLQPYIGkEIEAK	k8: Acetyl (+42.01)

Rv2783c_gpsI	6	DGLVHISkLGK	k8: Acetyl (+42.01)
Rv2783c_gpsI	6	IDEIkTQVVQR	k5: Acetyl (+42.01)
Rv2783c_gpsI	6	IDEIkTQVVQR	k5: Acetyl (+42.01)
Rv2783c_gpsI	6	VEDVVNVGDkLR	k10: Acetyl (+42.01)
Rv2783c_gpsI	6	VEIADIDkR	k8: Acetyl (+42.01)
Rv2783c_gpsI	6	VPVDkIGEVIGPK	k5: Acetyl (+42.01)
Rv3628_ppa	3	HFFVHYkDLEPGK	k7: Acetyl (+42.01)
Rv3628_ppa	3	HFFVHYkDLEPGK	k7: Acetyl (+42.01)
Rv3628_ppa	3	HFFVHYkDLEPGK	k7: Acetyl (+42.01)
Rv2460c_clpP2	1	DTDRDkILTAEEAK	k6: Acetyl (+42.01)
Rv2185c_TB16.3	1	LIDGALkDLK	k7: Acetyl (+42.01)
Rv1306_atpF	1	AEQQVASTLQTAHEQLkR	k17: Acetyl (+42.01)
Rv2299c_htpG	1	VLSTIkDVQSSRPEDYR	k6: Acetyl (+42.01)
Rv1932_tpx	1	DLPFAQkR	k7: Acetyl (+42.01)
Rv2031c_hspX	3	DGQLTIkAER	k7: Acetyl (+42.01)
Rv2031c_hspX	3	SEFAYGSFVR	
Rv2031c_hspX	3	TVSLPVGADEDDIKATYDK	
Rv3596c_clpC1	3	EFDEkIAEAR	k5: Acetyl (+42.01)
Rv3596c_clpC1	3	VLkEINTR	k3: Acetyl (+42.01)
Rv3596c_clpC1	3	YIEkDAALER	k4: Acetyl (+42.01)
Rv1448c_tal	1	IVDRPNLFIkIPATK	k10: Acetyl (+42.01)
Rv1521_fadD25	1	DLLIVYGR	
Rv2534c_efp	1	VVDkTFNAGVK	k4: Acetyl (+42.01)
Rv0971c_echA7	1	YYLTGEkFGAR	k7: Acetyl (+42.01)
Rv1211_Rv1211	1	TGDGPLEATkEGR	k10: Acetyl (+42.01)
Rv1201c_dapD	1	GPVTVYGVDkFPR	k10: Acetyl (+42.01)
Rv1248c_Rv1248c	2	DFTEIkFR	k6: Acetyl (+42.01)
Rv1248c_Rv1248c	2	VDGFAGAQYKk	k11: Acetyl (+42.01)
Rv0824c_desA1	1	SVDPVELEkLR	k9: Acetyl (+42.01)
Rv0706_rplV	1	TSHITVVVESR	
Rv1925_fadD31	2	NIkYVGDLVAYR	k3: Acetyl (+42.01)
Rv1925_fadD31	2	NIkYVGDLVAYR	k3: Acetyl (+42.01)
Rv0685_tuf	5	AFDQIDNAPEER	
Rv0685_tuf	5	GITINIAHVEYQTDKR	
Rv0685_tuf	5	PGTTTPHTEFEGQVYILSkDEGGR	k19: Acetyl (+42.01)
Rv0685_tuf	5	TTLTAAITK	
Rv0685_tuf	5	VSALkALEGDAK	k5: Acetyl (+42.01)
Rv3520c_Rv3520c	1	ALkPITHPLR	k3: Acetyl (+42.01)
Rv0440_groEL2	15	AGAATEVELkER	k10: Acetyl (+42.01)
Rv0440_groEL2	15	GLNALADAVK	

Rv0440_groEL2	15	GTFkSVAVK	k4: Acetyl (+42.01)
Rv0440_groEL2	15	IGAELVkEVAK	k7: Acetyl (+42.01)
Rv0440_groEL2	15	LAkLAGGVAVIK	k3: Acetyl (+42.01)
Rv0440_groEL2	15	NVAAGANPLGLkR	k12: Acetyl (+42.01)
Rv0440_groEL2	15	NVVLEKk	k7: Acetyl (+42.01)
Rv0440_groEL2	15	QEIENSDSDYDREkLQER	k14: Acetyl (+42.01)
Rv0440_groEL2	15	QEIENSDSDYDREkLQER	k14: Acetyl (+42.01)
Rv0440_groEL2	15	qIAFNSGLEPGVVAEkVR	n-term: Gln->pyro-Glu (-17.03), k16: Acetyl (+42.01)
Rv0440_groEL2	15	VALEAPLK	
Rv0440_groEL2	15	VSTVkDLLPLLEK	k5: Acetyl (+42.01)
Rv0440_groEL2	15	VSTVkDLLPLLEK	k5: Acetyl (+42.01)
Rv0440_groEL2	15	VTETLLkGAK	k7: Acetyl (+42.01)
Rv0440_groEL2	15	VVVTkDETTIVEGAGDTDAIAGR	k5: Acetyl (+42.01)
Rv3648c_cspA	2	TLEENQkVEFEIGHSPK	k7: Acetyl (+42.01)
Rv3648c_cspA	2	VEFEIGHSPK	
Rv3029c_fixA	1	TNIVVLIK	
Rv3458c_rpsD	1	IkESEYLLQLQEK	k2: Acetyl (+42.01)
Rv3846_sodA	1	GANDAVAkLEEAR	k8: Acetyl (+42.01)
Rv0667_rpoB	2	LHHLVDDkIHAR	k8: Acetyl (+42.01)
Rv0667_rpoB	2	LHHLVDDkIHAR	k8: Acetyl (+42.01)
Rv3581c_ispF	3	HVVVLITQHGYR	
Rv3581c_ispF	3	HVVVLITQHGYR	
Rv3581c_ispF	3	HVVVLITQHGYR	
Rv3274c_fadE25	1	GANGISAFmVHKDDEGFTVGPkER	m9: Oxidation (+15.99), k22: Acetyl (+42.01)
Rv2992c_gltS	1	DALIEGLALkPR	k10: Acetyl (+42.01)
Rv0815c_cysA2	1	VkLLDGGR	k2: Acetyl (+42.01)
Rv3285_accA3	1	NFLPAPGPVTkFHPPSGPGVR	k11: Acetyl (+42.01)
Rv2703_sigA	1	AVEkFDYTK	k4: Acetyl (+42.01)
Rv0831c_Rv0831c	1	LkDELLRQ	k2: Acetyl (+42.01)
Rv3417c_groEL1	1	LAkLAGGVAVIK	k3: Acetyl (+42.01)
Rv2882c_frr	2	EGEAGEDEVGRAEkDLDK	k14: Acetyl (+42.01)
Rv2882c_frr	2	TTHQYVTQIDELVkHK	k14: Acetyl (+42.01)
Rv0002_dnaN	2	ALPNkPVDVHVEGNR	k5: Acetyl (+42.01)
Rv0002_dnaN	2	LLDAEFPkFR	k8: Acetyl (+42.01)
Rv0489_gpm1	1	HYGALQGLDkAETK	k10: Acetyl (+42.01)
Rv1463_Rv1463	1	YAESQHGGILLITHYTR	
Rv3774_echA21	1	YASADAkFSVR	k7: Acetyl (+42.01)

Rv2211c_gcvT	1	AALLAEkAAGPR	k7: Acetyl (+42.01)
Rv2244_acpM	3	IESENPDAVANVQAR	
Rv2244_acpM	3	TVGDVVAYIQK	
Rv2244_acpM	3	TVGDVVAYIQK	
Rv1627c_Rv1627c	1	SFTEkHLGSVAGVPSVR	k5: Acetyl (+42.01)
Rv3457c_rpoA	1	TESDLLDIR	
Rv1308_atpA	2	HVLIIFDDLTK	
Rv1308_atpA	2	LTEVIkNFK	k6: Acetyl (+42.01)
Rv2241_aceE	2	GYALGkHFEGR	k6: Acetyl (+42.01)
Rv2241_aceE	2	TFkEVLR	k3: Acetyl (+42.01)
Rv2476c_gdh	3	ASGQkDLATLSVAAR	k5: Acetyl (+42.01)
Rv2476c_gdh	3	ASGQkDLATLSVAAR	k5: Acetyl (+42.01)
Rv2476c_gdh	3	LLPkVLADVQR	k4: Acetyl (+42.01)
Rv3396c_guaA	1	LLFkDEVR	k4: Acetyl (+42.01)
Rv1475c_acn	1	NYADVFkGDDR	k7: Acetyl (+42.01)
Rv0281_Rv0281	1	TkYFDEYFR	k2: Acetyl (+42.01)
Rv0462_lpdC	2	ALPNEDADVSkEIEK	k11: Acetyl (+42.01)
Rv0462_lpdC	2	NAELVHIFTkDAK	k10: Acetyl (+42.01)
Rv0668_rpoC	1	TFHQGGVGEDITGGLPR	
Rv3105c_prfB	1	VLQAkLLER	k5: Acetyl (+42.01)
Rv0716_rplE	1	SIAQFkLR	k6: Acetyl (+42.01)
Rv0683_rpsG	1	TGTDPVITLkR	k10: Acetyl (+42.01)
Rv2140c_TB18.6	1	YYVAVHAVkVEK	k9: Acetyl (+42.01)

Table 4.10. Peptides Identified by Anti-Acetyl-Lysine Enrichment from ∆MtPat Normoxia Trypsinized Lysate.

Protein name	Total spectrum count	Peptide sequence	Variable modifications identified by spectrum
Rv2031c_hspX	3	DGQLTIkAER	k7: Acetyl (+42.01)
Rv2031c_hspX	3	SEFAYGSFVR	
Rv2031c_hspX	3	TVSLPVGADEDDIK	
Rv2145c_wag31	1	ANAEQILGEAR	
Rv2220_glnA1	2	DEkVEYVDVR	k3: Acetyl (+42.01)
Rv2220_glnA1	2	TPDDVFkLAK	k7: Acetyl (+42.01)
Rv0147_Rv0147	1	ITAALTkFR	k7: Acetyl (+42.01)
Rv1636_TB15.3	2	LIIASAYLPQHEDAR	
Rv1636_TB15.3	2	VDVLIVHTT	
Rv0580c_Rv0580c	1	TQLmVVSFTGR	m4: Oxidation (+15.99)
Rv3800c_pks13	1	GGYLkDIK	k5: Acetyl (+42.01)
Rv1390_rpoZ	1	YALVIYAAK	
Rv1310_atpD	2	TISLQPTDGLVR	
Rv1310_atpD	2	TVLIQEmINR	m7: Oxidation (+15.99)
Rv3274c_fadE25	3	DDEGFTVGPkER	k10: Acetyl (+42.01)
Rv3274c_fadE25	3	EIAPHAAEVDEkAR	k12: Acetyl (+42.01)
Rv3274c_fadE25	3	ITQIYEGTNQIQR	
Rv0934_pstS1	1	VLAAmYQGTIK	m5: Oxidation (+15.99)
Rv1037c_esxI	1	NFQVIYEQANAHGQK	
Rv1388_mihF	2	GGTNLTQVLK	
Rv1388_mihF	2	RGGTNLTQVLK	
Rv2996c_serA1	1	TKPGVIIVNAAR	
Rv1144_Rv1144	1	DLASkLIR	k5: Acetyl (+42.01)
Rv2385_mbtJ	1	AmTYVAQFIR	m2: Oxidation (+15.99)
Rv3528c_Rv3528c	1	ALDkYPVK	k4: Acetyl (+42.01)
Rv1827_garA	2	FLLDQAITSAGR	
Rv1827_garA	2	LVFLTGPK	
Rv2605c_tesB2	1	ASQQQVWLR	
Rv0350_dnaK	4	DAGQIAGLNVLR	
Rv0350_dnaK	4	FkGTSGIDLTK	k2: Acetyl (+42.01)
Rv0350_dnaK	4	IQEGSGLSkEDIDR	k9: Acetyl (+42.01)
Rv0350_dnaK	4	kYTAPEISAR	k1: Acetyl (+42.01)
Rv0896_gltA2	1	VYkNYDPR	k3: Acetyl (+42.01)
Rv2429_ahpD	1	AALPEYAkDIK	k8: Acetyl (+42.01)
Rv0503c_cmaA2	1	SHYDkSNEFFK	k5: Acetyl (+42.01)

Rv1391_dfp	2	kGcDLLVVNAVGEGR	k1: Acetyl (+42.01), c3: Carbamidomethyl (+57.02)
Rv1391_dfp	2	RkGcDLLVVNAVGEGR	k2: Acetyl (+42.01), c4: Carbamidomethyl (+57.02)
Rv0860_fadB	1	LEAkALER	k4: Acetyl (+42.01)
Rv0282_eccA3	1	LVVIIAGYR	
Rv0247c_Rv0247c	1	LQQTQTPDLAVR	
Rv0569_Rv0569	1	FGAVQSAILHAR	
Rv2785c_rpsO	1	GLLLLVGR	
Rv1023_eno	1	VAkYNQLLR	k3: Acetyl (+42.01)
Rv1133c_metE	1	WAVGAFR	
Rv1630_rpsA	4	AWLEQTQSEVR	
Rv1630_rpsA	4	DLQPYIGKEIEAk	k13: Acetyl (+42.01)
Rv1630_rpsA	4	DLQPYIGKEIEAk	k13: Acetyl (+42.01)
Rv1630_rpsA	4	RAWLEQTQSEVR	
Rv2783c_gpsI	3	DGLVHISkLGK	k8: Acetyl (+42.01)
Rv2783c_gpsI	3	IDEIkTQVVQR	k5: Acetyl (+42.01)
Rv2783c_gpsI	3	VEIADIDkR	k8: Acetyl (+42.01)
Rv2626c_hrp1	2	EHDIGALPIcGDDDR	c10: Carbamidomethyl (+57.02)
Rv2626c_hrp1	2	HLPEHAIVQFVK	
Rv2509_Rv2509	1	GSGVHVTVLAPGPVR	
Rv3628_ppa	2	HFFVHYkDLEPGK	k7: Acetyl (+42.01)
Rv3628_ppa	2	HFFVHYkDLEPGK	k7: Acetyl (+42.01)
Rv0707_rpsC	1	ADLEkLTGK	k5: Acetyl (+42.01)
Rv2185c_TB16.3	1	LIDGALkDLK	k7: Acetyl (+42.01)
Rv3131_Rv3131	1	TVLTLAVR	
Rv2524c_fas	1	GSQYAIAGTVR	
Rv1058_fadD14	1	AFLADkVVR	k6: Acetyl (+42.01)
Rv0222_echA1	1	ILIITINRPK	
Rv3596c_clpC1	1	VLkEINTR	k3: Acetyl (+42.01)
Rv1925_fadD31	1	NIkYVGDLVAYR	k3: Acetyl (+42.01)
Rv1819c_bacA	1	NEkLNAAFR	k3: Acetyl (+42.01)
Rv3676_crp	2	LYIIISGK	
Rv3676_crp	2	QLLQLAQR	
Rv0655_mkl	1	LALVGLGGDEKk	k12: Acetyl (+42.01)
Rv0951_sucC	1	AGGVkYAATPQDAYEHAK	k5: Acetyl (+42.01)
Rv1368_lprF	1	IYDPGIILDkDR	k10: Acetyl (+42.01)
Rv1201c_dapD	1	GPVTVYGVDkFPR	k10: Acetyl (+42.01)
Rv1521_fadD25	1	DLLIVYGR	
Rv0702_rplD	1	QVLVVIGR	
Rv0005_gyrB	1	LLKDkDPNLTGDDIR	k5: Acetyl (+42.01)

Rv1248c_Rv1248c	1	DFTEIkFR	k6: Acetyl (+42.01)
Rv3051c_nrdE	1	IQFDkDR	k5: Acetyl (+42.01)
Rv0824c_desA1	1	SVDPVELEkLR	k9: Acetyl (+42.01)
Rv1079_metB	1	LIDkVFTR	k4: Acetyl (+42.01)
Rv0701_rplC	1	VTVLNLLVHK	
Rv1996_Rv1996	1	QVAmVVLGYR	m4: Oxidation (+15.99)
Rv0685_tuf	3	TTLTAAITK	
Rv0685_tuf	3	VLHDkFPDLNETK	k5: Acetyl (+42.01)
Rv0685_tuf	3	VSALkALEGDAK	k5: Acetyl (+42.01)
Rv3520c_Rv3520c	1	ALkPITHPLR	k3: Acetyl (+42.01)
Rv0440_groEL2	16	AGAATEVELkER	k10: Acetyl (+42.01)
Rv0440_groEL2	16	AGAATEVELkER	k10: Acetyl (+42.01)
Rv0440_groEL2	16	AVEkVTETLLK	k4: Acetyl (+42.01)
Rv0440_groEL2	16	DLLPLLEK	
Rv0440_groEL2	16	GLNALADAVK	
Rv0440_groEL2	16	GTFkSVAVK	k4: Acetyl (+42.01)
Rv0440_groEL2	16	IGAELVkEVAK	k7: Acetyl (+42.01)
Rv0440_groEL2	16	LAGGVAVIK	
Rv0440_groEL2	16	LAkLAGGVAVIK	k3: Acetyl (+42.01)
Rv0440_groEL2	16	NVAAGANPLGLK	
Rv0440_groEL2	16	NVAAGANPLGLkR	k12: Acetyl (+42.01)
Rv0440_groEL2	16	qEIENSDSDYDREkLQER	n-term: Gln->pyro-Glu (-17.03), k14: Acetyl (+42.01)
Rv0440_groEL2	16	QEIENSDSDYDREkLQER	k14: Acetyl (+42.01)
Rv0440_groEL2	16	QIAFNSGLEPGVVAEK	
Rv0440_groEL2	16	VALEAPLK	
Rv0440_groEL2	16	VTETLLkGAK	k7: Acetyl (+42.01)
Rv3029c_fixA	3	AVEEALQIR	
Rv3029c_fixA	3	FPSFkGImAAK	k5: Acetyl (+42.01), m8: Oxidation (+15.99)
Rv3029c_fixA	3	TNIVVLIK	
Rv3846_sodA	1	GANDAVAkLEEAR	k8: Acetyl (+42.01)
Rv1837c_glcB	1	DELQAQIDkWHR	k9: Acetyl (+42.01)
Rv0462_lpdC	2	NAELVHIFTkDAK	k10: Acetyl (+42.01)
Rv0462_lpdC	2	VAGVHFLmkK	m8: Oxidation (+15.99), k9: Acetyl (+42.01)
Rv3418c_groES	1	DVLAVVSk	k8: Acetyl (+42.01)
Rv0815c_cysA2	2	SSHTWFVLR	
Rv0815c_cysA2	2	VkLLDGGR	k2: Acetyl (+42.01)
Rv3028c_fixB	1	AAVDSGYYPGQFQVGQTGK	
Rv2889c_tsf	1	IGEkLELR	k4: Acetyl (+42.01)

Rv0873_fadE10	1	TEAFLVkLR	k7: Acetyl (+42.01)
Rv2703_sigA	1	AVEkFDYTK	k4: Acetyl (+42.01)
Rv0831c_Rv0831c	1	LkDELLR	k2: Acetyl (+42.01)
Rv1259_udgB	1	PVPGWGSkR	k8: Acetyl (+42.01)
Rv0231_fadE4	1	GVEkDTFFETVAR	k4: Acetyl (+42.01)
Rv0933_pstB	1	LSGGQQQLLcLAR	c10: Carbamidomethyl (+57.02)
Rv3417c_groEL1	3	LAGGVAVIK	
Rv3417c_groEL1	3	LAkLAGGVAVIK	k3: Acetyl (+42.01)
Rv3417c_groEL1	3	SDSDWDREkLGER	k9: Acetyl (+42.01)
Rv0363c_fba	1	PLLAISAQR	
Rv0002_dnaN	2	ALPNkPVDVHVEGNR	k5: Acetyl (+42.01)
Rv0002_dnaN	2	LLDAEFPkFR	k8: Acetyl (+42.01)
Rv3692_moxR2	1	GHVLLEGVPGVAK	
Rv2986c_hupB	1	AELIDVLTQK	
Rv2211c_gcvT	1	AALLAEkAAGPR	k7: Acetyl (+42.01)
Rv1479_moxR1	1	GHVLLEGVPGVAK	
Rv2238c_ahpE	1	DQNQQLVTLR	
Rv2244_acpM	3	IESENPDAVANVQAR	
Rv2244_acpM	3	TVGDVVAYIQK	
Rv2244_acpM	3	TVGDVVAYIQK	
Rv0066c_icd2	1	IFYKDAFAk	k9: Acetyl (+42.01)
Rv2711_ideR	1	LDQSGPTVSQTVSR	
Rv3248c_sahH	1	SIIVLSEGR	
Rv3457c_rpoA	3	LHQLGLSLK	
Rv3457c_rpoA	3	TESDLLDIR	
Rv3457c_rpoA	3	TLVELFGLAR	
Rv1308_atpA	4	AISLLLR	
Rv1308_atpA	4	HVLIIFDDLTK	
Rv1308_atpA	4	LTEVIkNFK	k6: Acetyl (+42.01)
Rv1308_atpA	4	TAVcVDTILNQR	c4: Carbamidomethyl (+57.02)
Rv0154c_fadE2	1	AAWTIDQHGNkEAR	k11: Acetyl (+42.01)
Rv2241_aceE	2	GYALGkHFEGR	k6: Acetyl (+42.01)
Rv2241_aceE	2	TFkEVLR	k3: Acetyl (+42.01)
Rv2476c_gdh	2	LLPkVLADVQR	k4: Acetyl (+42.01)
Rv2476c_gdh	2	LLVLAQAR	
Rv3396c_guaA	1	LLFkDEVR	k4: Acetyl (+42.01)
Rv1475c_acn	1	DHIEAIANWDPK	
Rv3858c_gltD	1	ADPGGFLkYTHR	k8: Acetyl (+42.01)
Rv0668_rpoC	1	TLKPEkDGLFcEK	k6: Acetyl (+42.01), c11: Carbamidomethyl (+57.02)
Rv0718_rpsH	1	LkANIAQILK	k2: Acetyl (+42.01)

Rv3105c_prfB	1	VLQAkLLER	k5: Acetyl (+42.01)
Rv0683_rpsG	1	TGTDPVITLkR	k10: Acetyl (+42.01)
Rv2572c_aspS	1	DHGGVIFIDLR	

Table 4.11. Peptides Identified by Anti-Acetyl-Lysine Enrichment from ∆MtPat Hypoxia Trypsinized Lysate.

Protein name	Total spectrum count	Peptide sequence	Variable modifications identified by spectrum
Rv2145c_wag31	1	TYLESQLEELGQR	
Rv2220_glnA1	2	DEkVEYVDVR	k3: Acetyl (+42.01)
Rv2220_glnA1	2	TPDDVFkLAK	k7: Acetyl (+42.01)
Rv0242c_fabG4	1	AALEkDYDLVGNNLGGR	k5: Acetyl (+42.01)
Rv0271c_fadE6	1	AGQLIAEGHATkLLNLR	k12: Acetyl (+42.01)
Rv1636_TB15.3	2	VTGTAPIYEILHDAkER	k15: Acetyl (+42.01)
Rv1636_TB15.3	2	VTGTAPIYEILHDAkER	k15: Acetyl (+42.01)
Rv3800c_pks13	1	GGYLkDIK	k5: Acetyl (+42.01)
Rv1310_atpD	1	TISLQPTDGLVR	
Rv3099c_Rv3099c	1	SQDVELGGDkELAGHILER	k10: Acetyl (+42.01)
Rv2996c_serA1	3	AQGINLIIHYVDRPGALGK	
Rv2996c_serA1	3	AQGINLIIHYVDRPGALGK	
Rv2996c_serA1	3	TPETAGLIDkEALAK	k10: Acetyl (+42.01)
Rv1144_Rv1144	1	DLASkLIR	k5: Acetyl (+42.01)
Rv3417c_groEL1	2	HVVLAkAFGGPTVTNDGVTVAR	k6: Acetyl (+42.01)
Rv3417c_groEL1	2	LAkLAGGVAVIK	k3: Acetyl (+42.01)
Rv3248c_sahH	1	SIIVLSEGR	
Rv3418c_groES	5	DVLAVVSk	k8: Acetyl (+42.01)
Rv3418c_groES	5	IPLDVAEGDTVIYSkYGGTEIK	k15: Acetyl (+42.01)
Rv3418c_groES	5	RIPLDVAEGDTVIYSkYGGTEIK	k16: Acetyl (+42.01)
Rv3418c_groES	5	VNIkPLEDK	k4: Acetyl (+42.01)
Rv3418c_groES	5	YNGEEYLILSAR	
Rv3710_leuA	1	AIVHFYNSTSILQR	
Rv0896_gltA2	1	mFTVLFALGR	m1: Oxidation (+15.99)
Rv2429_ahpD	2	AALPEYAkDIK	k8: Acetyl (+42.01)
Rv2429_ahpD	2	DIkLNLSSITR	k3: Acetyl (+42.01)
Rv0860_fadB	4	GYSEkLEAK	k5: Acetyl (+42.01)
Rv0860_fadB	4	LEAkALER	k4: Acetyl (+42.01)
Rv0860_fadB	4	LVAEkDSITGVVVASAK	k5: Acetyl (+42.01)
Rv0860_fadB	4	LVAEkDSITGVVVASAK	k5: Acetyl (+42.01)
Rv0821c_phoY2	1	mGALALHVAkIAR	m1: Oxidation (+15.99), k10: Acetyl (+42.01)
Rv0282_eccA3	1	LVVIIAGYR	
Rv0569_Rv0569	1	FGAVQSAILHAR	

Rv1290c_Rv1290c	1	QmVDIALR	m2: Oxidation (+15.99)
Rv0933_pstB	1	LTVIIVTHNLAQAAR	
Rv1133c_metE	2	LHLPPLPTTTIGSYPQTSAIR	
Rv1133c_metE	2	SELEAVAATLR	
Rv1630_rpsA	2	DLQPYIGkEIEAK	k8: Acetyl (+42.01)
Rv1630_rpsA	2	VRDLQPYIGkEIEAK	k10: Acetyl (+42.01)
Rv2783c_gpsI	3	DGLVHISkLGK	k8: Acetyl (+42.01)
Rv2783c_gpsI	3	LRVEIADIDkR	k10: Acetyl (+42.01)
Rv2783c_gpsI	3	VEDVVNVGDkLR	k10: Acetyl (+42.01)
Rv2606c_snzP	2	ATTFFDDPDVLAkVSR	k13: Acetyl (+42.01)
Rv2606c_snzP	2	ATTFFDDPDVLAkVSR	k13: Acetyl (+42.01)
Rv3628_ppa	1	HFFVHYkDLEPGK	k7: Acetyl (+42.01)
Rv3029c_fixA	2	FPSFkGImAAK	k5: Acetyl (+42.01), m8: Oxidation (+15.99)
Rv3029c_fixA	2	TNIVVLIK	
Rv2185c_TB16.3	1	LIDGALkDLK	k7: Acetyl (+42.01)
Rv3001c_ilvC	1	LVADVEGGNkQLEELRR	k10: Acetyl (+42.01)
Rv2928_tesA	1	QAAPTLYIFPHAGGTAkDYVAFSR	k17: Acetyl (+42.01)
Rv2031c_hspX	7	AELPGVDPDkDVDImVR	k10: Acetyl (+42.01), m15: Oxidation (+15.99)
Rv2031c_hspX	7	DGQLTIkAER	k7: Acetyl (+42.01)
Rv2031c_hspX	7	GILTVSVAVSEGKPTEK	
Rv2031c_hspX	7	SEFAYGSFVR	
Rv2031c_hspX	7	TVSLPVGADEDDIK	
Rv2031c_hspX	7	TVSLPVGADEDDIkATYDK	k14: Acetyl (+42.01)
Rv2031c_hspX	7	TVSLPVGADEDDIkATYDK	k14: Acetyl (+42.01)
Rv2780_ald	1	HGQILFTFLHLAASR	
Rv2213_pepB	1	DLVNTPPSHLFPAEFAkR	k17: Acetyl (+42.01)
Rv0350_dnaK	8	FkGTSGIDLTK	k2: Acetyl (+42.01)
Rv0350_dnaK	8	IVNEPTAAALAYGLDKGEkEQR	k19: Acetyl (+42.01)
Rv0350_dnaK	8	NQAETLVYQTEKFVk	k15: Acetyl (+42.01)
Rv0350_dnaK	8	NQAETLVYQTEkFVK	k12: Acetyl (+42.01)
Rv0350_dnaK	8	QATkDAGQIAGLNVLR	k4: Acetyl (+42.01)
Rv0350_dnaK	8	qATkDAGQIAGLNVLR	n-term: Gln->pyro-Glu (-17.03), k4: Acetyl (+42.01)
Rv0350_dnaK	8	qATkDAGQIAGLNVLR	n-term: Gln->pyro-Glu (-17.03), k4: Acetyl (+42.01)
Rv0350_dnaK	8	VPEDTLNkVDAAVAEAK	k8: Acetyl (+42.01)
Rv0248c_Rv0248c	1	HSYDVVVIGAGGAGLR	

Rv1448c_tal	1	IVDRPNLFIkIPATK	k10: Acetyl (+42.01)
Rv1925_fadD31	2	NIkYVGDLVAYR	k3: Acetyl (+42.01)
Rv1925_fadD31	2	NIkYVGDLVAYR	k3: Acetyl (+42.01)
Rv1240_mdh	1	GRIDkSTAELADER	k5: Acetyl (+42.01)
Rv1521_fadD25	1	DLLIVYGR	
Rv1612_trpB	1	GAVIVVNLSGR	
Rv2839c_infB	1	GLLkPIYEENQLGR	k4: Acetyl (+42.01)
Rv0818_Rv0818	1	GRPLDLTYkEFELLK	k9: Acetyl (+42.01)
Rv2949c_Rv2949c	1	LTQTNDPLGEVmAASHIETFKEEAk	m12: Oxidation (+15.99), k25: Acetyl (+42.01)
Rv0652_rplL	4	EAkDLVDGAPKPLLEK	k3: Acetyl (+42.01)
Rv0652_rplL	4	EAkDLVDGAPKPLLEK	k3: Acetyl (+42.01)
Rv0652_rplL	4	EAkDLVDGAPKPLLEK	k3: Acetyl (+42.01)
Rv0652_rplL	4	EIVSGLGLK	
Rv1751_Rv1751	1	AGVQVTLLEkHGDFLR	k10: Acetyl (+42.01)
Rv1192_Rv1192	1	DLLDkLHSR	k5: Acetyl (+42.01)
Rv1201c_dapD	1	RGPVTVYGVDkFPR	k11: Acetyl (+42.01)
Rv0005_gyrB	1	LLKDkDPNLTGDDIR	k5: Acetyl (+42.01)
Rv3389c_htdY	1	LSVVTEVADIQDkGEGK	k13: Acetyl (+42.01)
Rv1248c_Rv1248c	1	DFTEIkFR	k6: Acetyl (+42.01)
Rv0824c_desA1	1	SVDPVELEkLR	k9: Acetyl (+42.01)
Rv2572c_aspS	1	DHGGVIFIDLR	
Rv0685_tuf	11	ELLAAQEFDEDAPVVR	
Rv0685_tuf	11	GITINIAHVEYQTDK	
Rv0685_tuf	11	GITINIAHVEYQTDK	
Rv0685_tuf	11	GITINIAHVEYQTDkR	k15: Acetyl (+42.01)
Rv0685_tuf	11	GQVVTKPGTTTPHTEFEGQVYILSkDEGGR	k25: Acetyl (+42.01)
Rv0685_tuf	11	GQVVTKPGTTTPHTEFEGQVYILSkDEGGR	k25: Acetyl (+42.01)
Rv0685_tuf	11	HTPFFNNYRPQFYFR	
Rv0685_tuf	11	PGTTTPHTEFEGQVYILSkDEGGR	k19: Acetyl (+42.01)
Rv0685_tuf	11	VLHDkFPDLNETK	k5: Acetyl (+42.01)
Rv0685_tuf	11	VLHDKFPDLNETkAFDQIDNAPEER	k13: Acetyl (+42.01)
Rv0685_tuf	11	VSALkALEGDAK	k5: Acetyl (+42.01)
Rv0440_groEL2	28	AGAATEVELkER	k10: Acetyl (+42.01)
Rv0440_groEL2	28	AGAATEVELkER	k10: Acetyl (+42.01)
Rv0440_groEL2	28	AVEkVTETLLK	k4: Acetyl (+42.01)
Rv0440_groEL2	28	DLLPLLEK	
Rv0440_groEL2	28	EIELEDPYEkIGAELVK	k10: Acetyl (+42.01)
Rv0440_groEL2	28	FDkGYISGYFVTDPER	k3: Acetyl (+42.01)
Rv0440_groEL2	28	GLNALADAVK	

Rv0440_groEL2	28	GTFkSVAVK	k4: Acetyl (+42.01)
Rv0440_groEL2	28	GTFkSVAVK	k4: Acetyl (+42.01)
Rv0440_groEL2	28	GYISGYFVTDPER	
Rv0440_groEL2	28	IGAELVkEVAK	k7: Acetyl (+42.01)
Rv0440_groEL2	28	KTDDVAGDGTTTATVLAQALVR	
Rv0440_groEL2	28	KVVVTkDETTIVEGAGDTDAIAGR	k6: Acetyl (+42.01)
Rv0440_groEL2	28	LAkLAGGVAVIK	k3: Acetyl (+42.01)
Rv0440_groEL2	28	NVAAGANPLGLK	
Rv0440_groEL2	28	NVAAGANPLGLkR	k12: Acetyl (+42.01)
Rv0440_groEL2	28	QEIENSDSDYDREkLQER	k14: Acetyl (+42.01)
Rv0440_groEL2	28	QIAFNSGLEPGVVAEK	
Rv0440_groEL2	28	QIAFNSGLEPGVVAEkVR	k16: Acetyl (+42.01)
Rv0440_groEL2	28	QIAFNSGLEPGVVAEkVR	k16: Acetyl (+42.01)
Rv0440_groEL2	28	QIAFNSGLEPGVVAEkVR	k16: Acetyl (+42.01)
Rv0440_groEL2	28	qIAFNSGLEPGVVAEkVR	n-term: Gln->pyro-Glu (-17.03), k16: Acetyl (+42.01)
Rv0440_groEL2	28	TDDVAGDGTTTATVLAQALVR	
Rv0440_groEL2	28	VALEAPLK	
Rv0440_groEL2	28	VSTVkDLLPLLEK	k5: Acetyl (+42.01)
Rv0440_groEL2	28	VTETLLkGAK	k7: Acetyl (+42.01)
Rv0440_groEL2	28	VVVTkDETTIVEGAGDTDAIAGR	k5: Acetyl (+42.01)
Rv0440_groEL2	28	VVVTkDETTIVEGAGDTDAIAGR	k5: Acetyl (+42.01)
Rv3648c_cspA	1	TLEENQkVEFEIGHSPK	k7: Acetyl (+42.01)
Rv1596_nadC	1	LGLGDAALIkDNHVAAAGSVVDALR	k10: Acetyl (+42.01)
Rv1388_mihF	2	RGGTNLTQVLkDAESDEVLGK	k11: Acetyl (+42.01)
Rv1388_mihF	2	RGGTNLTQVLkDAESDEVLGK	k11: Acetyl (+42.01)
Rv2454c_Rv2454c	1	FPYYLETYGFHSIHGR	
Rv3458c_rpsD	2	IkESEYLLQLQEK	k2: Acetyl (+42.01)
Rv3458c_rpsD	2	IkESEYLLQLQEK	k2: Acetyl (+42.01)
Rv1658_argG	1	GFVYVHGLSSkLAAR	k11: Acetyl (+42.01)
Rv3846_sodA	1	GANDAVAkLEEAR	k8: Acetyl (+42.01)
Rv1837c_glcB	3	GDLAAAVDkDGTAFLR	k9: Acetyl (+42.01)
Rv1837c_glcB	3	GDLAAAVDkDGTAFLR	k9: Acetyl (+42.01)
Rv1837c_glcB	3	GDLAAAVDkDGTAFLR	k9: Acetyl (+42.01)
Rv0667_rpoB	1	STLEkDNTVGTDEALLDIYRK	k5: Acetyl (+42.01)
Rv3274c_fadE25	2	DDEGFTVGPkER	k10: Acetyl (+42.01)
Rv3274c_fadE25	2	EIAPHAAEVDEkAR	k12: Acetyl (+42.01)
Rv0815c_cysA2	1	VkLLDGGR	k2: Acetyl (+42.01)
Rv3285_accA3	1	NFLPAPGPVTkFHPPSGPGVR	k11: Acetyl (+42.01)
Rv2889c_tsf	1	IGEkLELR	k4: Acetyl (+42.01)

Rv0873_fadE10	1	TEAFLVkLR	k7: Acetyl (+42.01)
Rv2703_sigA	2	AVEkFDYTK	k4: Acetyl (+42.01)
Rv2703_sigA	2	IPVHmVEVINkLGR	m5: Oxidation (+15.99), k11: Acetyl (+42.01)
Rv0270_fadD2	2	FKPALVLEDIEkHK	k12: Acetyl (+42.01)
Rv0270_fadD2	2	ILDQLEkTEPKPDLSSLK	k7: Acetyl (+42.01)
Rv0009_ppiA	1	TVANFVGLAQGTK	
Rv0231_fadE4	1	GVEkDTFFETVAR	k4: Acetyl (+42.01)
Rv2882c_frr	2	LVVIkPYEANQLR	k5: Acetyl (+42.01)
Rv2882c_frr	2	TTHQYVTQIDELVkHK	k14: Acetyl (+42.01)
Rv0363c_fba	1	DkLDSYVRPLLAISAQR	k2: Acetyl (+42.01)
Rv0002_dnaN	1	ALPNkPVDVHVEGNR	k5: Acetyl (+42.01)
Rv0489_gpm1	1	HYGALQGLDkAETK	k10: Acetyl (+42.01)
Rv1463_Rv1463	1	YAESQHGGILLITHYTR	
Rv3774_echA21	1	ELALTGkNIDAAR	k7: Acetyl (+42.01)
Rv2986c_hupB	2	AELIDVLTQK	
Rv2986c_hupB	2	AELIDVLTQkLGSDR	k10: Acetyl (+42.01)
Rv2244_acpM	4	IPDEDLAGLR	
Rv2244_acpM	4	TVGDVVAYIQK	
Rv2244_acpM	4	TVGDVVAYIQK	
Rv2244_acpM	4	YGVkIPDEDLAGLR	k4: Acetyl (+42.01)
Rv2788_sirR	1	LAEQGLVDHEkYGAVTLTDSGR	k11: Acetyl (+42.01)
Rv0641_rplA	1	mSKTSKAYRAAAAK	m1: Oxidation (+15.99)
Rv3592_mhuD	1	INAIEVPAGAGPELEkR	k16: Acetyl (+42.01)
Rv3457c_rpoA	2	TDFDkLILDVETK	k5: Acetyl (+42.01)
Rv3457c_rpoA	2	TLVELFGLAR	
Rv1308_atpA	3	GFAATGGGSVVPDEHVEALDEDKLAk	k26: Acetyl (+42.01)
Rv1308_atpA	3	HVLIIFDDLTK	
Rv1308_atpA	3	LTEVIkNFK	k6: Acetyl (+42.01)
Rv3528c_Rv3528c	1	LLDLGEkHYFR	k7: Acetyl (+42.01)
Rv0548c_menB	1	FkQTDADVGSFDGGYGSAYLAR	k2: Acetyl (+42.01)
Rv2241_aceE	2	GYALGkHFEGR	k6: Acetyl (+42.01)
Rv2241_aceE	2	TFkEVLR	k3: Acetyl (+42.01)
Rv2476c_gdh	2	ELEALPSEkEIAR	k9: Acetyl (+42.01)
Rv2476c_gdh	2	LLPkVLADVQR	k4: Acetyl (+42.01)
Rv3396c_guaA	1	LLFkDEVR	k4: Acetyl (+42.01)
Rv0462_lpdC	5	ALPNEDADVSkEIEK	k11: Acetyl (+42.01)
Rv0462_lpdC	5	ALPNEDADVSKEIEkQFK	k15: Acetyl (+42.01)
Rv0462_lpdC	5	DGVAQELkAEK	k8: Acetyl (+42.01)
Rv0462_lpdC	5	NAELVHIFTkDAK	k10: Acetyl (+42.01)

Rv0462_lpdC	5	NEGYDVVVAkFPFTANAK	k10: Acetyl (+42.01)
Rv0668_rpoC	1	LGYLLDLAPkDLEK	k10: Acetyl (+42.01)
Rv3246c_mtrA	2	VEkDPENPTVVLTVR	k3: Acetyl (+42.01)
Rv3246c_mtrA	2	VEkDPENPTVVLTVR	k3: Acetyl (+42.01)
Rv3801c_fadD32	1	TGDYGTYFkDHLYIAGR	k9: Acetyl (+42.01)
Rv3105c_prfB	1	VLQAkLLER	k5: Acetyl (+42.01)
Rv0683_rpsG	1	TGTDPVITLkR	k10: Acetyl (+42.01)
Rv2140c_TB18.6	1	YYVAVHAVKVEk	k12: Acetyl (+42.01)

Table 4.12. Peptides Identified by Anti-Acetyl-Lysine Enrichment from ∆Rv1151 (mtCobB) Normoxia Trypsinized Lysate.

Protein name	Total spectrum count	Peptide sequence	Variable modifications identified by spectrum
Rv3033_Rv3033	1	NQVANIISDkLFQR	k10: Acetyl (+42.01)
Rv0379_secE2	1	LEVSFkmR	k6: Acetyl (+42.01), m7: Oxidation (+15.99)
Rv1751_Rv1751	1	AGVQVTLLEkHGDFLR	k10: Acetyl (+42.01)
Rv2220_glnA1	1	TPDDVFkLAK	k7: Acetyl (+42.01)
Rv0384c_clpB	1	LQLQVSLPAK	
Rv3648c_cspA	2	TLEENQkVEFEIGHSPK	k7: Acetyl (+42.01)
Rv3648c_cspA	2	VEFEIGHSPkGPQATGVR	k10: Acetyl (+42.01)
Rv1636_TB15.3	3	AADILkDESYK	k6: Acetyl (+42.01)
Rv1636_TB15.3	3	VDVLIVHTT	
Rv1636_TB15.3	3	VTGTAPIYEILHDAkER	k15: Acetyl (+42.01)
Rv0580c_Rv0580c	2	SLLHTPLAGPLR	
Rv0580c_Rv0580c	2	TQLmVVSFTGR	m4: Oxidation (+15.99)
Rv3800c_pks13	4	DEVQQLHEHQkTQTAEEIAR	k11: Acetyl (+42.01)
Rv3800c_pks13	4	GGYLkDIK	k5: Acetyl (+42.01)
Rv3800c_pks13	4	TYLEAGQIDGFVR	
Rv3800c_pks13	4	VPVFVFHPAGGSTVVYEPLLGR	
Rv0632c_echA3	1	GGFELAYR	
Rv1390_rpoZ	1	YALVIYAAK	
Rv3401_Rv3401	1	FGLFHLLQASAR	
Rv3592_mhuD	2	INAIEVPAGAGPELEkR	k16: Acetyl (+42.01)
Rv3592_mhuD	2	INAIEVPAGAGPELEkR	k16: Acetyl (+42.01)
Rv1310_atpD	2	TISLQPTDGLVR	
Rv1310_atpD	2	VVDLLTPYVR	
Rv3274c_fadE25	1	DDEGFTVGPkER	k10: Acetyl (+42.01)
Rv2713_sthA	1	TQHVIGkEVDVVR	k7: Acetyl (+42.01)
Rv3569c_hsaD	1	LSkFSVAPTR	k3: Acetyl (+42.01)
Rv1037c_esxI	1	NFQVIYEQANAHGQK	
Rv2504c_scoA	1	TVSSYVGENkEFAR	k10: Acetyl (+42.01)
Rv2996c_serA1	2	AQGINLIIHYVDR	
Rv2996c_serA1	2	AQGINLIIHYVDRPGALGK	
Rv1144_Rv1144	1	DLASkLIR	k5: Acetyl (+42.01)
Rv2385_mbtJ	1	AmTYVAQFIR	m2: Oxidation (+15.99)
Rv3248c_sahH	2	TGNLVTkNSLTPDVR	k7: Acetyl (+42.01)
Rv3248c_sahH	2	TGNLVTkNSLTPDVR	k7: Acetyl (+42.01)

Rv2203_Rv2203	1	GQVQGIAQLLFQR	
Rv3224_Rv3224	2	DGANIALIAkTAEPHPK	k10: Acetyl (+42.01)
Rv3224_Rv3224	2	TAEPHPkLPGTVFTAAK	k7: Acetyl (+42.01)
Rv0350_dnaK	10	DAGQIAGLNVLR	
Rv0350_dnaK	10	EIAAHNkLLGSFELTGIPPAPR	k7: Acetyl (+42.01)
Rv0350_dnaK	10	FkGTSGIDLTK	k2: Acetyl (+42.01)
Rv0350_dnaK	10	GTSGIDLTkDK	k9: Acetyl (+42.01)
Rv0350_dnaK	10	IQEGSGLSkEDIDR	k9: Acetyl (+42.01)
Rv0350_dnaK	10	IQEGSGLSkEDIDR	k9: Acetyl (+42.01)
Rv0350_dnaK	10	IVNEPTAAALAYGLDKGEk	k19: Acetyl (+42.01)
Rv0350_dnaK	10	NQAETLVYQTEkFVK	k12: Acetyl (+42.01)
Rv0350_dnaK	10	qATkDAGQIAGLNVLR	n-term: Gln->pyro-Glu (-17.03), k4: Acetyl (+42.01)
Rv0350_dnaK	10	VPEDTLNkVDAAVAEAK	k8: Acetyl (+42.01)
Rv2429_ahpD	2	AALPEYAkDIK	k8: Acetyl (+42.01)
Rv2429_ahpD	2	DIkLNLSSITR	k3: Acetyl (+42.01)
Rv0684_fusA1	1	ASAGHIYAVIGLK	
Rv0896_gltA2	2	ILAkLGGDDSLLGIAK	k4: Acetyl (+42.01)
Rv0896_gltA2	2	mFTVLFALGR	m1: Oxidation (+15.99)
Rv0860_fadB	2	GYSEkLEAK	k5: Acetyl (+42.01)
Rv0860_fadB	2	LEAkALER	k4: Acetyl (+42.01)
Rv0821c_phoY2	1	mGALALHVAkIAR	m1: Oxidation (+15.99), k10: Acetyl (+42.01)
Rv0282_eccA3	2	ADLDkFLDTNEGLR	k5: Acetyl (+42.01)
Rv0282_eccA3	2	LVVIIAGYR	
Rv3295_Rv3295	1	AFFAAVVkDEADR	k8: Acetyl (+42.01)
Rv0569_Rv0569	2	FGAVQSAILHAR	
Rv0569_Rv0569	2	GLIIEVR	
Rv2753c_dapA	1	ALASHPNIVGVkDAK	k12: Acetyl (+42.01)
Rv3850_Rv3850	1	DVETkQFVSAVTNR	k5: Acetyl (+42.01)
Rv0933_pstB	2	LTVIIVTHNLAQAAR	
Rv0933_pstB	2	LTVIIVTHNLAQAAR	
Rv1023_eno	1	VAkYNQLLR	k3: Acetyl (+42.01)
Rv0148_Rv0148	1	VALFGNDGANFDkPPSVQDVAAR	k13: Acetyl (+42.01)
Rv1133c_metE	1	VLAELkEALGQGIPAR	k6: Acetyl (+42.01)
Rv2783c_gpsI	5	DGLVHISkLGK	k8: Acetyl (+42.01)
Rv2783c_gpsI	5	IDEIkTQVVQR	k5: Acetyl (+42.01)
Rv2783c_gpsI	5	LRVEIADIDkR	k10: Acetyl (+42.01)
Rv2783c_gpsI	5	VEDVVNVGDkLR	k10: Acetyl (+42.01)

Rv2783c_gpsI	5	VEIADIDkR	k8: Acetyl (+42.01)
Rv2158c_murE	1	GQGFLALVDYAHkPEALR	k13: Acetyl (+42.01)
Rv2509_Rv2509	1	GSGVHVTVLAPGPVR	
Rv3628_ppa	4	DLEPGkFVK	k6: Acetyl (+42.01)
Rv3628_ppa	4	HFFVHYkDLEPGK	k7: Acetyl (+42.01)
Rv3628_ppa	4	HFFVHYkDLEPGK	k7: Acetyl (+42.01)
Rv3628_ppa	4	HFFVHYkDLEPGK	k7: Acetyl (+42.01)
Rv3029c_fixA	3	FPSFkGImAAK	k5: Acetyl (+42.01), m8: Oxidation (+15.99)
Rv3029c_fixA	3	FPSFkGImAAK	k5: Acetyl (+42.01), m8: Oxidation (+15.99)
Rv3029c_fixA	3	TNIVVLIK	
Rv2185c_TB16.3	1	LIDGALkDLK	k7: Acetyl (+42.01)
Rv1932_tpx	1	DLPFAQkR	k7: Acetyl (+42.01)
Rv0818_Rv0818	1	GRPLDLTYkEFELLK	k9: Acetyl (+42.01)
Rv3849_espR	1	AHGLPSAAQQkVLDR	k11: Acetyl (+42.01)
Rv2031c_hspX	6	DGQLTIkAER	k7: Acetyl (+42.01)
Rv2031c_hspX	6	GILTVSVAVSEGKPTEK	
Rv2031c_hspX	6	GILTVSVAVSEGKPTEK	
Rv2031c_hspX	6	SEFAYGSFVR	
Rv2031c_hspX	6	TVSLPVGADEDDIK	
Rv2031c_hspX	6	TVSLPVGADEDDIkATYDK	k14: Acetyl (+42.01)
Rv2213_pepB	1	DLVNTPPSHLFPAEFAkR	k17: Acetyl (+42.01)
Rv1617_pykA	1	qVDkSLLELAR	n-term: Gln->pyro-Glu (-17.03), k4: Acetyl (+42.01)
Rv1448c_tal	1	IVDRPNLFIkIPATK	k10: Acetyl (+42.01)
Rv1925_fadD31	2	NIkYVGDLVAYR	k3: Acetyl (+42.01)
Rv1925_fadD31	2	NIkYVGDLVAYR	k3: Acetyl (+42.01)
Rv2626c_hrp1	1	HLPEHAIVQFVK	
Rv3676_crp	1	LYIIISGK	
Rv2839c_infB	1	VHELAkELGVTSK	k6: Acetyl (+42.01)
Rv0652_rplL	5	EAkDLVDGAPKPLLEK	k3: Acetyl (+42.01)
Rv0652_rplL	5	EAkDLVDGAPKPLLEK	k3: Acetyl (+42.01)
Rv0652_rplL	5	EAkDLVDGAPKPLLEK	k3: Acetyl (+42.01)
Rv0652_rplL	5	EIVSGLGLK	
Rv0652_rplL	5	IGVIkVVR	k5: Acetyl (+42.01)
Rv0655_mkl	2	AQAAILDDLEGTHkYAVHEIGQ	k14: Acetyl (+42.01)
Rv0655_mkl	2	LALVGLGGDEKk	k12: Acetyl (+42.01)
Rv0636_hadB	1	FTAVVPVPNDGkGAELVFNGR	k12: Acetyl (+42.01)
Rv0155_pntAa	1	GGQTLIGFLAPR	

Rv1306_atpF	2	AEQQVASTLQTAHEQLkR	k17: Acetyl (+42.01)
Rv1306_atpF	2	AEQQVASTLQTAHEQLkR	k17: Acetyl (+42.01)
Rv2744c_35kd_ag	1	qLADIEkLQVNVR	n-term: Gln->pyro-Glu (-17.03), k7: Acetyl (+42.01)
Rv1201c_dapD	2	GPVTVYGVDkFPR	k10: Acetyl (+42.01)
Rv1201c_dapD	2	RGPVTVYGVDkFPR	k11: Acetyl (+42.01)
Rv1521_fadD25	3	DLLIVYGR	
Rv1521_fadD25	3	IkDLLIVYGR	k2: Acetyl (+42.01)
Rv1521_fadD25	3	LVAIIELKk	k9: Acetyl (+42.01)
Rv0702_rplD	1	QVLVVIGR	
Rv1629_polA	1	FTPEAVVEkYGLTPR	k9: Acetyl (+42.01)
Rv1248c_Rv1248c	1	DFTEIkFR	k6: Acetyl (+42.01)
Rv3868_eccA1	1	LVVIIAGYSSDIDR	
Rv0685_tuf	9	GITINIAHVEYQTDK	
Rv0685_tuf	9	GITINIAHVEYQTDKR	
Rv0685_tuf	9	GQVVTKPGTTTPHTEFEGQVYILSkDEGGR	k25: Acetyl (+42.01)
Rv0685_tuf	9	LLDQGQAGDNVGLLLR	
Rv0685_tuf	9	LLDQGQAGDNVGLLLR	
Rv0685_tuf	9	TTVTGVEmFR	m8: Oxidation (+15.99)
Rv0685_tuf	9	VLHDkFPDLNETK	k5: Acetyl (+42.01)
Rv0685_tuf	9	VLHDKFPDLNETkAFDQIDNAPEER	k13: Acetyl (+42.01)
Rv0685_tuf	9	VSALkALEGDAK	k5: Acetyl (+42.01)
Rv3520c_Rv3520c	1	ALkPITHPLR	k3: Acetyl (+42.01)
Rv0440_groEL2	25	AGAATEVELkER	k10: Acetyl (+42.01)
Rv0440_groEL2	25	AGAATEVELkER	k10: Acetyl (+42.01)
Rv0440_groEL2	25	DETTIVEGAGDTDAIAGR	
Rv0440_groEL2	25	DLLPLLEK	
Rv0440_groEL2	25	EIELEDPYEkIGAELVK	k10: Acetyl (+42.01)
Rv0440_groEL2	25	FDkGYISGYFVTDPER	k3: Acetyl (+42.01)
Rv0440_groEL2	25	GLNALADAVK	
Rv0440_groEL2	25	GTFkSVAVK	k4: Acetyl (+42.01)
Rv0440_groEL2	25	GTFkSVAVK	k4: Acetyl (+42.01)
Rv0440_groEL2	25	GYISGYFVTDPER	
Rv0440_groEL2	25	IGAELVkEVAK	k7: Acetyl (+42.01)
Rv0440_groEL2	25	KTDDVAGDGTTTATVLAQALVR	
Rv0440_groEL2	25	kVVVTKDETTIVEGAGDTDAIAGR	k1: Acetyl (+42.01)
Rv0440_groEL2	25	LAkLAGGVAVIK	k3: Acetyl (+42.01)
Rv0440_groEL2	25	NVAAGANPLGLkR	k12: Acetyl (+42.01)
Rv0440_groEL2	25	NVAAGANPLGLkR	k12: Acetyl (+42.01)
Rv0440_groEL2	25	QEIENSDSDYDREkLQER	k14: Acetyl (+42.01)

Rv0440_groEL2	25	QEIENSDSDYDREkLQER	k14: Acetyl (+42.01)
Rv0440_groEL2	25	QIAFNSGLEPGVVAEK	
Rv0440_groEL2	25	QIAFNSGLEPGVVAEkVR	k16: Acetyl (+42.01)
Rv0440_groEL2	25	qIAFNSGLEPGVVAEkVR	n-term: Gln->pyro-Glu (-17.03), k16: Acetyl (+42.01)
Rv0440_groEL2	25	QIAFNSGLEPGVVAEkVR	k16: Acetyl (+42.01)
Rv0440_groEL2	25	VALEAPLK	
Rv0440_groEL2	25	VTETLLKGAk	k10: Acetyl (+42.01)
Rv0440_groEL2	25	VVVTkDETTIVEGAGDTDAIAGR	k5: Acetyl (+42.01)
Rv3131_Rv3131	1	TVLTLAVR	
Rv3246c_mtrA	2	VEkDPENPTVVLTVR	k3: Acetyl (+42.01)
Rv3246c_mtrA	2	VEkDPENPTVVLTVR	k3: Acetyl (+42.01)
Rv1388_mihF	2	GGTNLTQVLK	
Rv1388_mihF	2	GGTNLTQVLkDAESDEVLGK	k10: Acetyl (+42.01)
Rv0157_pntB	1	GVPVkYAIHPVAGR	k5: Acetyl (+42.01)
Rv2145c_wag31	1	TYLESQLEELGQR	
Rv0513_Rv0513	1	LAEIVkIYPEADGR	k6: Acetyl (+42.01)
Rv3598c_lysS	1	GIADSLGLEkDPAIHDNR	k10: Acetyl (+42.01)
Rv1658_argG	1	GFVYVHGLSSkLAAR	k11: Acetyl (+42.01)
Rv3846_sodA	2	GANDAVAkLEEAR	k8: Acetyl (+42.01)
Rv3846_sodA	2	GANDAVAkLEEAR	k8: Acetyl (+42.01)
Rv1181_pks4	1	FAAAVQAALkDGYR	k10: Acetyl (+42.01)
Rv1837c_glcB	1	GDLAAAVDkDGTAFLR	k9: Acetyl (+42.01)
Rv0667_rpoB	2	STLEkDNTVGTDEALLDIYR	k5: Acetyl (+42.01)
Rv0667_rpoB	2	STLEkDNTVGTDEALLDIYR	k5: Acetyl (+42.01)
Rv3688c_Rv3688c	1	ELSDDEVIkVLAR	k9: Acetyl (+42.01)
Rv0462_lpdC	2	ALPNEDADVSkEIEK	k11: Acetyl (+42.01)
Rv0462_lpdC	2	VAGVHFLmkK	m8: Oxidation (+15.99), k9: Acetyl (+42.01)
Rv3581c_ispF	2	HVVVLITQHGYR	
Rv3581c_ispF	2	HVVVLITQHGYR	
Rv3418c_groES	3	RIPLDVAEGDTVIYSkYGGTEIK	k16: Acetyl (+42.01)
Rv3418c_groES	3	RIPLDVAEGDTVIYSkYGGTEIK	k16: Acetyl (+42.01)
Rv3418c_groES	3	VNIkPLEDK	k4: Acetyl (+42.01)
Rv0815c_cysA2	1	VkLLDGGR	k2: Acetyl (+42.01)
Rv3028c_fixB	1	AAVDSGYYPGQFQVGQTGK	
Rv2889c_tsf	3	AEGKPEQALPkIVEGR	k11: Acetyl (+42.01)
Rv2889c_tsf	3	GDDAAAAHAVALQIAALR	
Rv2889c_tsf	3	IGEkLELR	k4: Acetyl (+42.01)

Rv0873_fadE10	1	TEAFLVkLR	k7: Acetyl (+42.01)
Rv0951_sucC	2	AGGVkYAATPQDAYEHAK	k5: Acetyl (+42.01)
Rv0951_sucC	2	VPVNAVkGVDLDFAR	k7: Acetyl (+42.01)
Rv0831c_Rv0831c	2	AQVSSIVGLER	
Rv0831c_Rv0831c	2	ELkHLLINDLPIER	k3: Acetyl (+42.01)
Rv0884c_serC	1	SLHLTYGEFSAkFASAVSK	k12: Acetyl (+42.01)
Rv0009_ppiA	1	TVANFVGLAQGTK	
Rv3417c_groEL1	1	LAkLAGGVAVIK	k3: Acetyl (+42.01)
Rv2882c_frr	1	DLDkTTHQYVTQIDELVK	k4: Acetyl (+42.01)
Rv0231_fadE4	2	GVEkDTFFETVAR	k4: Acetyl (+42.01)
Rv0231_fadE4	2	GVEkDTFFETVAR	k4: Acetyl (+42.01)
Rv0363c_fba	2	DkLDSYVRPLLAISAQR	k2: Acetyl (+42.01)
Rv0363c_fba	2	LRPDILAQGQQVAAAK	
Rv0002_dnaN	1	ALPNkPVDVHVEGNR	k5: Acetyl (+42.01)
Rv1488_Rv1488	1	NVVGGmTLEQTLTSR	m6: Oxidation (+15.99)
Rv0489_gpm1	1	HYGALQGLDkAETK	k10: Acetyl (+42.01)
Rv1463_Rv1463	1	YAESQHGGILLITHYTR	
Rv1436_gap	1	GLmTTIHAYTQDQNLQDGPHkDLR	m3: Oxidation (+15.99), k21: Acetyl (+42.01)
Rv0066c_icd2	1	IFYkDAFAK	k4: Acetyl (+42.01)
Rv2244_acpM	4	IPDEDLAGLR	
Rv2244_acpM	4	TVGDVVAYIQK	
Rv2244_acpM	4	TVGDVVAYIQK	
Rv2244_acpM	4	YGVkIPDEDLAGLR	k4: Acetyl (+42.01)
Rv3804c_fbpA	1	VQFQSGGANSPALYLLDGLR	
Rv1886c_fbpB	1	VQFQSGGNNSPAVYLLDGLR	
Rv1379_pyrR	1	IAHQIIEkTALDDPVGPDAPR	k8: Acetyl (+42.01)
Rv3457c_rpoA	2	NFGQkSIDEVK	k5: Acetyl (+42.01)
Rv3457c_rpoA	2	TLVELFGLAR	
Rv1308_atpA	6	AISLLLR	
Rv1308_atpA	6	ALELQAPSVVHR	
Rv1308_atpA	6	HVLIIFDDLTK	
Rv1308_atpA	6	HVLIIFDDLTK	
Rv1308_atpA	6	LTEVIkNFK	k6: Acetyl (+42.01)
Rv1308_atpA	6	TGEVLSVPVGDGFLGR	
Rv0005_gyrB	1	LLKDkDPNLTGDDIR	k5: Acetyl (+42.01)
Rv2241_aceE	2	GYALGkHFEGR	k6: Acetyl (+42.01)
Rv2241_aceE	2	TFkEVLR	k3: Acetyl (+42.01)
Rv2476c_gdh	5	ASGQkDLATLSVAAR	k5: Acetyl (+42.01)
Rv2476c_gdh	5	ASGQkDLATLSVAAR	k5: Acetyl (+42.01)

Rv2476c_gdh	5	ELEALPSEkEIAR	k9: Acetyl (+42.01)
Rv2476c_gdh	5	LLPkVLADVQR	k4: Acetyl (+42.01)
Rv2476c_gdh	5	LTDDDkLLVLAQAR	k6: Acetyl (+42.01)
Rv3396c_guaA	1	LLFkDEVR	k4: Acetyl (+42.01)
Rv3858c_gltD	1	ADPGGFLkYTHR	k8: Acetyl (+42.01)
Rv0718_rpsH	1	LkANIAQILK	k2: Acetyl (+42.01)
Rv3801c_fadD32	2	TGDYGTYFK	
Rv3801c_fadD32	2	TGDYGTYFkDHLYIAGR	k9: Acetyl (+42.01)
Rv3105c_prfB	1	VLQAkLLER	k5: Acetyl (+42.01)
Rv2468c_Rv2468c	1	FAIYLGDLGR	
Rv0716_rplE	1	SIAQFkLR	k6: Acetyl (+42.01)
Rv1872c_lldD2	2	AIEILQTGVIR	
Rv1872c_lldD2	2	DLAPLLQFNRPQFDTSkR	k17: Acetyl (+42.01)
Rv0683_rpsG	1	TGTDPVITLkR	k10: Acetyl (+42.01)
Rv2159c_Rv2159c	1	mKFVNHIEPVAPR	m1: Oxidation (+15.99), n-term: Acetyl (+42.01)
Rv2188c_pimB	1	kGQDTLVTALPSIR	k1: Acetyl (+42.01)

Table 4.13. Peptides Identified by Anti-Acetyl-Lysine Enrichment from ∆Rv1151 (mtCobB) Hypoxia Trypsinized Lysate.

Protein name	Total spectrum count	Peptide sequence	Variable modifications identified by spectrum
Rv1308_atpA	4	GFAATGGGSVVPDEHVEALDEDKLAk	k26: Acetyl (+42.01)
Rv1308_atpA	4	HVLIIFDDLTK	
Rv1308_atpA	4	LTEVIkNFK	k6: Acetyl (+42.01)
Rv1308_atpA	4	TAVcVDTILNQR	c4: Carbamidomethyl (+57.02)
Rv2940c_mas	1	LLTLGWQQR	
Rv2462c_tig	1	YGQAVAESDVQPLGRPNIEVTK	
Rv2145c_wag31	2	GSAAPVDSNADAGGFDQFNR	
Rv2145c_wag31	2	TYLESQLEELGQR	
Rv2220_glnA1	2	HYIGGLLHHAPSLLAFTNPTVNSYK	
Rv2220_glnA1	2	SVFDDGLAFDGSSIR	
Rv0384c_clpB	1	LQLQVSLPAK	
Rv3699_Rv3699	1	AAVSkYWK	k5: Acetyl (+42.01)
Rv0147_Rv0147	1	ITAALTkFR	k7: Acetyl (+42.01)
Rv3029c_fixA	2	AVEEALQIR	
Rv3029c_fixA	2	TNIVVLIK	
Rv3800c_pks13	4	HSVYFTHGIR	
Rv3800c_pks13	4	NWVGkAVGK	k5: Acetyl (+42.01)
Rv3800c_pks13	4	TRGGYLkDIK	k7: Acetyl (+42.01)
Rv3800c_pks13	4	YIKPGGEPIHDVEYWkK	k16: Acetyl (+42.01)
Rv0957_purH	1	AGVTLYLTGAR	
Rv1656_argF	1	ALLVWLLER	
Rv0632c_echA3	2	GGFELAYR	
Rv0632c_echA3	2	SAYQQATGLAK	
Rv0704_rplB	1	SAGSSIQLLGK	
Rv3592_mhuD	2	AHAVENSPGFLGFQLLRPVK	
Rv3592_mhuD	2	INAIEVPAGAGPELEkR	k16: Acetyl (+42.01)
Rv1310_atpD	3	FTQAGSEVSTLLGR	
Rv1310_atpD	3	GVEVIDTGR	
Rv1310_atpD	3	TISLQPTDGLVR	
Rv3569c_hsaD	1	LSkFSVAPTR	k3: Acetyl (+42.01)
Rv2391_sirA	1	DWGIAkFR	k6: Acetyl (+42.01)
Rv2958c_Rv2958c	1	LSLSVSAR	
Rv2996c_serA1	2	AQGINLIIHYVDRPGALGK	
Rv2996c_serA1	2	TKPGVIIVNAAR	

Rv2385_mbtJ	1	AmTYVAQFIR	m2: Oxidation (+15.99)
Rv0244c_fadE5	1	GLSLYFVPK	
Rv1437_pgk	1	SVANLkDLLAEGVSGR	k6: Acetyl (+42.01)
Rv1390_rpoZ	1	YALVIYAAK	
Rv1827_garA	1	LVFLTGPK	
Rv0859_fadA	1	LKPAFEGLAALGGFDDVALQkYH WVEK	k21: Acetyl (+42.01)
Rv0810c_Rv0810c	1	ELkYSSPQTDFQR	k3: Acetyl (+42.01)
Rv3283_sseA	1	SSHTWFVLTHLLGK	
Rv0350_dnaK	10	AALGGSDISAIK	
Rv0350_dnaK	10	DAGQIAGLNVLR	
Rv0350_dnaK	10	IQEGSGLSkEDIDR	k9: Acetyl (+42.01)
Rv0350_dnaK	10	ITQDLLDR	
Rv0350_dnaK	10	KYTAPEISAR	
Rv0350_dnaK	10	NQAETLVYQTEK	
Rv0350_dnaK	10	NQAETLVYQTEKFVk	k15: Acetyl (+42.01)
Rv0350_dnaK	10	NQAETLVYQTEkFVK	k12: Acetyl (+42.01)
Rv0350_dnaK	10	VVDWLVDKFk	k10: Acetyl (+42.01)
Rv0350_dnaK	10	YTAPEISAR	
Rv0896_gltA2	2	LPGWIAHWR	
Rv0896_gltA2	2	VYkNYDPR	k3: Acetyl (+42.01)
Rv3489_Rv3489	1	SDHGEIGDVEPLADSTASQAR	
Rv2429_ahpD	2	AALPEYAkDIK	k8: Acetyl (+42.01)
Rv2429_ahpD	2	DIkLNLSSITR	k3: Acetyl (+42.01)
Rv0489_gpm1	1	HYGALQGLDkAETK	k10: Acetyl (+42.01)
Rv3747_Rv3747	1	LNVQGGVLSR	
Rv3874_esxB	2	TDAATLAQEAGNFER	
Rv3874_esxB	2	TQIDQVESTAGSLQGQWR	
Rv0860_fadB	7	ANPDGAGVQPWDKk	k14: Acetyl (+42.01)
Rv0860_fadB	7	GAGFYEYADGK	
Rv0860_fadB	7	GYSEkLEAK	k5: Acetyl (+42.01)
Rv0860_fadB	7	LEAkALER	k4: Acetyl (+42.01)
Rv0860_fadB	7	LVAEkDSITGVVVASAK	k5: Acetyl (+42.01)
Rv0860_fadB	7	LVAEkDSITGVVVASAK	k5: Acetyl (+42.01)
Rv0860_fadB	7	TFFAGGDVK	
Rv3028c_fixB	1	AAVDSGYYPGQFQVGQTGK	
Rv0282_eccA3	1	LVVIIAGYR	
Rv1483_fabG1	1	GIGLAIAQR	
Rv0041_leuS	1	FVYPGPDGEVEVFQEFGkIGK	k18: Acetyl (+42.01)
Rv2115c_mpa	1	EQLENAVGSHAPTR	
Rv0247c_Rv0247c	1	LQQTQTPDLAVR	

Rv2986c_hupB	2	AELIDVLTQK	
Rv2986c_hupB	2	AELIDVLTQkLGSDR	k10: Acetyl (+42.01)
Rv0854_Rv0854	1	SQDGkYELTPK	k5: Acetyl (+42.01)
Rv0569_Rv0569	2	FGAVQSAILHAR	
Rv0569_Rv0569	2	GLIIEVR	
Rv2524c_fas	1	GSQYAIAGTVR	
Rv2785c_rpsO	1	GLLLLVGR	
Rv3566c_nat	2	VASWYASTHPASkFVTGLTAAVITDDAR	k13: Acetyl (+42.01)
Rv3566c_nat	2	VASWYASTHPASkFVTGLTAAVITDDAR	k13: Acetyl (+42.01)
Rv0652_rplL	3	EAkDLVDGAPKPLLEK	k3: Acetyl (+42.01)
Rv0652_rplL	3	EAkDLVDGAPKPLLEK	k3: Acetyl (+42.01)
Rv0652_rplL	3	EIVSGLGLK	
Rv0433_Rv0433	1	WAEFEGFVYDQKk	k13: Acetyl (+42.01)
Rv0148_Rv0148	2	VALFGNDGANFDkPPSVQDVAAR	k13: Acetyl (+42.01)
Rv0148_Rv0148	2	VHLYGGYHVLR	
Rv0467_icl1	1	SAEQIQQEWDTNPR	
Rv1133c_metE	5	EALGQGIPARPVIIGPITFLLLSK	
Rv1133c_metE	5	SWLAFGAEK	
Rv1133c_metE	5	TLVAGVVDGR	
Rv1133c_metE	5	WAVGAFR	
Rv1133c_metE	5	WFDTNYHYLVPEIGPSTTFTLHPGK	
Rv1630_rpsA	4	AWGTIEALKEkDEAVK	k11: Acetyl (+42.01)
Rv1630_rpsA	4	AWLEQTQSEVR	
Rv1630_rpsA	4	GTVIEVVK	
Rv1630_rpsA	4	RAWLEQTQSEVR	
Rv0905_echA6	1	VVAPDAFFQFPTSkYGLALDNWSIR	k14: Acetyl (+42.01)
Rv2783c_gpsI	2	DGLVHISkLGK	k8: Acetyl (+42.01)
Rv2783c_gpsI	2	VEIADIDkR	k8: Acetyl (+42.01)
Rv0824c_desA1	1	SVDPVELEkLR	k9: Acetyl (+42.01)
Rv3628_ppa	2	DLEPGkFVK	k6: Acetyl (+42.01)
Rv3628_ppa	2	HFFVHYkDLEPGK	k7: Acetyl (+42.01)
Rv2460c_clpP2	1	ILTAEEAkDYGIIDTVLEYR	k8: Acetyl (+42.01)
Rv0707_rpsC	1	AAGGEEAAPDAAAPVEAQSTES	
Rv1886c_fbpB	1	VQFQSGGNNSPAVYLLDGLR	
Rv2299c_htpG	1	DGQQQIFYATGETR	
Rv0054_ssb	1	QTGEWkDGEALFLR	k6: Acetyl (+42.01)
Rv3001c_ilvC	1	VGVIGYGSQGHAHSLSLR	
Rv2031c_hspX	5	GILTVSVAVSEGKPTEK	

Rv2031c_hspX	5	SEFAYGSFVR	
Rv2031c_hspX	5	TEQkDFDGRSEFAYGSFVR	k4: Acetyl (+42.01)
Rv2031c_hspX	5	TVSLPVGADEDDIKATYDK	
Rv2031c_hspX	5	TVSLPVGADEDDIkATYDK	k14: Acetyl (+42.01)
Rv2780_ald	1	HGQILFTFLHLAASR	
Rv0155_pntAa	1	GGQTLIGFLAPR	
Rv2699c_Rv2699c	1	RTETDDVSEDSLEELkAR	k16: Acetyl (+42.01)
Rv0248c_Rv0248c	2	GQYAETEEEADQWLkDNDSAR	k15: Acetyl (+42.01)
Rv0248c_Rv0248c	2	HSYDVVVIGAGGAGLR	
Rv2467_pepN	1	FAVTQSGAAPGAGETR	
Rv3596c_clpC1	1	SQVEEIIGQGGQQAPSGHIPFTPR	
Rv1658_argG	1	GFVYVHGLSSkLAAR	k11: Acetyl (+42.01)
Rv3418c_groES	13	EKPQEGTVVAVGPGR	
Rv3418c_groES	13	EKPQEGTVVAVGPGRWDEDGEK	
Rv3418c_groES	13	ILVQANEAETTTASGLVIPDTAK	
Rv3418c_groES	13	IPLDVAEGDTVIYSkYGGTEIK	k15: Acetyl (+42.01)
Rv3418c_groES	13	RIPLDVAEGDTVIYSk	k16: Acetyl (+42.01)
Rv3418c_groES	13	RIPLDVAEGDTVIYSK	
Rv3418c_groES	13	RIPLDVAEGDTVIYSkYGGTEIK	k16: Acetyl (+42.01)
Rv3418c_groES	13	VNIKPLEDK	
Rv3418c_groES	13	VNIKPLEDkILVQANEAETTTASG LVIPDTAK	k9: Acetyl (+42.01)
Rv3418c_groES	13	WDEDGEkRIPLDVAEGDTVIYSK	k7: Acetyl (+42.01)
Rv3418c_groES	13	WDEDGEkRIPLDVAEGDTVIYSK	k7: Acetyl (+42.01)
Rv3418c_groES	13	YNGEEYLILSAR	
Rv3418c_groES	13	YNGEEYLILSAR	
Rv1629_polA	1	FTPEAVVEkYGLTPR	k9: Acetyl (+42.01)
Rv1240_mdh	2	ALNAVAADDVR	
Rv1240_mdh	2	GASSAASAASATIDAAR	
Rv1521_fadD25	2	DLLIVYGR	
Rv1521_fadD25	2	SAAHGHPDILYLQYTSGSTR	
Rv0379_secE2	1	SVYkVIDIIGTSPTSWEQAAAEAV QR	k4: Acetyl (+42.01)
Rv3676_crp	1	LYIIISGK	
Rv2839c_infB	1	GASLSDFADK	
Rv0639_nusG	1	SKPGDWYVVHSYAGYENK	
Rv3875_esxA	1	LAAAWGGSGSEAYQGVQQK	
Rv1391_dfp	1	RkGcDLLVVNAVGEGR	k2: Acetyl (+42.01), c4: Carbamidomethyl (+57.02)
Rv0636_hadB	1	GAELVFNGR	
Rv0046c_ino1	1	SEHQSLPAPEASTEVR	

Rv0951_sucC	1	AGGVkYAATPQDAYEHAK	k5: Acetyl (+42.01)
Rv1201c_dapD	1	RGPVTVYGVDkFPR	k11: Acetyl (+42.01)
Rv3852_hns	1	SAPPKPAEAPVSLQQR	
Rv0702_rplD	1	QVLVVIGR	
Rv1248c_Rv1248c	1	DFTEIkFR	k6: Acetyl (+42.01)
Rv0009_ppiA	1	TVANFVGLAQGTK	
Rv0296c_Rv0296c	3	ENLLIVHWHDLGR	
Rv0296c_Rv0296c	3	ENLLIVHWHDLGR	
Rv0296c_Rv0296c	3	ENLLIVHWHDLGR	
Rv0706_rplV	1	TSHITVVVESR	
Rv1925_fadD31	2	NIkYVGDLVAYR	k3: Acetyl (+42.01)
Rv1925_fadD31	2	NIkYVGDLVAYR	k3: Acetyl (+42.01)
Rv1596_nadC	2	ALQkYAVR	k4: Acetyl (+42.01)
Rv1596_nadC	2	LGLGDAALIkDNHVAAAGSVVD ALR	k10: Acetyl (+42.01)
Rv0685_tuf	12	AFDQIDNAPEER	
Rv0685_tuf	12	ELLAAQEFDEDAPVVR	
Rv0685_tuf	12	GITINIAHVEYQTDK	
Rv0685_tuf	12	GITINIAHVEYQTDKR	
Rv0685_tuf	12	GITINIAHVEYQTDKR	
Rv0685_tuf	12	HTPFFNNYR	
Rv0685_tuf	12	HTPFFNNYRPQFYFR	
Rv0685_tuf	12	LLDQGQAGDNVGLLLR	
Rv0685_tuf	12	PGTTTPHTEFEGQVYILSkDEGG R	k19: Acetyl (+42.01)
Rv0685_tuf	12	TTLTAAITK	
Rv0685_tuf	12	VLHDkFPDLNETK	k5: Acetyl (+42.01)
Rv0685_tuf	12	VLHDkFPDLNETK	k5: Acetyl (+42.01)
Rv0440_groEL2	33	AGAATEVELkER	k10: Acetyl (+42.01)
Rv0440_groEL2	33	AGAATEVELkER	k10: Acetyl (+42.01)
Rv0440_groEL2	33	AGAATEVELkERK	k10: Acetyl (+42.01)
Rv0440_groEL2	33	DETTIVEGAGDTDAIAGR	
Rv0440_groEL2	33	DETTIVEGAGDTDAIAGR	
Rv0440_groEL2	33	DETTIVEGAGDTDAIAGR	
Rv0440_groEL2	33	EIELEDPYEkIGAELVK	k10: Acetyl (+42.01)
Rv0440_groEL2	33	FDkGYISGYFVTDPER	k3: Acetyl (+42.01)
Rv0440_groEL2	33	GLNALADAVK	
Rv0440_groEL2	33	GTFkSVAVK	k4: Acetyl (+42.01)
Rv0440_groEL2	33	GYISGYFVTDPER	
Rv0440_groEL2	33	KTDDVAGDGTTTATVLAQALVR	
Rv0440_groEL2	33	KVVVTkDETTIVEGAGDTDAIAG	k6: Acetyl (+42.01)

		R	
Rv0440_groEL2	33	LAGGVAVIK	
Rv0440_groEL2	33	LAkLAGGVAVIK	k3: Acetyl (+42.01)
Rv0440_groEL2	33	NVAAGANPLGLK	
Rv0440_groEL2	33	NVAAGANPLGLkR	k12: Acetyl (+42.01)
Rv0440_groEL2	33	QEIENSDSDYDREkLQER	k14: Acetyl (+42.01)
Rv0440_groEL2	33	qEIENSDSDYDREkLQER	n-term: Gln->pyro-Glu (-17.03), k14: Acetyl (+42.01)
Rv0440_groEL2	33	qEIENSDSDYDREkLQER	n-term: Gln->pyro-Glu (-17.03), k14: Acetyl (+42.01)
Rv0440_groEL2	33	QIAFNSGLEPGVVAEK	
Rv0440_groEL2	33	qIAFNSGLEPGVVAEK	n-term: Gln->pyro-Glu (-17.03)
Rv0440_groEL2	33	qIAFNSGLEPGVVAEkVR	n-term: Gln->pyro-Glu (-17.03), k16: Acetyl (+42.01)
Rv0440_groEL2	33	qIAFNSGLEPGVVAEkVR	n-term: Gln->pyro-Glu (-17.03), k16: Acetyl (+42.01)
Rv0440_groEL2	33	QIAFNSGLEPGVVAEkVR	k16: Acetyl (+42.01)
Rv0440_groEL2	33	QIAFNSGLEPGVVAEkVR	k16: Acetyl (+42.01)
Rv0440_groEL2	33	SALQNAASIAGLFLTTEAVVADKPEK	
Rv0440_groEL2	33	TDDVAGDGTTTATVLAQALVR	
Rv0440_groEL2	33	VALEAPLK	
Rv0440_groEL2	33	VSTVkDLLPLLEK	k5: Acetyl (+42.01)
Rv0440_groEL2	33	VTETLLK	
Rv0440_groEL2	33	VTETLLkGAK	k7: Acetyl (+42.01)
Rv0440_groEL2	33	VVVTkDETTIVEGAGDTDAIAGR	k5: Acetyl (+42.01)
Rv3648c_cspA	2	TLEENQkVEFEIGHSPK	k7: Acetyl (+42.01)
Rv3648c_cspA	2	VEFEIGHSPK	
Rv3246c_mtrA	1	VEkDPENPTVVLTVR	k3: Acetyl (+42.01)
Rv2246_kasB	1	YAINNSFGFGGHNVAIAFGR	
Rv0157_pntB	1	GVPVkYAIHPVAGR	k5: Acetyl (+42.01)
Rv2454c_Rv2454c	1	FPYYLETYGFHSIHGR	
Rv3846_sodA	1	GANDAVAkLEEAR	k8: Acetyl (+42.01)
Rv3270_ctpC	2	ASEWVDkLR	k7: Acetyl (+42.01)
Rv3270_ctpC	2	ASEWVDkLRR	k7: Acetyl (+42.01)
Rv3281_accE5	1	VSGTNEVSDGNETNNPAPVSR	
Rv1015c_rplY	1	TIQHADLLVVR	
Rv1837c_glcB	2	DELQAQIDkWHR	k9: Acetyl (+42.01)
Rv1837c_glcB	2	GDLAAAVDkDGTAFLR	k9: Acetyl (+42.01)
Rv0667_rpoB	2	GENIPEPGIPESFK	
Rv0667_rpoB	2	GTFIINGTER	
Rv1643_rplT	1	EQQLHSLNYAYR	
Rv3581c_ispF	1	HVVVLITQHGYR	

Rv3274c_fadE25	4	DDEGFTVGPkER	k10: Acetyl (+42.01)
Rv3274c_fadE25	4	EIAPHAAEVDEkAR	k12: Acetyl (+42.01)
Rv3274c_fadE25	4	GSPTTELYFENcR	c12: Carbamidomethyl (+57.02)
Rv3274c_fadE25	4	ITQIYEGTNQIQR	
Rv0815c_cysA2	4	DFVDAQQFSkLLSER	k10: Acetyl (+42.01)
Rv0815c_cysA2	4	SDEELAkLYADAGLDNSK	k7: Acetyl (+42.01)
Rv0815c_cysA2	4	SSHTWFVLR	
Rv0815c_cysA2	4	SSHTWFVLR	
Rv1098c_fum	1	NILESFkLLTNVSR	k7: Acetyl (+42.01)
Rv2971_Rv2971	1	TPAQVLLR	
Rv3858c_gltD	1	ADPGGFLkYTHR	k8: Acetyl (+42.01)
Rv2889c_tsf	1	AEGKPEQALPkIVEGR	k11: Acetyl (+42.01)
Rv0873_fadE10	1	TEAFLVkLR	k7: Acetyl (+42.01)
Rv2703_sigA	2	AmADQARTIR	m2: Oxidation (+15.99)
Rv2703_sigA	2	AVEkFDYTK	k4: Acetyl (+42.01)
Rv0831c_Rv0831c	1	AQVSSIVGLER	
Rv0211_pckA	3	GNDWYFR	
Rv0211_pckA	3	VFFVNWFR	
Rv0211_pckA	3	VVFTDGSEEEFQR	
Rv3417c_groEL1	6	AEIDKSDSDWDREkLGER	k14: Acetyl (+42.01)
Rv3417c_groEL1	6	AEIDKSDSDWDREkLGER	k14: Acetyl (+42.01)
Rv3417c_groEL1	6	EVGLEVLGSAR	
Rv3417c_groEL1	6	LAGGVAVIK	
Rv3417c_groEL1	6	LAkLAGGVAVIK	k3: Acetyl (+42.01)
Rv3417c_groEL1	6	SDSDWDREkLGER	k9: Acetyl (+42.01)
Rv0281_Rv0281	1	TkYFDEYFR	k2: Acetyl (+42.01)
Rv0363c_fba	1	DkLDSYVRPLLAISAQR	k2: Acetyl (+42.01)
Rv0002_dnaN	1	LLDAEFPkFR	k8: Acetyl (+42.01)
Rv3692_moxR2	2	GATALLGTAR	
Rv3692_moxR2	2	GHVLLEGVPGVAK	
Rv1463_Rv1463	3	YAESQHGGILLITHYTR	
Rv1463_Rv1463	3	YAESQHGGILLITHYTR	
Rv1463_Rv1463	3	YIHPEYVHVFVGGR	
Rv1636_TB15.3	5	AADILkDESYK	k6: Acetyl (+42.01)
Rv1636_TB15.3	5	LIIASAYLPQHEDAR	
Rv1636_TB15.3	5	LLGSVPANVSR	
Rv1636_TB15.3	5	VDVLIVHTT	
Rv1636_TB15.3	5	VTGTAPIYEILHDAkER	k15: Acetyl (+42.01)
Rv0407_fgd1	1	GASIYDVPDGGVPVYIAAGGPAV AkYAGR	k25: Acetyl (+42.01)
Rv3710_leuA	2	AIVHFYNSTSILQR	

Rv3710_leuA	2	cVEQAAkYPGTQWR	c1: Carbamidomethyl (+57.02), k7: Acetyl (+42.01)
Rv1479_moxR1	2	GHVLLEGVPGVAK	
Rv1479_moxR1	2	SWVAFGASPR	
Rv2954c_Rv2954c	1	HFHSIFYLR	
Rv2244_acpM	5	IESENPDAVANVQAR	
Rv2244_acpM	5	IESENPDAVANVQAR	
Rv2244_acpM	5	IPDEDLAGLR	
Rv2244_acpM	5	LEEENPEAAQALR	
Rv2244_acpM	5	TVGDVVAYIQK	
Rv0688_Rv0688	1	EFYDEkDIALR	k6: Acetyl (+42.01)
Rv2711_ideR	1	LDQSGPTVSQTVSR	
Rv3248c_sahH	4	GVPVFAWK	
Rv3248c_sahH	4	GVTEETTTGVLR	
Rv3248c_sahH	4	HSLIDGINR	
Rv3248c_sahH	4	VLIcGYGDVGK	c4: Carbamidomethyl (+57.02)
Rv3457c_rpoA	4	GYVPAVQNR	
Rv3457c_rpoA	4	LHQLGLSLK	
Rv3457c_rpoA	4	NFGQkSIDEVK	k5: Acetyl (+42.01)
Rv3457c_rpoA	4	TLVELFGLAR	
Rv2605c_tesB2	1	ASQQQVWLR	
Rv0701_rplC	1	VNKPLTGQYTAAGVNPR	
Rv2241_aceE	2	GYALGkHFEGR	k6: Acetyl (+42.01)
Rv2241_aceE	2	TFkEVLR	k3: Acetyl (+42.01)
Rv2476c_gdh	1	ASGQkDLATLSVAAR	k5: Acetyl (+42.01)
Rv3396c_guaA	1	LLFkDEVR	k4: Acetyl (+42.01)
Rv1475c_acn	2	GTLLLGVR	
Rv1475c_acn	2	NYADVFkGDDRWR	k7: Acetyl (+42.01)
Rv0154c_fadE2	1	AAWTIDQHGNkEAR	k11: Acetyl (+42.01)
Rv0566c_Rv0566c	1	AAVDVFKEk	k9: Acetyl (+42.01)
Rv0462_lpdC	2	ALPNEDADVSKEIEkQFK	k15: Acetyl (+42.01)
Rv0462_lpdC	2	NEGYDVVVAkFPFTANAK	k10: Acetyl (+42.01)
Rv0668_rpoC	5	DAGFYWATR	
Rv0668_rpoC	5	DGLFcEkIFGPTR	c5: Carbamidomethyl (+57.02), k7: Acetyl (+42.01)
Rv0668_rpoC	5	DWEcYcGkYK	c4: Carbamidomethyl (+57.02), c6: Carbamidomethyl (+57.02), k8: Acetyl (+42.01)
Rv0668_rpoC	5	LGYLLDLAPKDLEk	k14: Acetyl (+42.01)
Rv0668_rpoC	5	TLKPEkDGLFcEK	k6: Acetyl (+42.01), c11: Carbamidomethyl (+57.02)
Rv3597c_lsr2	1	GRIPADVIDAYHAAT	

Rv3801c_fadD32	1	TGDYGTYFkDHLYIAGR	k9: Acetyl (+42.01)
Rv2468c_Rv2468c	1	FAIYLGDLGR	
Rv0716_rplE	1	SIAQFkLR	k6: Acetyl (+42.01)
Rv0683_rpsG	2	TGTDPVITLkR	k10: Acetyl (+42.01)
Rv0683_rpsG	2	WLVGYSR	
Rv1002c_Rv1002c	1	QYQVQRPWLGTVR	

Bibliography

Allison, K.R., Brynildsen, M.P., and Collins, J.J. (2011). Metabolite-enabled eradication of bacterial persisters by aminoglycosides. Nature *473*, 216-220.

Anderson, K.L., Roberts, C., Disz, T., Vonstein, V., Hwang, K., Overbeek, R., Olson, P.D., Projan, S.J., and Dunman, P.M. (2006). Characterization of the Staphylococcus aureus heat shock, cold shock, stringent, and SOS responses and their effects on log-phase mRNA turnover. J Bacteriol *188*, 6739-6756.

Andries, K., Verhasselt, P., Guillemont, J., Gohlmann, H.W., Neefs, J.M., Winkler, H., Van Gestel, J., Timmerman, P., Zhu, M., Lee, E.*, et al.* (2005). A diarylquinoline drug active on the ATP synthase of Mycobacterium tuberculosis. Science *307*, 223-227.

Assfalg, V., Huser, N., Reim, D., Kaiser-Moore, S., Rossmann-Bloeck, T., Weighardt, H., Novotny, A.R., Stangl, M.J., Holzmann, B., and Emmanuel, K.L. (2010). Combined immunosuppressive and antibiotic therapy improves

bacterial clearance and survival of polymicrobial septic peritonitis. Shock *33*, 155-161.

Atrih, A., Zollner, P., Allmaier, G., and Foster, S.J. (1996). Structural analysis of Bacillus subtilis 168 endospore peptidoglycan and its role during differentiation. J Bacteriol *178*, 6173-6183.

Bacon, J., Dover, L.G., Hatch, K.A., Zhang, Y., Gomes, J.M., Kendall, S., Wernisch, L., Stoker, N.G., Butcher, P.D., Besra, G.S.*, et al.* (2007). Lipid composition and transcriptional response of Mycobacterium tuberculosis grown under iron-limitation in continuous culture: identification of a novel wax ester. Microbiology *153*, 1435-1444.

Baek, S.H., Li, A.H., and Sassetti, C.M. (2011). Metabolic regulation of mycobacterial growth and antibiotic sensitivity. PLoS Biol *9*, e1001065.

Baeza, I., Ibanez, M., Wong, C., Chavez, P., Gariglio, P., and Oro, J. (1991). Possible prebiotic significance of polyamines in the condensation, protection, encapsulation, and biological properties of DNA. Orig Life Evol Biosph *21*, 225-242.

Bai, G., Knapp, G.S., and McDonough, K.A. (2011). Cyclic AMP signalling in mycobacteria: redirecting the conversation with a common currency. Cell Microbiol *13*, 349-358.

Balaban, N.Q., Merrin, J., Chait, R., Kowalik, L., and Leibler, S. (2004). Bacterial persistence as a phenotypic switch. Science *305*, 1622-1625.

Banerjee, A., Adolph, R.S., Gopalakrishnapai, J., Kleinboelting, S., Emmerich, C., Steegborn, C., and Visweswariah, S.S. (2015). A universal stress protein (USP) in mycobacteria binds cAMP. J Biol Chem *290*, 12731-12743.

Beste, D.J., Bonde, B., Hawkins, N., Ward, J.L., Beale, M.H., Noack, S., Noh, K., Kruger, N.J., Ratcliffe, R.G., and McFadden, J. (2011). (1)(3)C metabolic flux analysis identifies an unusual route for pyruvate dissimilation in mycobacteria which requires isocitrate lyase and carbon dioxide fixation. PLoS Pathog *7*, e1002091.

Betts, J.C., Lukey, P.T., Robb, L.C., McAdam, R.A., and Duncan, K. (2002). Evaluation of a nutrient starvation model of Mycobacterium tuberculosis persistence by gene and protein expression profiling. Mol Microbiol *43*, 717-731.

Blumenthal, A., Trujillo, C., Ehrt, S., and Schnappinger, D. (2010). Simultaneous analysis of multiple Mycobacterium tuberculosis knockdown mutants in vitro and in vivo. PLoS One *5*, e15667.

Boshoff, H.I., and Barry, C.E., 3rd (2005). Tuberculosis - metabolism and respiration in the absence of growth. Nat Rev Microbiol *3*, 70-80.

Boshoff, H.I., Reed, M.B., Barry, C.E., 3rd, and Mizrahi, V. (2003). DnaE2 polymerase contributes to in vivo survival and the emergence of drug resistance in Mycobacterium tuberculosis. Cell *113*, 183-193.

Bourassa, L., and Camilli, A. (2009). Glycogen contributes to the environmental persistence and transmission of Vibrio cholerae. Mol Microbiol *72*, 124-138.

Bourigault, M.L., Vacher, R., Rose, S., Olleros, M.L., Janssens, J.P., Quesniaux, V.F., and Garcia, I. (2013). Tumor necrosis factor neutralization combined with chemotherapy enhances Mycobacterium tuberculosis clearance and reduces lung pathology. Am J Clin Exp Immunol *2*, 124-134.

Brown, M.R., Allison, D.G., and Gilbert, P. (1988). Resistance of bacterial biofilms to antibiotics: a growth-rate related effect? J Antimicrob Chemother *22*, 777-780.

Burton, B.M., Marquis, K.A., Sullivan, N.L., Rapoport, T.A., and Rudner, D.Z. (2007). The ATPase SpoIIIE transports DNA across fused septal membranes during sporulation in Bacillus subtilis. Cell *131*, 1301-1312.

Castano-Cerezo, S., Bernal, V., Blanco-Catala, J., Iborra, J.L., and Canovas, M. (2011). cAMP-CRP co-ordinates the expression of the protein acetylation pathway with central metabolism in Escherichia coli. Mol Microbiol *82*, 1110-1128.

Chen, Z., Odstrcil, E.A., Tu, B.P., and McKnight, S.L. (2007). Restriction of DNA replication to the reductive phase of the metabolic cycle protects genome integrity. Science *316*, 1916-1919.

Choder, M. (1991). A general topoisomerase I-dependent transcriptional repression in the stationary phase in yeast. Genes Dev *5*, 2315-2326.

Cole, J.J. (1999). Aquatic Microbiology for Ecosystem Scientists: New and Recycled Paradigms in Ecological Microbiology. Ecosystems *2*, 215-225.

Corper, H.J., and Cohn, M.L. (1933). The viability and virulence of old cultures of tuercule bacilli. Am Rev Tuberc *28*, 856-874.

Crosby, H.A., Heiniger, E.K., Harwood, C.S., and Escalante-Semerena, J.C. (2010). Reversible N epsilon-lysine acetylation regulates the activity of acyl-CoA synthetases involved in anaerobic benzoate catabolism in Rhodopseudomonas palustris. Mol Microbiol *76*, 874-888.

Crosby, H.A., Pelletier, D.A., Hurst, G.B., and Escalante-Semerena, J.C. (2012). System-wide studies of N-lysine acetylation in Rhodopseudomonas palustris reveal substrate specificity of protein acetyltransferases. J Biol Chem *287*, 15590-15601.

Cunningham, A.F., and Spreadbury, C.L. (1998). Mycobacterial stationary phase induced by low oxygen tension: cell wall thickening and localization of the 16-kilodalton alpha-crystallin homolog. J Bacteriol *180*, 801-808.

Daniel, J., Deb, C., Dubey, V.S., Sirakova, T.D., Abomoelak, B., Morbidoni, H.R., and Kolattukudy, P.E. (2004). Induction of a novel class of diacylglycerol acyltransferases and triacylglycerol accumulation in

Mycobacterium tuberculosis as it goes into a dormancy-like state in culture. J Bacteriol *186*, 5017-5030.

Daniel, J., Maamar, H., Deb, C., Sirakova, T.D., and Kolattukudy, P.E. (2011). Mycobacterium tuberculosis uses host triacylglycerol to accumulate lipid droplets and acquires a dormancy-like phenotype in lipid-loaded macrophages. PLoS Pathog *7*, e1002093.

Diacon, A.H., Dawson, R., von Groote-Bidlingmaier, F., Symons, G., Venter, A., Donald, P.R., van Niekerk, C., Everitt, D., Winter, H., Becker, P*., et al.* (2012). 14-day bactericidal activity of PA-824, bedaquiline, pyrazinamide, and moxifloxacin combinations: a randomised trial. Lancet *380*, 986-993.

Drlica, K., Malik, M., Kerns, R.J., and Zhao, X. (2008). Quinolone-mediated bacterial death. Antimicrob Agents Chemother *52*, 385-392.

Du, Y., Zhang, H., He, Y., Huang, F., and He, Z.G. (2012). Mycobacterium smegmatis Lsr2 physically and functionally interacts with a new flavoprotein involved in bacterial resistance to oxidative stress. J Biochem *152*, 479-486.

Duwat, P., Sourice, S., Cesselin, B., Lamberet, G., Vido, K., Gaudu, P., Le Loir, Y., Violet, F., Loubiere, P., and Gruss, A. (2001). Respiration capacity of

the fermenting bacterium Lactococcus lactis and its positive effects on growth and survival. J Bacteriol *183*, 4509-4516.

Eagle, H. (1952). Experimental approach to the problem of treatment failure with penicillin. I. Group A streptococcal infection in mice. Am J Med *13*, 389-399.

Engel, P., Kramer, R., and Unden, G. (1994). Transport of C4-dicarboxylates by anaerobically grown Escherichia coli. Energetics and mechanism of exchange, uptake and efflux. Eur J Biochem *222*, 605-614.

Eoh, H., and Rhee, K.Y. (2013). Multifunctional essentiality of succinate metabolism in adaptation to hypoxia in Mycobacterium tuberculosis. Proc Natl Acad Sci U S A *110*, 6554-6559.

Errington, J. (2003). Regulation of endospore formation in Bacillus subtilis. Nat Rev Microbiol *1*, 117-126.

Fang, X., Wallqvist, A., and Reifman, J. (2012). Modeling phenotypic metabolic adaptations of Mycobacterium tuberculosis H37Rv under hypoxia. PLoS Comput Biol *8*, e1002688.

Favrot, L., Blanchard, J.S., and Vergnolle, O. (2016). Bacterial GCN5-Related N-Acetyltransferases: From Resistance to Regulation. Biochemistry *55*, 989-1002.

Ferraris, D.M., Spallek, R., Oehlmann, W., Singh, M., and Rizzi, M. (2015). Structures of citrate synthase and malate dehydrogenase of Mycobacterium tuberculosis. Proteins *83*, 389-394.

Finkel, S.E. (2006). Long-term survival during stationary phase: evolution and the GASP phenotype. Nat Rev Microbiol *4*, 113-120.

Fischer, E., and Sauer, U. (2003). A novel metabolic cycle catalyzes glucose oxidation and anaplerosis in hungry Escherichia coli. J Biol Chem *278*, 46446-46451.

Ford, C.B., Lin, P.L., Chase, M.R., Shah, R.R., Iartchouk, O., Galagan, J., Mohaideen, N., Ioerger, T.R., Sacchettini, J.C., Lipsitch, M.*, et al.* (2011). Use of whole genome sequencing to estimate the mutation rate of Mycobacterium tuberculosis during latent infection. Nat Genet *43*, 482-486.

Ford, C.B., Shah, R.R., Maeda, M.K., Gagneux, S., Murray, M.B., Cohen, T., Johnston, J.C., Gardy, J., Lipsitch, M., and Fortune, S.M. (2013).

Mycobacterium tuberculosis mutation rate estimates from different lineages predict substantial differences in the emergence of drug-resistant tuberculosis. Nat Genet *45*, 784-790.

Franzblau, S.G., Witzig, R.S., McLaughlin, J.C., Torres, P., Madico, G., Hernandez, A., Degnan, M.T., Cook, M.B., Quenzer, V.K., Ferguson, R.M*., et al.* (1998). Rapid, low-technology MIC determination with clinical Mycobacterium tuberculosis isolates by using the microplate Alamar Blue assay. J Clin Microbiol *36*, 362-366.

Fuge, E.K., Braun, E.L., and Werner-Washburne, M. (1994). Protein synthesis in long-term stationary-phase cultures of Saccharomyces cerevisiae. J Bacteriol *176*, 5802-5813.

Galagan, J.E., Minch, K., Peterson, M., Lyubetskaya, A., Azizi, E., Sweet, L., Gomes, A., Rustad, T., Dolganov, G., Glotova, I*., et al.* (2013). The Mycobacterium tuberculosis regulatory network and hypoxia. Nature *499*, 178-183.

Garton, N.J., Christensen, H., Minnikin, D.E., Adegbola, R.A., and Barer, M.R. (2002). Intracellular lipophilic inclusions of mycobacteria in vitro and in sputum. Microbiology *148*, 2951-2958.

Gee, C.L., Papavinasasundaram, K.G., Blair, S.R., Baer, C.E., Falick, A.M., King, D.S., Griffin, J.E., Venghatakrishnan, H., Zukauskas, A., Wei, J.R.*, et al.* (2012). A phosphorylated pseudokinase complex controls cell wall synthesis in mycobacteria. Sci Signal *5*, ra7.

Gengenbacher, M., Rao, S.P., Pethe, K., and Dick, T. (2010). Nutrient-starved, non-replicating Mycobacterium tuberculosis requires respiration, ATP synthase and isocitrate lyase for maintenance of ATP homeostasis and viability. Microbiology *156*, 81-87.

Georgellis, D., Barlow, T., Arvidson, S., and von Gabain, A. (1993). Retarded RNA turnover in Escherichia coli: a means of maintaining gene expression during anaerobiosis. Mol Microbiol *9*, 375-381.

Gill, W.P., Harik, N.S., Whiddon, M.R., Liao, R.P., Mittler, J.E., and Sherman, D.R. (2009). A replication clock for Mycobacterium tuberculosis. Nat Med *15*, 211-214.

Gomez, J.E., and McKinney, J.D. (2004). M. tuberculosis persistence, latency, and drug tolerance. Tuberculosis (Edinb) *84*, 29-44.

Gong, C., Bongiorno, P., Martins, A., Stephanou, N.C., Zhu, H., Shuman, S., and Glickman, M.S. (2005). Mechanism of nonhomologous end-joining in mycobacteria: a low-fidelity repair system driven by Ku, ligase D and ligase C. Nat Struct Mol Biol *12*, 304-312.

Gray, J.V., Petsko, G.A., Johnston, G.C., Ringe, D., Singer, R.A., and Werner-Washburne, M. (2004). "Sleeping beauty": quiescence in Saccharomyces cerevisiae. Microbiol Mol Biol Rev *68*, 187-206.

Griffin, J.E., Gawronski, J.D., Dejesus, M.A., Ioerger, T.R., Akerley, B.J., and Sassetti, C.M. (2011). High-resolution phenotypic profiling defines genes essential for mycobacterial growth and cholesterol catabolism. PLoS Pathog *7*, e1002251.

Griffin, J. E., A. K. Pandey, S. A. Gilmore, V. Mizrahi, J. D. McKinney, C. R. Bertozzi, and C. M. Sassetti. (2012). Cholesterol catabolism by Mycobacterium tuberculosis requires transcriptional and metabolic adaptations." Chem Biol *19* (2):218-27.

Groat, R.G., Schultz, J.E., Zychlinsky, E., Bockman, A., and Matin, A. (1986). Starvation proteins in Escherichia coli: kinetics of synthesis and role in starvation survival. J Bacteriol *168*, 486-493.

Gupta, R., Barkan, D., Redelman-Sidi, G., Shuman, S., and Glickman, M.S. (2011). Mycobacteria exploit three genetically distinct DNA double-strand break repair pathways. Mol Microbiol *79*, 316-330.

Gupta, R., Lavollay, M., Mainardi, J.L., Arthur, M., Bishai, W.R., and Lamichhane, G. (2010). The Mycobacterium tuberculosis protein LdtMt2 is a nonclassical transpeptidase required for virulence and resistance to amoxicillin. Nat Med *16*, 466-469.

Gurumurthy, M., Rao, M., Mukherjee, T., Rao, S.P., Boshoff, H.I., Dick, T., Barry, C.E., 3rd, and Manjunatha, U.H. (2013). A novel F(420) -dependent anti-oxidant mechanism protects Mycobacterium tuberculosis against oxidative stress and bactericidal agents. Mol Microbiol *87*, 744-755.

Hasan, M. R., M. Rahman, S. Jaques, E. Purwantini, and L. Daniels. (2010). Glucose 6-phosphate accumulation in mycobacteria: implications for a novel F420-dependent anti-oxidant defense system. J Biol Chem *285* (25):19135-44.

Hett, E.C., and Rubin, E.J. (2008). Bacterial growth and cell division: a mycobacterial perspective. Microbiol Mol Biol Rev *72*, 126-156, table of contents.

Honaker, R.W., Dhiman, R.K., Narayanasamy, P., Crick, D.C., and Voskuil, M.I. (2010). DosS responds to a reduced electron transport system to induce the Mycobacterium tuberculosis DosR regulon. J Bacteriol *192*, 6447-6455.

Hugonnet, J.E., Tremblay, L.W., Boshoff, H.I., Barry, C.E., 3rd, and Blanchard, J.S. (2009). Meropenem-clavulanate is effective against extensively drug-resistant Mycobacterium tuberculosis. Science *323*, 1215-1218.

Hussain, S., Malik, M., Shi, L., Gennaro, M.L., and Drlica, K. (2009). In vitro model of mycobacterial growth arrest using nitric oxide with limited air. Antimicrob Agents Chemother *53*, 157-161.

Jona, G., Choder, M., and Gileadi, O. (2000). Glucose starvation induces a drastic reduction in the rates of both transcription and degradation of mRNA in yeast. Biochim Biophys Acta *1491*, 37-48.

Jones, S.E., and Lennon, J.T. (2010). Dormancy contributes to the maintenance of microbial diversity. Proc Natl Acad Sci U S A *107*, 5881-5886.

Kadouri, D., Jurkevitch, E., Okon, Y., and Castro-Sowinski, S. (2005). Ecological and agricultural significance of bacterial polyhydroxyalkanoates. Crit Rev Microbiol *31*, 55-67.

Kalscheuer, R., Stoveken, T., Malkus, U., Reichelt, R., Golyshin, P.N., Sabirova, J.S., Ferrer, M., Timmis, K.N., and Steinbuchel, A. (2007). Analysis of storage lipid accumulation in Alcanivorax borkumensis: Evidence for alternative triacylglycerol biosynthesis routes in bacteria. J Bacteriol *189*, 918-928.

Kana, B.D., Gordhan, B.G., Downing, K.J., Sung, N., Vostroktunova, G., Machowski, E.E., Tsenova, L., Young, M., Kaprelyants, A., Kaplan, G.*, et al.* (2008). The resuscitation-promoting factors of Mycobacterium tuberculosis are required for virulence and resuscitation from dormancy but are collectively dispensable for growth in vitro. Mol Microbiol *67*, 672-684.

Kang, C.M., Abbott, D.W., Park, S.T., Dascher, C.C., Cantley, L.C., and Husson, R.N. (2005). The Mycobacterium tuberculosis serine/threonine

kinases PknA and PknB: substrate identification and regulation of cell shape. Genes Dev *19*, 1692-1704.

Keren, I., Kaldalu, N., Spoering, A., Wang, Y., and Lewis, K. (2004a). Persister cells and tolerance to antimicrobials. FEMS Microbiol Lett *230*, 13-18.

Keren, I., Shah, D., Spoering, A., Kaldalu, N., and Lewis, K. (2004b). Specialized persister cells and the mechanism of multidrug tolerance in Escherichia coli. J Bacteriol *186*, 8172-8180.

Kim, J.H., O'Brien, K.M., Sharma, R., Boshoff, H.I., Rehren, G., Chakraborty, S., Wallach, J.B., Monteleone, M., Wilson, D.J., Aldrich, C.C.*, et al.* (2013). A genetic strategy to identify targets for the development of drugs that prevent bacterial persistence. Proc Natl Acad Sci U S A *110*, 19095-19100.

Kohanski, M.A., Dwyer, D.J., Hayete, B., Lawrence, C.A., and Collins, J.J. (2007). A common mechanism of cellular death induced by bactericidal antibiotics. Cell *130*, 797-810.

Kreidl, K.O., Green, G.R., and Wren, S.M. (2002). Intravascular hemolysis from a Clostridium perfringens liver abscess. J Am Coll Surg *194*, 387.

Kumar, P., Arora, K., Lloyd, J.R., Lee, I.Y., Nair, V., Fischer, E., Boshoff, H.I., and Barry, C.E., 3rd (2012). Meropenem inhibits D,D-carboxypeptidase activity in Mycobacterium tuberculosis. Mol Microbiol *86*, 367-381.

Kunkel, T.A. (2004). DNA replication fidelity. J Biol Chem *279*, 16895-16898.

Lacour, S., and Landini, P. (2004). SigmaS-dependent gene expression at the onset of stationary phase in Escherichia coli: function of sigmaS-dependent genes and identification of their promoter sequences. J Bacteriol *186*, 7186-7195.

Lam, H., Oh, D.C., Cava, F., Takacs, C.N., Clardy, J., de Pedro, M.A., and Waldor, M.K. (2009). D-amino acids govern stationary phase cell wall remodeling in bacteria. Science *325*, 1552-1555.

Lavollay, M., Arthur, M., Fourgeaud, M., Dubost, L., Marie, A., Veziris, N., Blanot, D., Gutmann, L., and Mainardi, J.L. (2008). The peptidoglycan of stationary-phase Mycobacterium tuberculosis predominantly contains cross-links generated by L,D-transpeptidation. J Bacteriol *190*, 4360-4366.

Lee, H.J., Lang, P.T., Fortune, S.M., Sassetti, C.M., and Alber, T. (2012). Cyclic AMP regulation of protein lysine acetylation in Mycobacterium tuberculosis. Nat Struct Mol Biol *19*, 811-818.

Lee, Y. V., H. A. Wahab, and Y. S. Choong. (2015). Potential inhibitors for isocitrate lyase of Mycobacterium tuberculosis and non-M. tuberculosis: a summary. Biomed Res Int 2015:895453.

Leistikow, R. L., R. A. Morton, I. L. Bartek, I. Frimpong, K. Wagner, and M. I. Voskuil. (2010). The Mycobacterium tuberculosis DosR regulon assists in metabolic homeostasis and enables rapid recovery from nonrespiring dormancy. J Bacteriol *192* (6):1662-70.

Lenaerts, A.J., Gruppo, V., Brooks, J.V., and Orme, I.M. (2003). Rapid in vivo screening of experimental drugs for tuberculosis using gamma interferon gene-disrupted mice. Antimicrob Agents Chemother *47*, 783-785.

Lenhart, J.S., Schroeder, J.W., Walsh, B.W., and Simmons, L.A. (2012). DNA repair and genome maintenance in Bacillus subtilis. Microbiol Mol Biol Rev *76*, 530-564.

Lewis, D.L., and Gattie, D.K. (1988). Prediction of substrate removal rates of attached microorganisms and of relative contributions of attached and suspended communities at field sites. Appl Environ Microbiol *54*, 434-440.

Lewis, K. (2007). Persister cells, dormancy and infectious disease. Nat Rev Microbiol *5*, 48-56.

Long, J.E., DeJesus, M., Ward, D., Baker, R.E., Ioerger, T., and Sassetti, C.M. (2015). Identifying essential genes in Mycobacterium tuberculosis by global phenotypic profiling. Methods Mol Biol *1279*, 79-95.

Magge, A., Setlow, B., Cowan, A.E., and Setlow, P. (2009). Analysis of dye binding by and membrane potential in spores of Bacillus species. J Appl Microbiol *106*, 814-824.

Martinez, A., and Kolter, R. (1997). Protection of DNA during oxidative stress by the nonspecific DNA-binding protein Dps. J Bacteriol *179*, 5188-5194.

Marton, L.J., and Pegg, A.E. (1995). Polyamines as targets for therapeutic intervention. Annu Rev Pharmacol Toxicol *35*, 55-91.

McDermott, W. (1958). Microbial persistence. Yale J Biol Med *30*, 257-291.

McDonough, K.A., and Rodriguez, A. (2011). The myriad roles of cyclic AMP in microbial pathogens: from signal to sword. Nat Rev Microbiol *10*, 27-38.

Mir, M., Asong, J., Li, X., Cardot, J., Boons, G.J., and Husson, R.N. (2011). The extracytoplasmic domain of the Mycobacterium tuberculosis Ser/Thr kinase PknB binds specific muropeptides and is required for PknB localization. PLoS Pathog *7*, e1002182.

Mitchison, D.A., and Coates, A.R. (2004). Predictive in vitro models of the sterilizing activity of anti-tuberculosis drugs. Curr Pharm Des *10*, 3285-3295.

Morth, J.P., Gosmann, S., Nowak, E., and Tucker, P.A. (2005). A novel two-component system found in Mycobacterium tuberculosis. FEBS Lett *579*, 4145-4148.

Mukamolova, G.V., Kaprelyants, A.S., Young, D.I., Young, M., and Kell, D.B. (1998). A bacterial cytokine. Proc Natl Acad Sci U S A *95*, 8916-8921.

Munoz-Elias, E.J., and McKinney, J.D. (2005). Mycobacterium tuberculosis isocitrate lyases 1 and 2 are jointly required for in vivo growth and virulence. Nat Med *11*, 638-644.

Munoz-Elias, E.J., Timm, J., Botha, T., Chan, W.T., Gomez, J.E., and McKinney, J.D. (2005). Replication dynamics of Mycobacterium tuberculosis in chronically infected mice. Infect Immun *73*, 546-551.

Musk, D.J., Jr., and Hergenrother, P.J. (2006). Chemical countermeasures for the control of bacterial biofilms: effective compounds and promising targets. Curr Med Chem *13*, 2163-2177.

Nambi, S., Basu, N., and Visweswariah, S.S. (2010). cAMP-regulated protein lysine acetylases in mycobacteria. J Biol Chem *285*, 24313-24323.

Nambi, S., Gupta, K., Bhattacharyya, M., Ramakrishnan, P., Ravikumar, V., Siddiqui, N., Thomas, A.T., and Visweswariah, S.S. (2013). Cyclic AMP-dependent protein lysine acylation in mycobacteria regulates fatty acid and propionate metabolism. J Biol Chem *288*, 14114-14124.

Nambi, S., Long, J.E., Mishra, B.B., Baker, R., Murphy, K.C., Olive, A.J., Nguyen, H.P., Shaffer, S.A., and Sassetti, C.M. (2015). The Oxidative Stress Network of Mycobacterium tuberculosis Reveals Coordination between Radical Detoxification Systems. Cell Host Microbe *17*, 829-837.

Neidhardt, F.C. (1999). Bacterial growth: constant obsession with dN/dt. J Bacteriol *181*, 7405-7408.

Nguyen, D., Joshi-Datar, A., Lepine, F., Bauerle, E., Olakanmi, O., Beer, K., McKay, G., Siehnel, R., Schafhauser, J., Wang, Y*., et al.* (2011). Active starvation responses mediate antibiotic tolerance in biofilms and nutrient-limited bacteria. Science *334*, 982-986.

Noy, T., Xu, H., and Blanchard, J.S. (2014). Acetylation of acetyl-CoA synthetase from Mycobacterium tuberculosis leads to specific inactivation of the adenylation reaction. Arch Biochem Biophys *550-551*, 42-49.

Ohniwa, R.L., Morikawa, K., Kim, J., Ohta, T., Ishihama, A., Wada, C., and Takeyasu, K. (2006). Dynamic state of DNA topology is essential for genome condensation in bacteria. Embo j *25*, 5591-5602.

Paz, I., Abramovitz, L., and Choder, M. (1999). Starved Saccharomyces cerevisiae cells have the capacity to support internal initiation of translation. J Biol Chem *274*, 21741-21745.

Pedersen, S. (1986). The chain growth rate for protein synthesis varies in Escherichia coli. In The Molecular Biology of Bacterial Growth, M.

Schaechter, F.C. Neidhardt, J.L. Ingraham, N.O. Kjeldgaard, ed. (Boston, Mass: Jones and Bartlett, Inc.), pp. 13-20.

Pernthaler, A., and Amann, R. (2004). Simultaneous fluorescence in situ hybridization of mRNA and rRNA in environmental bacteria. Appl Environ Microbiol *70*, 5426-5433.

Potera, C. (2010). Antibiotic Resistance: Biofilm dispersing agent rejuvenates older antibiotics. Environ Heath Perspect *118*, A288.

Primm, T.P., Andersen, S.J., Mizrahi, V., Avarbock, D., Rubin, H., and Barry, C.E., 3rd (2000). The stringent response of Mycobacterium tuberculosis is required for long-term survival. J Bacteriol *182*, 4889-4898.

Prlic, A., S. Bliven, P. W. Rose, W. F. Bluhm, C. Bizon, A. Godzik, and P. E. Bourne. (2010). Pre-calculated protein structure alignments at the RCSB PDB website. Bioinformatics *26* (23):2983-5.

Purwantini, E., and Mukhopadhyay, B. (2009). Conversion of NO2 to NO by reduced coenzyme F420 protects mycobacteria from nitrosative damage. Proc Natl Acad Sci U S A *106*, 6333-6338.

Radunz, A., and Schmid, G.H. (2000). Wax esters and triglycerides as storage substances in seeds of Buxus sempervirens. Eur J Lipid Sci Tech *102*, 734-738.

Ramirez-Guadiana, F.H., Barraza-Salas, M., Ramirez-Ramirez, N., Ortiz-Cortes, M., Setlow, P., and Pedraza-Reyes, M. (2012). Alternative excision repair of ultraviolet B- and C-induced DNA damage in dormant and developing spores of Bacillus subtilis. J Bacteriol *194*, 6096-6104.

Rao, P.K., and Li, Q. (2009). Protein turnover in mycobacterial proteomics. Molecules *14*, 3237-3258.

Rao, S.P., Alonso, S., Rand, L., Dick, T., and Pethe, K. (2008). The protonmotive force is required for maintaining ATP homeostasis and viability of hypoxic, nonreplicating Mycobacterium tuberculosis. Proc Natl Acad Sci U S A *105*, 11945-11950.

Reeve, C.A., Amy, P.S., and Matin, A. (1984). Role of protein synthesis in the survival of carbon-starved Escherichia coli K-12. J Bacteriol *160*, 1041-1046.

Rittershaus, E.S., Baek, S.H., and Sassetti, C.M. (2013). The normalcy of dormancy: common themes in microbial quiescence. Cell Host Microbe *13*, 643-651.

Roszak, D.B., and Colwell, R.R. (1987). Survival strategies of bacteria in the natural environment. Microbiol Rev *51*, 365-379.

Rustad, T.R., Harrell, M.I., Liao, R., and Sherman, D.R. (2008). The enduring hypoxic response of Mycobacterium tuberculosis. PLoS One *3*, e1502.

Rustad, T.R., Minch, K.J., Brabant, W., Winkler, J.K., Reiss, D.J., Baliga, N.S., and Sherman, D.R. (2013). Global analysis of mRNA stability in Mycobacterium tuberculosis. Nucleic Acids Res *41*, 509-517.

Sala, C., Dhar, N., Hartkoorn, R.C., Zhang, M., Ha, Y.H., Schneider, P., and Cole, S.T. (2010). Simple model for testing drugs against nonreplicating Mycobacterium tuberculosis. Antimicrob Agents Chemother *54*, 4150-4158.

Sarathy, J., Dartois, V., Dick, T., and Gengenbacher, M. (2013). Reduced drug uptake in phenotypically resistant nutrient-starved nonreplicating Mycobacterium tuberculosis. Antimicrob Agents Chemother *57*, 1648-1653.

Sassetti, C.M., Boyd, D.H., and Rubin, E.J. (2003). Genes required for mycobacterial growth defined by high density mutagenesis. Mol Microbiol *48*, 77-84.

Sauer, U., Lasko, D.R., Fiaux, J., Hochuli, M., Glaser, R., Szyperski, T., Wuthrich, K., and Bailey, J.E. (1999). Metabolic flux ratio analysis of genetic and environmental modulations of Escherichia coli central carbon metabolism. J Bacteriol *181*, 6679-6688.

Schnappinger, D., O'Brien, K.M., and Ehrt, S. (2015). Construction of conditional knockdown mutants in mycobacteria. Methods Mol Biol *1285*, 151-175.

Schnorpfeil, M., Janausch, I.G., Biel, S., Kroger, A., and Unden, G. (2001). Generation of a proton potential by succinate dehydrogenase of Bacillus subtilis functioning as a fumarate reductase. Eur J Biochem *268*, 3069-3074.

Shah, I.M., Laaberki, M.H., Popham, D.L., and Dworkin, J. (2008). A eukaryotic-like Ser/Thr kinase signals bacteria to exit dormancy in response to peptidoglycan fragments. Cell *135*, 486-496.

Shaikh, A.S., Tang, Y.J., Mukhopadhyay, A., Martin, H.G., Gin, J., Benke, P.I., and Keasling, J.D. (2010). Study of stationary phase metabolism via isotopomer analysis of amino acids from an isolated protein. Biotechnol Prog *26*, 52-56.

Sherman, D.R., Voskuil, M., Schnappinger, D., Liao, R., Harrell, M.I., and Schoolnik, G.K. (2001). Regulation of the Mycobacterium tuberculosis hypoxic response gene encoding alpha -crystallin. Proc Natl Acad Sci U S A *98*, 7534-7539.

Sherrid, A.M., Rustad, T.R., Cangelosi, G.A., and Sherman, D.R. (2010). Characterization of a Clp protease gene regulator and the reaeration response in Mycobacterium tuberculosis. PLoS One *5*, e11622.

Shi, L., Sutter, B.M., Ye, X., and Tu, B.P. (2010). Trehalose is a key determinant of the quiescent metabolic state that fuels cell cycle progression upon return to growth. Mol Biol Cell *21*, 1982-1990.

Shi, W., Zhang, X., Jiang, X., Yuan, H., Lee, J.S., Barry, C.E., 3rd, Wang, H., Zhang, W., and Zhang, Y. (2011). Pyrazinamide inhibits trans-translation in Mycobacterium tuberculosis. Science *333*, 1630-1632.

Shuman, S., and Glickman, M.S. (2007). Bacterial DNA repair by non-homologous end joining. Nat Rev Microbiol *5*, 852-861.

Sillje, H.H., Paalman, J.W., ter Schure, E.G., Olsthoorn, S.Q., Verkleij, A.J., Boonstra, J., and Verrips, C.T. (1999). Function of trehalose and glycogen in cell cycle progression and cell viability in Saccharomyces cerevisiae. J Bacteriol *181*, 396-400.

Singh, R., Manjunatha, U., Boshoff, H.I., Ha, Y.H., Niyomrattanakit, P., Ledwidge, R., Dowd, C.S., Lee, I.Y., Kim, P., Zhang, L.*, et al.* (2008). PA-824 kills nonreplicating Mycobacterium tuberculosis by intracellular NO release. Science *322*, 1392-1395.

Sirakova, T.D., Deb, C., Daniel, J., Singh, H.D., Maamar, H., Dubey, V.S., and Kolattukudy, P.E. (2012). Wax ester synthesis is required for Mycobacterium tuberculosis to enter in vitro dormancy. PLoS One *7*, e51641.

Smith, R.M., and Williams, S.B. (2006). Circadian rhythms in gene transcription imparted by chromosome compaction in the cyanobacterium Synechococcus elongatus. Proc Natl Acad Sci U S A *103*, 8564-8569.

Squeglia, F., Marchetti, R., Ruggiero, A., Lanzetta, R., Marasco, D., Dworkin, J., Petoukhov, M., Molinaro, A., Berisio, R., and Silipo, A. (2011). Chemical basis of peptidoglycan discrimination by PrkC, a key kinase involved in bacterial resuscitation from dormancy. J Am Chem Soc *133*, 20676-20679.

Stallings, C.L., Stephanou, N.C., Chu, L., Hochschild, A., Nickels, B.E., and Glickman, M.S. (2009). CarD is an essential regulator of rRNA transcription required for Mycobacterium tuberculosis persistence. Cell *138*, 146-159.

Steinhaus, E.A., and Birkeland, J.M. (1939). Studies on the Life and Death of Bacteria: I. The Senescent Phase in Aging Cultures and the Probable Mechanisms Involved. J Bacteriol *38*, 249-261.

Stragier, P., and Losick, R. (1996). Molecular genetics of sporulation in Bacillus subtilis. Annu Rev Genet *30*, 297-241.

Summers, E.L., Meindl, K., Uson, I., Mitra, A.K., Radjainia, M., Colangeli, R., Alland, D., and Arcus, V.L. (2012). The structure of the oligomerization domain of Lsr2 from Mycobacterium tuberculosis reveals a mechanism for chromosome organization and protection. PLoS One *7*, e38542.

Talukder, A.A., Yanai, S., Nitta, T., Kato, A., and Yamada, M. (1996). RpoS-dependent regulation of genes expressed at late stationary phase in Escherichia coli. FEBS Lett *386*, 177-180.

Tews, I., Findeisen, F., Sinning, I., Schultz, A., Schultz, J.E., and Linder, J.U. (2005). The structure of a pH-sensing mycobacterial adenylyl cyclase holoenzyme. Science *308*, 1020-1023.

Tran, Q.H., and Unden, G. (1998). Changes in the proton potential and the cellular energetics of Escherichia coli during growth by aerobic and anaerobic respiration or by fermentation. Eur J Biochem *251*, 538-543.

Valcourt, J.R., Lemons, J.M., Haley, E.M., Kojima, M., Demuren, O.O., and Coller, H.A. (2012). Staying alive: metabolic adaptations to quiescence. Cell Cycle *11*, 1680-1696.

Vijayan, V., Zuzow, R., and O'Shea, E.K. (2009). Oscillations in supercoiling drive circadian gene expression in cyanobacteria. Proc Natl Acad Sci U S A *106*, 22564-22568.

Voskuil, M.I., Schnappinger, D., Visconti, K.C., Harrell, M.I., Dolganov, G.M., Sherman, D.R., and Schoolnik, G.K. (2003). Inhibition of respiration by nitric

oxide induces a Mycobacterium tuberculosis dormancy program. J Exp Med *198*, 705-713.

Wang, Q., Zhang, Y., Yang, C., Xiong, H., Lin, Y., Yao, J., Li, H., Xie, L., Zhao, W., Yao, Y*., et al.* (2010). Acetylation of metabolic enzymes coordinates carbon source utilization and metabolic flux. Science *327*, 1004-1007.

Watanabe, S., Zimmermann, M., Goodwin, M.B., Sauer, U., Barry, C.E., 3rd, and Boshoff, H.I. (2011). Fumarate reductase activity maintains an energized membrane in anaerobic Mycobacterium tuberculosis. PLoS Pathog *7*, e1002287.

Wayne, L.G. (1976). Dynamics of submerged growth of Mycobacterium tuberculosis under aerobic and microaerophilic conditions. Am Rev Respir Dis *114*, 807-811.

Wayne, L.G. (1977). Synchronized replication of Mycobacterium tuberculosis. Infect Immun *17*, 528-530.

Wayne, L.G., and Hayes, L.G. (1996). An in vitro model for sequential study of shiftdown of Mycobacterium tuberculosis through two stages of nonreplicating persistence. Infect Immun *64*, 2062-2069.

Wayne, L.G., and Sohaskey, C.D. (2001). Nonreplicating persistence of mycobacterium tuberculosis. Annu Rev Microbiol *55*, 139-163.

Werner-Washburne, M., Braun, E.L., Crawford, M.E., and Peck, V.M. (1996). Stationary phase in Saccharomyces cerevisiae. Mol Microbiol *19*, 1159-1166.

Wolfe, A.J. (2005). The acetate switch. Microbiol Mol Biol Rev *69*, 12-50.

Xie, Z., Siddiqi, N., and Rubin, E.J. (2005). Differential antibiotic susceptibilities of starved Mycobacterium tuberculosis isolates. Antimicrob Agents Chemother *49*, 4778-4780.

Xu, H., Hegde, S.S., and Blanchard, J.S. (2011). Reversible acetylation and inactivation of Mycobacterium tuberculosis acetyl-CoA synthetase is dependent on cAMP. Biochemistry *50*, 5883-5892.

Ye, Y., and A. Godzik. (2003). Flexible structure alignment by chaining aligned fragment pairs allowing twists. Bioinformatics *19* Suppl 2:ii246-55.

Zhang, J., Sprung, R., Pei, J., Tan, X., Kim, S., Zhu, H., Liu, C.F., Grishin, N.V., and Zhao, Y. (2009a). Lysine acetylation is a highly abundant and evolutionarily conserved modification in Escherichia coli. Mol Cell Proteomics *8*, 215-225.

Zhang, N., Wu, J., and Oliver, S.G. (2009b). Gis1 is required for transcriptional reprogramming of carbon metabolism and the stress response during transition into stationary phase in yeast. Microbiology *155*, 1690-1698.

Zhang, Y., Wade, M.M., Scorpio, A., Zhang, H., and Sun, Z. (2003). Mode of action of pyrazinamide: disruption of Mycobacterium tuberculosis membrane transport and energetics by pyrazinoic acid. J Antimicrob Chemother *52*, 790-795.

Zhou, X., and Cegelski, L. (2012). Nutrient-dependent structural changes in S. aureus peptidoglycan revealed by solid-state NMR spectroscopy. Biochemistry *51*, 8143-8153.